

Document UCRL-TR-203529

This document contains 64 pages.

Neutrons and Granite: Transport and Activation

Peter J. Bedrossian

April 2004

*Lawrence Livermore National Laboratory
Livermore CA 94551*

**Work was performed at Lawrence Livermore National Laboratory under the
auspices of the University of California under US-DOE Contract W-7405-Eng-48.**

This document was prepared as an account of work sponsored by an agency of the United States Government. Neither the United States Government nor the University of California nor any of their employees, makes any warranty, express or implied, or assumes any legal liability or responsibility for the accuracy, completeness, or usefulness of any information, apparatus, product, or process disclosed, or represents that its use would not infringe privately owned rights. Reference herein to any specific commercial product, process, or service by trade name, trademark, manufacturer, or otherwise, does not necessarily constitute or imply its endorsement, recommendation, or favoring by the United States Government or the University of California. The views and opinions of authors expressed herein do not necessarily state or reflect those of the United States Government or the University of California, and shall not be used for advertising or product endorsement purposes.

This page intentionally left blank
to facilitate double-sided printing

Abstract

In typical ground materials, both energy deposition and radionuclide production by energetic neutrons vary with the incident particle energy in a non-monotonic way. We describe the overall balance of nuclear reactions involving neutrons impinging on granite to demonstrate these energy-dependencies. While granite is a useful surrogate for a broad range of soil and rock types, the incorporation of small amounts of water (hydrogen) does alter the balance of nuclear reactions.

This page intentionally left blank
to facilitate double-sided printing.

Table of Contents

Abstract	3
List of Tables	6
List of Figures	7
Introduction.....	9
Method	10
Results and Discussion	14
Neutron Transport and Energy Deposition in Dry Granite.....	14
Effect of composition variations	17
Generation of hazardous radioisotopes.....	17
Summary	19
Acknowledgments.....	19
Figures.....	20
Tables.....	34
Appendix A: Cross-Sections for Neutron Transport	38
Appendix B: Radionuclide Production Cross-Sections	46
Appendix C: Cross Section Sources for Radionuclide Production.....	56

List of Tables

Table 1: Composition of simplified granite used in this study. The calculations reflect the natural isotopic abundances for each element.....	34
Table 2: Radionuclides included in published lists of contaminant nuclides which may be created by neutron irradiation of ground. Those nuclides shown in red are radioactive. Note that not all of these radionuclides can be produced from the isotopes included in the simplified granite of Table 1, but they may be produced by neutron reactions with trace elements.....	35
Table 3: Available cross-sections for producing each of the radionuclides listed in Table 2. The reactions included in calculations described in this work are highlighted in yellow. Those which are not highlighted involve target nuclides which are not included in the simplified granite formulation considered here.	36
Table 4: Parent decay chains.....	37

List of Figures

Figure 1: Test problem geometry.....	20
Figure 2: Calculated cumulative energy deposition into granite from monoenergetic, planar neutron sources with incident angles as indicated. Note zero suppression on the vertical scale.....	21
Figure 3: Calculated cumulative energy deposition into granite and into the principal atomic components of granite individually from monoenergetic, planar neutron sources and normal incidence.....	21
Figure 4: Calculated cumulative energy deposition into granite by depth. This and all subsequent plots involve neutrons at normal incidence.....	22
Figure 5: Calculated $^{16}\text{O}(\text{n},\text{elastic})$ reactions in granite by depth for normal incidence..	22
Figure 6: Calculated $^{28}\text{Si}(\text{n},\text{elastic})$ reactions in granite by depth.	23
Figure 7: Calculated inelastic reactions of neutrons and ^{16}O in granite by depth.....	23
Figure 8: Calculated inelastic reactions of neutrons and ^{28}Si in granite by depth.	24
Figure 9: Calculated $^{16}\text{O}(\text{n},\alpha)$ reactions in granite by depth.....	24
Figure 10: Calculated $^{16}\text{O}(\text{n},\text{p})$ reactions in granite by depth.	25
Figure 11: Calculated $^{28}\text{Si}(\text{n},\alpha)$ reactions in granite by depth.....	25
Figure 12: Calculated $^{28}\text{Si}(\text{n},\text{d})$ reactions in granite by depth.....	26
Figure 13: Calculated $^{28}\text{Si}(\text{n},\gamma)$ reactions in granite by depth.	26
Figure 14: Calculated $^{28}\text{Si}(\text{n},\text{n}\alpha)$ reactions in granite by depth.	27
Figure 15: Calculated $^{28}\text{Si}(\text{n},\text{p})$ reactions in granite by depth.....	27
Figure 16: Calculated $^{28}\text{Si}(\text{n},\text{np})$ reactions in granite by depth.....	28
Figure 17: Calculated energy deposition by depth into the ^{16}O component of granite only. Other components are removed from the problem.	29
Figure 18: Calculated, total neutron reactions by depth into the ^{16}O component of granite only. Other components are removed from the problem.....	29
Figure 19: Calculated energy deposition by depth into the ^{28}Si component of granite only. Other components are removed from the problem.	30
Figure 20: Calculated, total neutron reactions by depth into the ^{28}Si component of granite only. Other components are removed from the problem.	30
Figure 21: Summary of the dominant reactions for neutrons incident on granite. Reactions involving ^{16}O are represented with solid curves, while reactions involving ^{28}Si are represented with dashed curves.....	31
Figure 22: Calculated energy deposition by depth in granite vs. percentage of added water.....	32
Figure 23: Effects of added water on neutron reactions in granite.	32
Figure 24: Total production of specific radioisotopes in granite from planar, monoenergetic neutron sources.....	33
Figure 25: (Appendix A) Neutron cross-sections for target ^{28}Si from ENDF/B-VI.8....	38
Figure 26: (Appendix A) Total Cross Section for neutrons incident on ^{28}Si , from ENDF/B-VI.8.....	39

Figure 27: (Appendix A) Neutron cross-sections for target ^{16}O from ENDF/B-VI.8.	40
Figure 28: (Appendix A) Neutron cross-sections for target ^{16}O from ENDL99.	41
Figure 29: (Appendix A) Total Cross Section for neutrons incident on ^{16}O , from both ENDF/B-VI.8 and ENDL99.	42
Figure 30: (Appendix A) ENDF/B-VI cross sections for dominant transmutation reactions in granite, <i>WEIGHTED BY THE ATOMIC COMPOSITIONS IN GRANITE</i> . The vertical scale is the cross section multiplied by the number of atoms/barn-cm of the target nuclide.	43
Figure 31: (Appendix A) Neutron elastic cross-sections for ^1H , ^{16}O , and ^{28}Si	44
Figure 32: (Appendix A) Capture cross-sections for ^1H , ^{16}O , and ^{28}Si	45

Introduction

The release of energetic neutrons in the vicinity of the earth's surface, as might occur in a nuclear explosion, will affect the ground in two ways: (i) collisions and nuclear reactions will transfer energy from the incident neutrons to the ground, resulting in ground heating that can lead to melting, vaporization, and shock generation; and (ii) neutron reactions can generate hazardous radionuclides.¹ Trace elements present in soil can be activated to generate non-negligible quantities of radioisotopes. Mitigation of collateral effects from the release of energetic neutrons requires a detailed understanding of the interaction of neutrons with the ground. The methodology described here provides a tool to evaluate collateral damage from radioisotope activation for specific conditions of neutron release, ground composition, and terrain. While this study uses simple models that capture the essential physics, the methodology is easily generalizable to a broad range of general neutron sources, ground compositions, and details of terrain.

Specifically, we consider a planar, monoenergetic neutron source at a height of 1m above granite. (Figure 1) Granite is a natural surrogate for many soils and rocks because it is composed primarily of SiO₂, and its composition closely approximates that of the earth's crust. Apart from Limestone, the more common soils and rocks on the earth's surface are composed primarily of Si and O. [1] Using MCNP, we calculate the energy deposition as a function of depth in the ground and correlate the energy deposition with neutron reactions taking place for each incident neutron energy. The production of hazardous radionuclides is included in the calculations. Finally, we consider small variations in granite composition.

¹ C. Bridgman, *The Effects of Nuclear Weapons* (VA: DTRA, 2001).

Method

All of the calculations described below used Version 5 of the MCNP code. A comprehensive description of the capabilities of the code and the underlying physics is provided in the documentation for the code.² Each calculation uses a planar source of monoenergetic neutrons of radius 10m, located 1m above the surface of the ground. The total problem radius within which neutrons and neutron-induced gammas are tallied is typically 100m. The source neutrons are all directed toward the ground, either at normal incidence or at a specified angle. The ground is partitioned into flat slabs with logarithmically-spaced boundaries parallel to the flat surface. The calculations were typically started with 20,000 census particles and with biasing such that particle importance increased with depth into the ground. We have used a simplified granite composition for the ground, given in Table 1.³ For reference we have included in the table the concentrations of various elements in the earth's crust, and in pure SiO₂. Because the dominant constituents of granite correspond generally to those in the earth's crust, the physics of neutron transport in granite may be expected to apply generally to a variety of soils and rocks with similar compositions. The model captures the essential features of the energy-dependence of neutron-ground coupling and demonstrates the calculation of radionuclide production rates. It can also be generalized easily to specific environments of interest.

All results are presented below in a normalized form and can therefore be scaled to arbitrary source strength. For example, energy deposition and reaction tallies are both normalized to the total incident energy fluence (number of source neutrons × energy per neutron), while radionuclide production calculations are normalized to the number of incident neutrons.

The Monte Carlo transport calculations described below use cross-sections from Release 8 of the ENDF/B-VI library where available. This is the most current library of

² "MCNP—A General Monte Carlo N-Particle Transport Code, Version 5," LANL document LA-UR-03-1987. (2003).

³ Source: T. S. Carman, private communication.

evaluated cross-sections included with Release 5 of MCNP. If no cross-section set is available in an ENDF library for a particular nuclide, then we use the ENDL-92 library. The latter is the most current release of an ENDL library which is available for use with MCNP.

In order to calculate radionuclide activation, we set up tallies for each reaction channel which might yield a particular radionuclide for which cross-sections are available. In this study we consider the hazardous radionuclides which are listed in either one of two standard lists.^{4, 5} The consolidated list of hazardous radionuclides is presented in Table 2 below. The isotopes on the list fall into two categories: those with shorter half-lives (minutes, hours) pose a direct radiation hazard until they are depleted by radioactive decay, while the longer-lived isotopes can enter the food chain and become incorporated in biological tissue. While this is not a comprehensive list of all radionuclides which may be produced by neutron activation of soil, it is representative of the two, broad classes of hazardous isotopes, and the methodology below is easily generalizable to include other isotopes as needed for specific cases.⁶

In order to calculate the number of radionuclides of a particular species produced in reactions, it is necessary to add the contributions from any reactions that might produce that nuclide. In general, the evaluated cross-sections for those reactions may be scattered among different libraries. Appendix G of the MCNP manual [2] lists the target nuclides included in each cross-section library accessible to MCNP but *not* the specific reactions included in each library for a particular target. Lists of specific reactions are available for some evaluated cross-section libraries.⁷ However, the specific task of locating cross-sections for each reaction that might generate a particular nuclide requires a *backward*

⁴ John Northrop, ed., *Handbook of Nuclear Weapon Effects*, (Alexandria, Virginia: Defense Special Weapons Agency, 1996), p. 8-22.

⁵ E. Teller, W. Talley, G. Higgins, and G. Johnson, *The Constructive Uses of Nuclear Explosives* (New York: McGraw-Hill, 1968), p, 107.

⁶ Isotope data cited in the tables are derived from R. Firestone and V. Shirley, eds, *Table of Isotopes*, (John Wiley, 1999).

⁷ See, for example, <<http://nuclear.llnl.gov>>.

directory which would provide targets, reactions, and source libraries for a given product nuclide. Because no such directory is generally available, we present one in Appendix C below. The table is generally applicable to any trace elements for which evaluated cross-sections are available. Only radioactive product nuclei are represented in that table. If more than one library contains a cross-section for a particular reaction, we select a cross-section for the purpose of this study according to the following hierarchy: (i) ENDF/B-IV^{8, 9}, (ii) ENDL92¹⁰, (iii) ACTL and (iv) 532dos. The first contains the most up-to-date evaluations and therefore represents the most current experimental data. Either of the first two libraries may be used for transport calculations. The third and fourth libraries on the list are vintage 1970-1980 libraries from LLNL and LANL respectively which may be used only for dosimetry, not transport. Neither is actively maintained at this time, for many relevant target isotopes they hold the only accessible, evaluated cross-section data available.

Appendix C offers a complete directory of evaluated cross-sections available for use with MCNP for the production of radioisotopes. Using that table, we present in Table 3 a list of the available cross-sections for production of the radionuclides listed in Table 2, with source libraries selected on the basis of the hierarchy given above. Of the reactions listed in Table 3, those which are highlighted are included in the calculations represented in this work. Those which are not highlighted involve target nuclei which are not included in the simplified granite formulation used for this study.

In principle a complete accounting of radionuclide production should include not only generation by direct neutron irradiation but also generation by decay of parent nuclei. Table 4 presents an accounting of possible parent nuclei for each of the radionuclides listed in Table 2. According to Appendix C, production cross-sections

⁸ J. M. Campbell, S. Frankle, and R. Little, "ENDF66: A continuous-Energy Neutron Data Library based on ENDF/B-VI Release 6," LANL Document LA-UR-03-0954.

⁹ J. Hendricks, S. Frankle, and J. Court, "ENDF/B-VI Data for MCNP," LANL Document LA-12891 (1994).

¹⁰ S. Frankle, "Summary Documentation for the ENDL92 Continuous-Energy Neutron Data Library," LANL Document LA-UR-96-327 (1996)

exist only for those few parent nuclei which are highlighted in Table 4. This component of radionuclide production is not included in the work described below.

We emphasize that this study is limited to the transport and reactions of neutrons and neutron-induced gammas. Other processes which might be consequences of energy deposition in the ground, such as hydrodynamics and material phase or strength evolution are beyond the scope of this work and should be addressed separately.

Results and Discussion

Neutron Transport and Energy Deposition in Dry Granite

Because the principal atomic components of granite are Si and O, we concentrate on the interaction of incident neutrons with each of those species. We shall show that combination of the results of neutron transport calculations for these two elements individually accounts for the essential features of neutron transport and energy deposition in granite. Because Si and O are also the dominant elemental species in most soils and rocks, with the exception of limestone, the results are applicable more generally.

The following discussion makes frequent reference to plots of evaluated cross-sections in Appendix A. Figures 25 and 26 present the evaluated cross-sections used in this study for ^{28}Si , while figures 27-29 present the evaluated cross-sections for ^{16}O targets. Figure 30 presents plots of the dominant transmutation reactions involving neutrons in granite, weighted by the concentration of each atomic species in the simplified granite formulation used in this work.

Figure 2 shows that the total energy deposition, normalized to the total source energy, for monoenergetic neutrons normally incident on granite rises strongly between incident energies of 1 and 2 MeV. As the source particle energy rises, the energy deposition falls to a minimum near 6MeV, then rises, peaks again near 9MeV, then falls off at higher energies. As the angle of incidence increases, the total energy deposition falls for all incident particle energies, but it falls slightly more strongly at lower energies (<7MeV). We shall show that the dependence of energy deposition on incident angle arises because lower-energy neutrons have a higher incidence of near-surface collisions which increase the likelihood of reflection and escape into the air.

In Figure 3, the energy deposition of incident neutrons is considered separately for ^{16}O and ^{28}Si , the two dominant nuclides in granite. Oxygen and silicon respond differently to incident neutrons at any given, incident energy. Only the oxygen target shows the sharp rise in energy deposition between 1 and 2 MeV. Above 2MeV, the oxygen target shows a decrease in energy deposition and a minum at 6 MeV, then rises

between 6 and 8MeV and falls off at higher energies. The silicon target shows a peak in energy deposition near 3MeV, then decreases to a minimum near 8MeV.

Figure 4 presents the depth profiles of energy deposition in granite from monoenergetic surface sources. This and all subsequent figures reflect the results of calculations with neutrons at normal incidence. The lowest-energy neutrons (1-2MeV) deposit a higher proportion of their energy near the surface than do higher-energy neutrons.

^{16}O is characterized by a very low cross-section for neutron capture across the range of incident particle energies considered in this work. (Figure 27) For the lowest incident neutron energies considered here, elastic scattering dominates. At higher energies, the (n,α) channel opens first. In contrast, ^{28}Si has non-negligible capture cross-sections throughout the range of incident particle energies considered here (Figure 25), and inelastic neutron scattering off ^{28}Si has a significant cross-section at lower energies than for ^{16}O .

Individual reaction tallies from MCNP calculations illustrate the consequences of these details of the ^{16}O and ^{28}Si neutron cross-sections. For the lowest incident neutron energies, elastic scattering off ^{16}O dominates. (Figure 5 and Figure 6) Inelastic scattering from ^{16}O is significant only for incident energies above 6MeV (Figure 7), but inelastic scattering from ^{28}Si is significant for incident energies $\geq 2\text{MeV}$ (Figure 8). For 1MeV incident neutrons, elastic scattering from ^{16}O leads to significant reflection from the surface. The $^{16}\text{O}(n,\alpha)$ reaction channel, which is endothermic, opens above 2 MeV. (Figure 9) The energy deposition into ^{16}O falls to a local minimum near 6MeV but rises at higher energies as inelastic scattering becomes significant. Another endothermic channel associated with the $^{16}\text{O}(n,p)$ reaction opens above 10MeV and leads to another decrease in energy deposition for incident particles exceeding that energy.

Because of the non-negligible capture cross section for 1MeV neutrons on ^{28}Si , absorption of neutrons by ^{28}Si in granite is significant but small relative to elastic scattering over all incident neutron energies (Figure 13), and appreciable energy is still absorbed by the silicon target in the absence of oxygen even for 1MeV incident neutrons. (Figure 3). The dip in energy deposition for the silicon target in Figure 3 is associated with two threshold reactions, the $^{28}\text{Si}(n,a)$ reaction (Figure 11) and of the $^{28}\text{Si}(n,p)$

reaction (Figure 15) The opening of other endothermic reaction channels for ^{28}Si at higher still higher energies (Figure 12, Figure 14, and Figure 16) is associated with decreases in the energy deposition by incident neutrons at the highest energies considered here.

Energy deposition and neutron reactions for ^{16}O alone are summarized in Figure 17 and Figure 18 respectively, and for ^{28}Si in Figure 19 and Figure 20 respectively. For 1MeV neutrons incident on ^{16}O with the density of oxygen in granite, most energy deposition takes place within 50cm of the surface. For incident energies $\geq 3\text{MeV}$ most energy deposition takes place within 1.8 m of the surface. In contrast, significant energy deposition into ^{28}Si with the density of silicon in granite takes place at depths exceeding 10m for all incident energies.

A coherent picture for the transport and energy deposition of incident neutrons in granite emerges from these considerations. Figure 21 shows that elastic scattering from ^{16}O dominates elastic scattering from ^{28}Si for all incident neutron energies. At the lowest energies the ^{28}Si absorption reaction is dominated by elastic scattering from ^{16}O . Therefore, lower-energy neutrons are confined near the surface by collisions, and the lowest-energy neutrons considered here (MeV) are most likely to be reflected back to air and deposit the lowest proportion of their energy in the granite. Other features of the deposition profile for normal incidence (red curve in Figure 2 and Figure 3) are predominantly consequences of the competition among different reaction channels in ^{16}O and ^{28}Si with various cross-sections and threshold energy as described above.

We note here the importance of treating all reactions for a given target nuclide with a consistent cross-section library. Figure 27 and Figure 28 present the evaluated cross - sections for neutron reacctions in the ENDF/B-VI and ENDL99 libraries, respectively. While the total cross-sections from the two libraries are very close (Figure 29), the individual cross-sections differ because the two libraries may partition individual physical processes among the various cross-sections in different ways. For example, ENDL99 defines a $^{16}\text{O}(\text{n},\text{n}\alpha)$ reaction. ENDF/B-VI instead folds that reaction into the cross-section for the inelastic reaction, $^{16}\text{O}(\text{n},\text{n}')$, and treats the $^{16}\text{O}(\text{n},\text{n}\alpha)$ reaction as two separate physical processes: (i) inelastic neutron scattering and promotion of the oxygen nuclide to an excited state, and (ii) alpha-decay of the excited state of ^{16}O to ^{12}C , which

is not included in scope of MCNP and is therefore not included in this work. The different shapes of the $^{16}\text{O}(\text{n},\text{n}'\gamma)$ cross-section curves from the two libraries above the $^{16}\text{O}(\text{n},\text{n}\alpha)$ threshold reflect the different treatments of this process.

Effect of composition variations

The calculations described above are easily generalized for variations in ground composition. As an example we consider the effect of water inclusion in granite. Figure 31 shows that the elastic cross-sections for ^1H , ^{16}O , and ^{28}Si are comparable in magnitude over the range of incident neutron energies considered in this work. Figure 32 shows that the capture cross-sections for ^1H and ^{28}Si are comparable in magnitude over the same range of neutron energies, except for resonances in the ^{28}Si capture cross-section. Figure 22 shows the energy deposition into granite from 14MeV incident neutrons increases monotonically with increasing water concentration from 68% to 72% of the total source energy for realistic variations in water content up through 5 weight percent. Figure 23 displays the variation of the two processes most susceptible to changing water content: elastic scattering and neutron capture. The occurrence of both processes per incident neutron energy fluence rises monotonically with water content for ^1H target nuclei and falls monotonically for ^{16}O and ^{28}Si target nuclei in the granite. We have seen above that elastic scattering from ^{16}O tended to promote reflection of neutrons and therefore to suppress energy deposition in the granite. However, the close mass match of the incident neutrons and the ^1H nuclei would tend to impart more kinetic energy to the hydrogen nuclei than to oxygen. Therefore, enhancement of elastic scattering from hydrogen at the expense of scattering from oxygen would be expected to enhance overall energy deposition in the granite.

Generation of hazardous radioisotopes

The radionuclides produced by neutron activation of ground constituents fall into two categories, each of which presents a different hazard. The short-lived isotopes, with half-lives of the order of hours and minutes, present a direct radiation hazard while they remain radioactive. Isotopes with longer half-lives can enter the food chain and therefore present a longer-term hazard. Representatives of both classes are included in the

calculations. In this work we calculate only the production of radioisotopes which can be generated by neutron irradiation of the simplified granite formulation. Other nuclides can be generated by neutron irradiation of trace elements, which can be added to calculations for specific environments as appropriate.

The figures in Appendix B present plots of all of the evaluated cross-sections available for the reactions represented in Table 3, organized by product nuclide. Figure 24 presents the results of MCNP calculations for the generation of each of the hazardous radioisotopes for which cross-sections involving the target nuclei in our simplified granite are available in the standard libraries. The energy-dependence of production of each nuclide is generally a result of the types of reactions included. A steady or slightly-falling curve in Figure 24 generally suggests domination by a capture reaction, whereas a sharply-rising curve suggests a threshold reaction. For example, the calculation of ^{45}Ca production includes two reactions, $^{44}\text{C}(\text{n},\gamma)$ and $^{48}\text{Ti}(\text{n},\alpha)$. The former is a capture reaction with a cross-section which decreases monotonically with increasing neutron energy above 1MeV. The latter reaction has a threshold above 6MeV, corresponding to the rise in ^{45}Ca production in granite for incident neutron energies above 6MeV.

Summary

Using a simplified model for the interaction of energetic neutrons with granite and the MCNP code, we find that the energy-dependence of energy deposition by neutrons in granite follows from a balance of competing nuclear reactions primarily involving ^{16}O and ^{28}Si targets. Incorporation of water in the granite enhances energy deposition. The strong dependence of the quantities of certain radionuclides generated by neutron irradiation on the energy of the incident neutrons follows from the energy-dependence of the cross-sections of the various reaction channels which contribute to production of each radionuclide.

Acknowledgments

The authors are grateful to T. Scott Carman, D. Dearborn, T. Hoover, and P. Stry, and T. Thomson for helpful discussions, to D. McNabb and M. McKinley for assistance with access to nuclear data, and to L. Chase and R. Harding for assistance with the code.

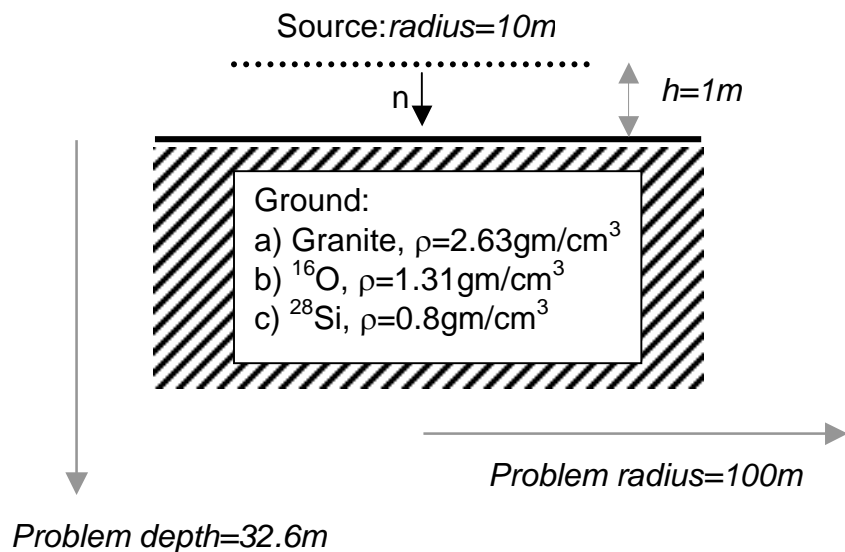
Figures

Figure 1: Test problem geometry.

**Neutron Energy Deposition in Granite
From a Plane Source 1m above Surface**
Calculated with MCNP

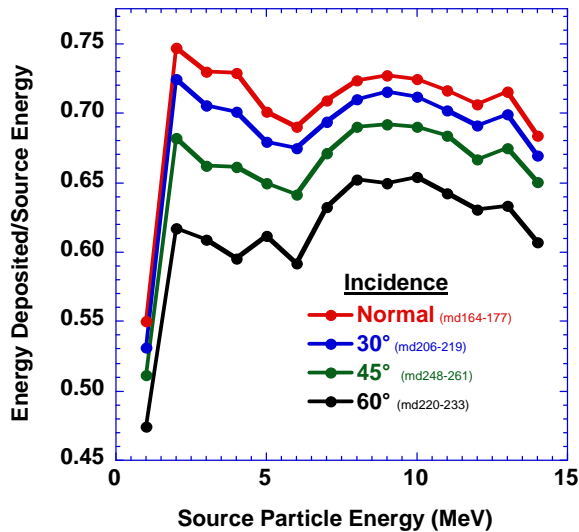


Figure 2: Calculated cumulative energy deposition into granite from monoenergetic, planar neutron sources with incident angles as indicated. Note zero suppression on the vertical scale.

**Neutron Energy Deposition
From a Plane Source 1m above Surface**
Calculated with MCNP

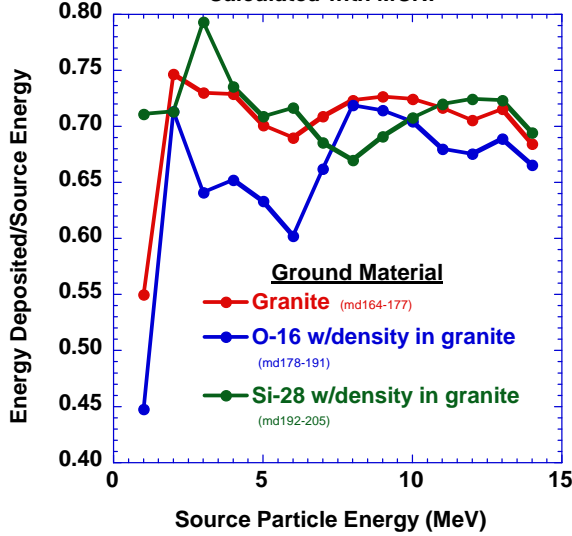


Figure 3: Calculated cumulative energy deposition into granite and into the principal atomic components of granite individually from monoenergetic, planar neutron sources and normal incidence.

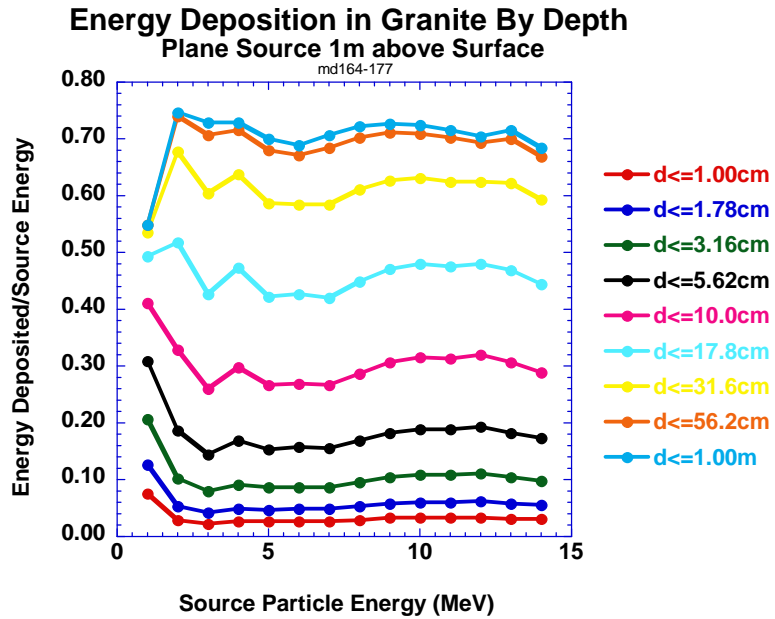


Figure 4: Calculated cumulative energy deposition into granite by depth. This and all subsequent plots involve neutrons at normal incidence.

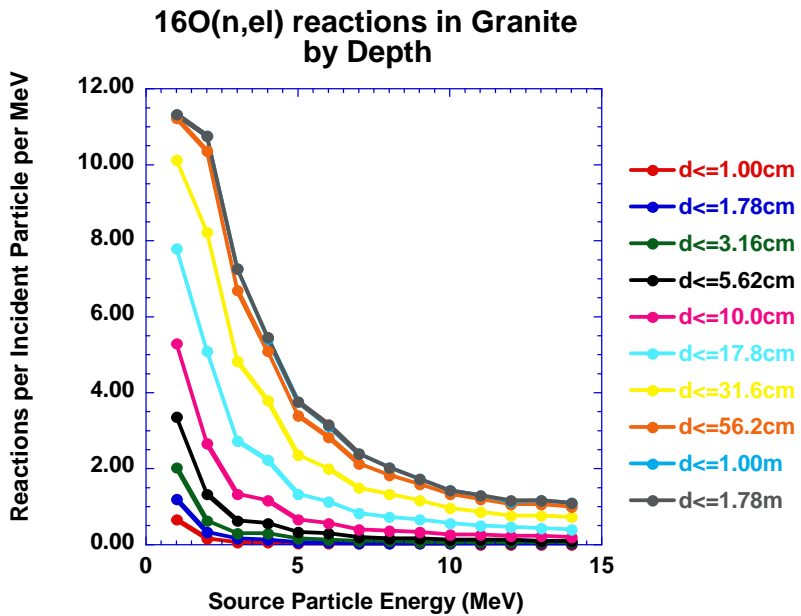


Figure 5: Calculated $^{16}\text{O}(\text{n},\text{elastic})$ reactions in granite by depth for normal incidence.

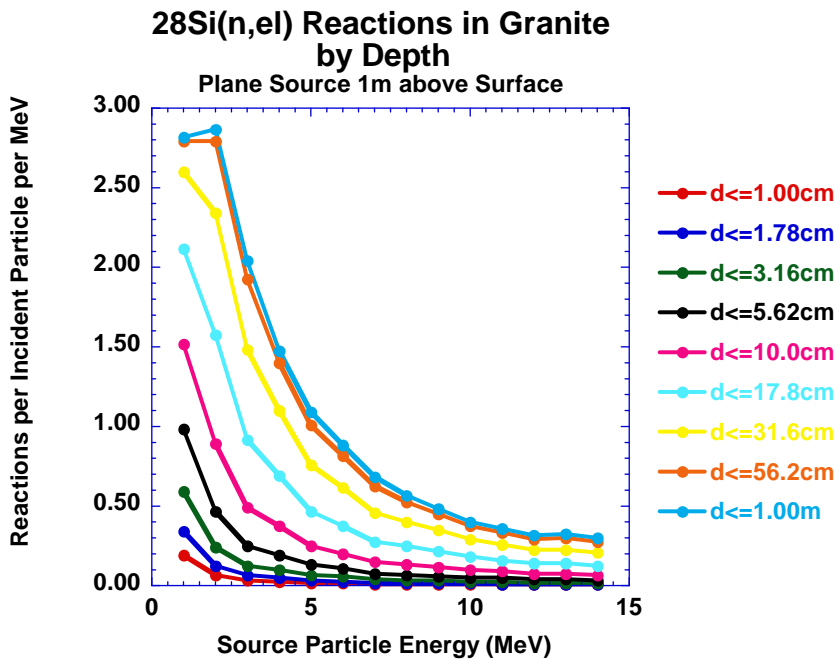


Figure 6: Calculated $^{28}\text{Si}(\text{n},\text{elastic})$ reactions in granite by depth.

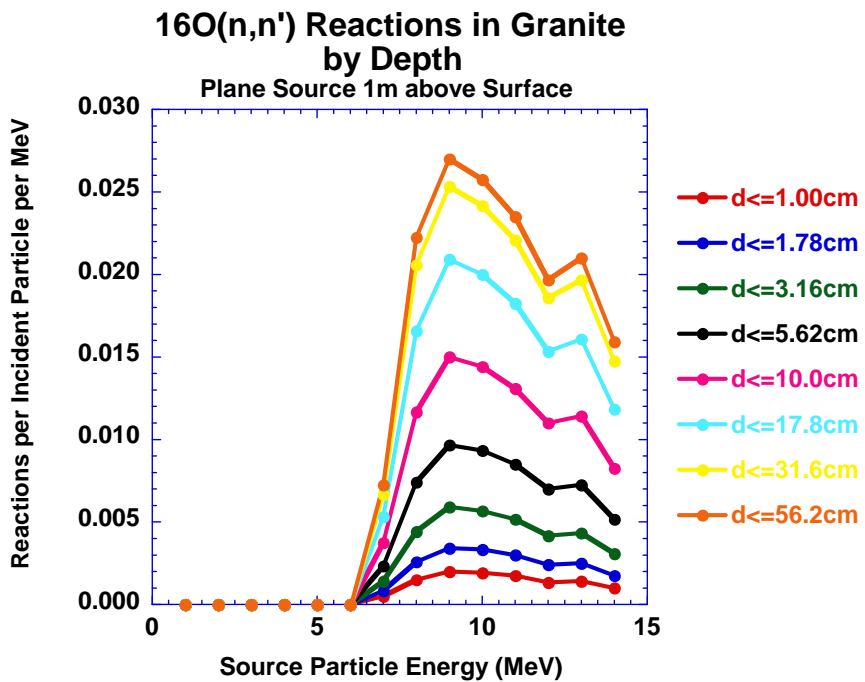


Figure 7: Calculated inelastic reactions of neutrons and ^{16}O in granite by depth.

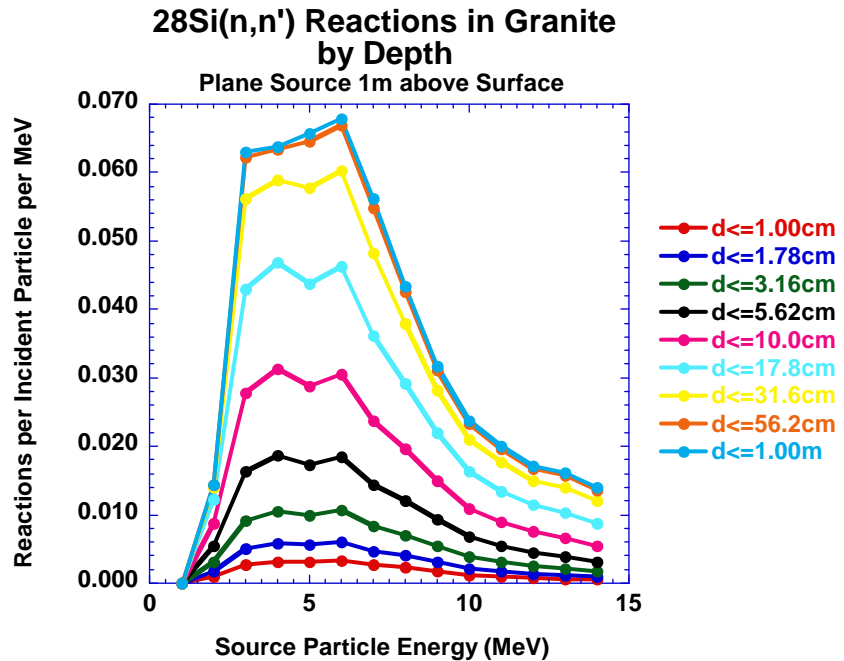


Figure 8: Calculated inelastic reactions of neutrons and ^{28}Si in granite by depth.

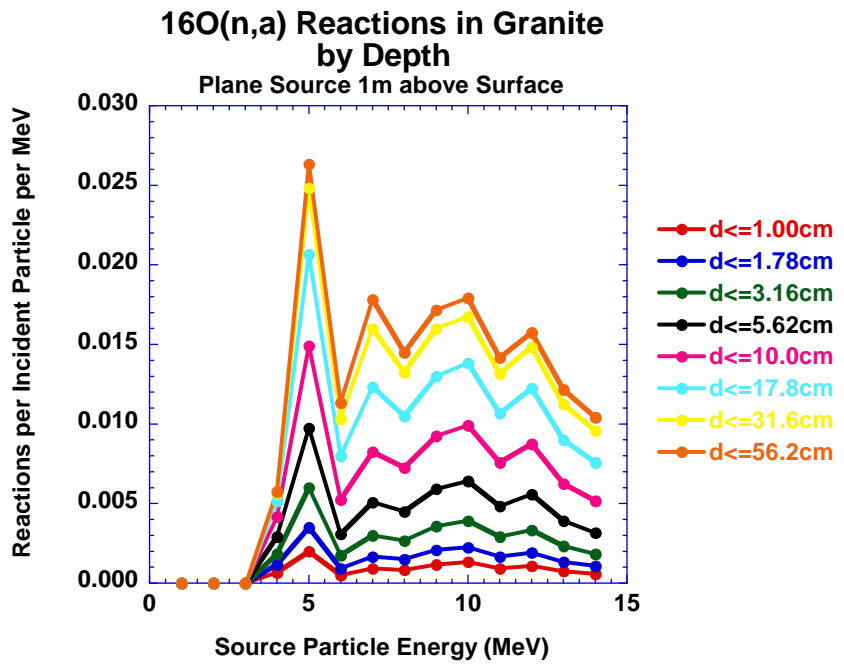


Figure 9: Calculated $^{16}\text{O}(\text{n},\alpha)$ reactions in granite by depth.

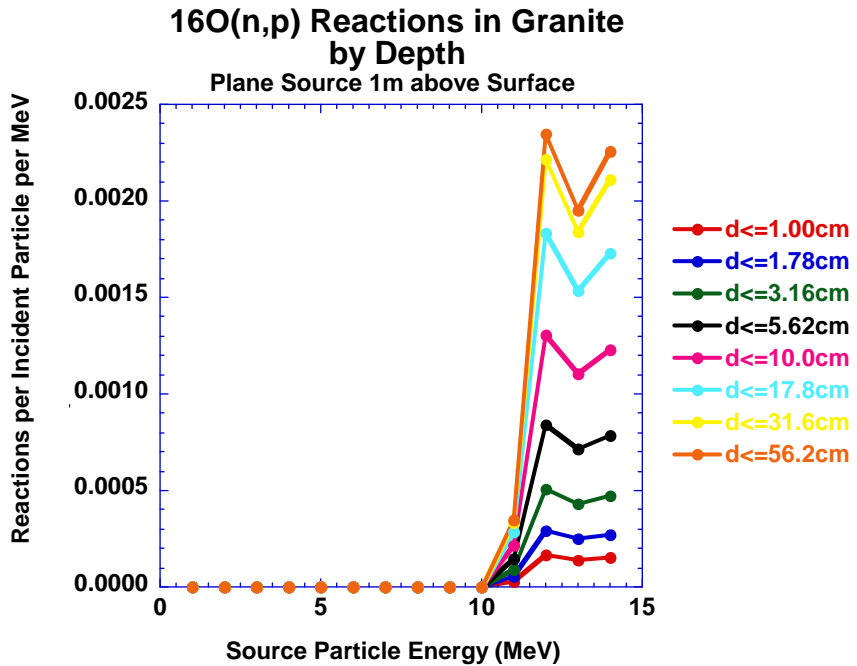


Figure 10: Calculated $^{16}\text{O}(\text{n},\text{p})$ reactions in granite by depth.

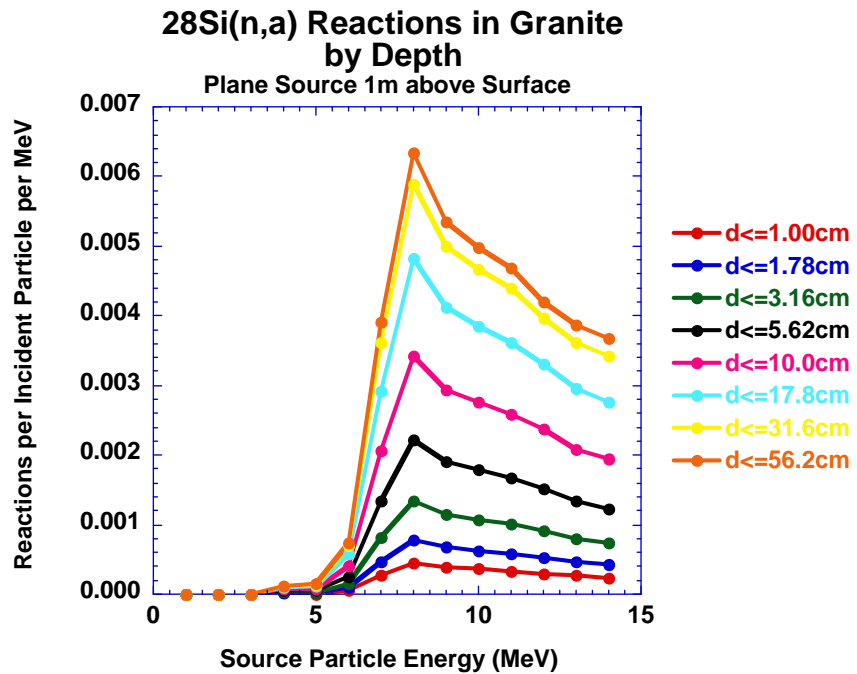


Figure 11: Calculated $^{28}\text{Si}(\text{n},\alpha)$ reactions in granite by depth.

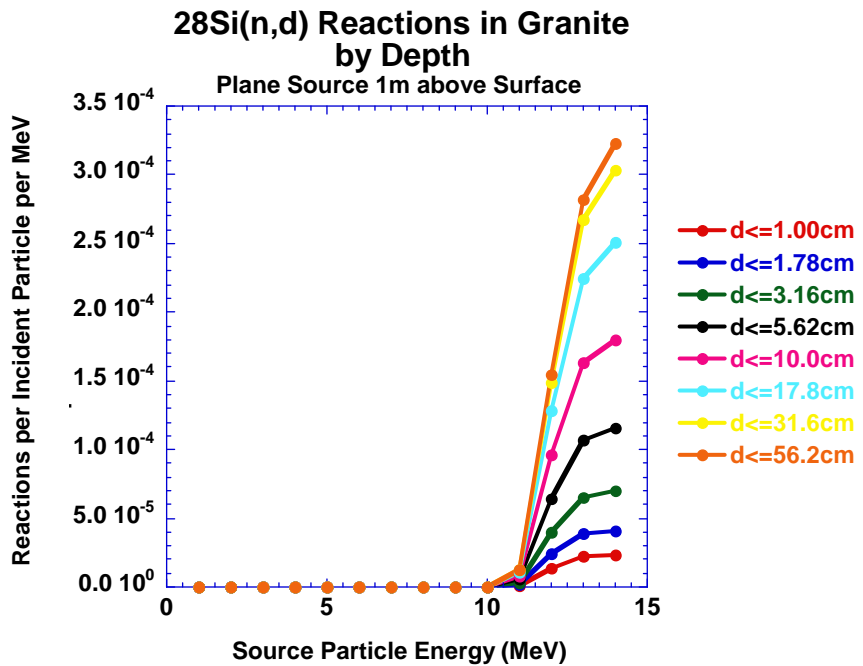


Figure 12: Calculated $^{28}\text{Si}(n,\text{d})$ reactions in granite by depth.

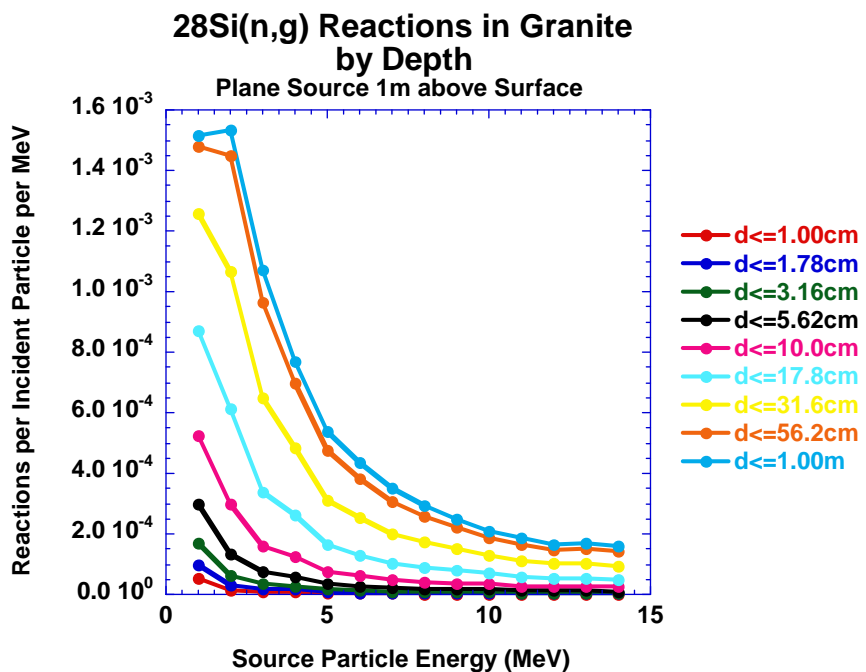


Figure 13: Calculated $^{28}\text{Si}(n,\gamma)$ reactions in granite by depth.

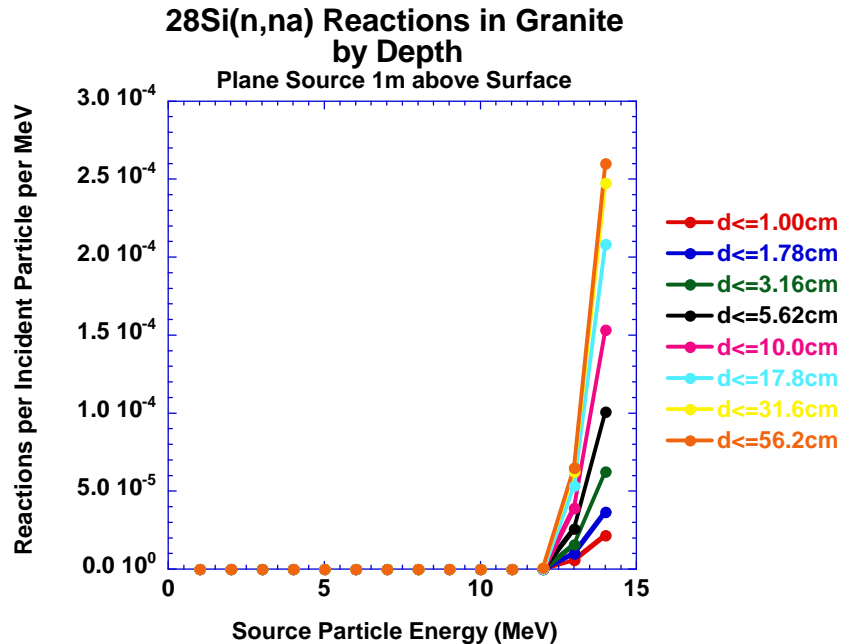


Figure 14: Calculated $^{28}\text{Si}(n,\text{n}\alpha)$ reactions in granite by depth.

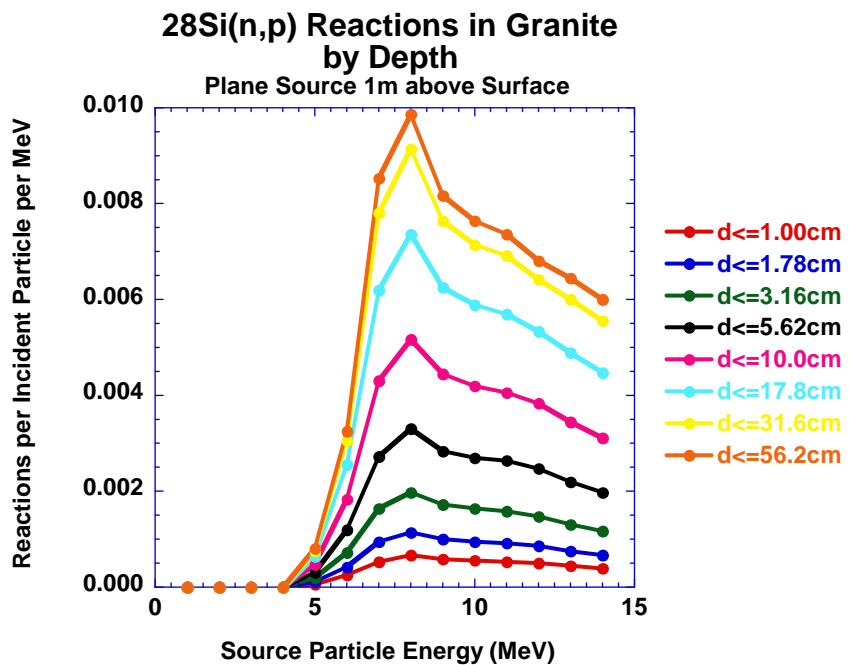


Figure 15: Calculated $^{28}\text{Si}(n,p)$ reactions in granite by depth.

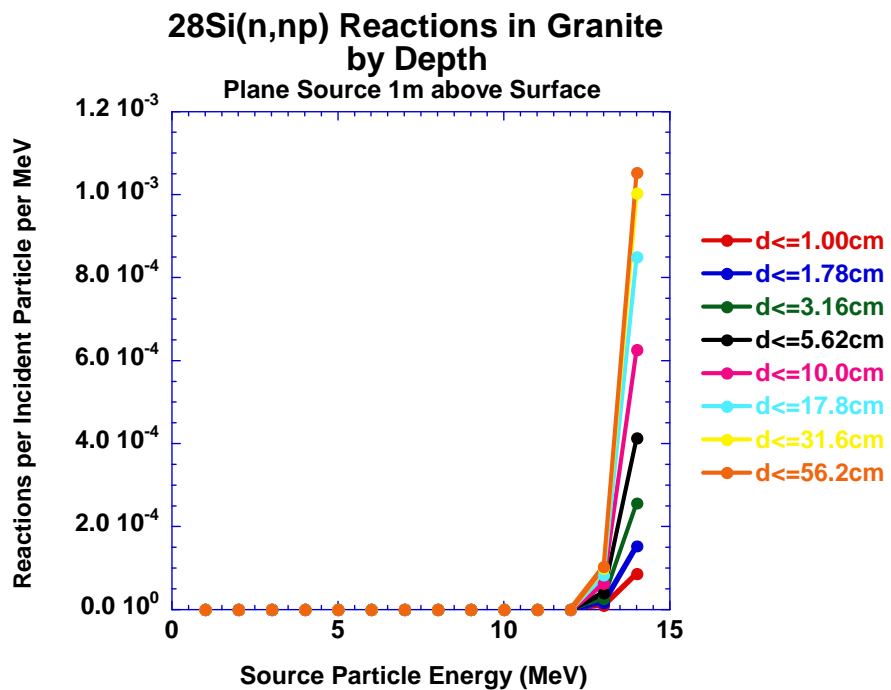


Figure 16: Calculated $^{28}\text{Si}(n,np)$ reactions in granite by depth.

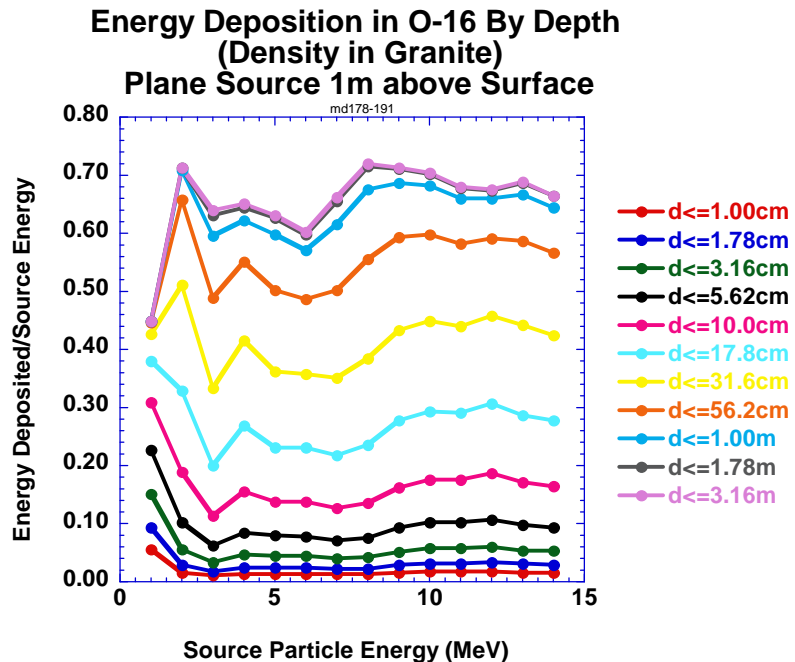


Figure 17: Calculated energy deposition by depth into the ^{16}O component of granite only. Other components are removed from the problem.

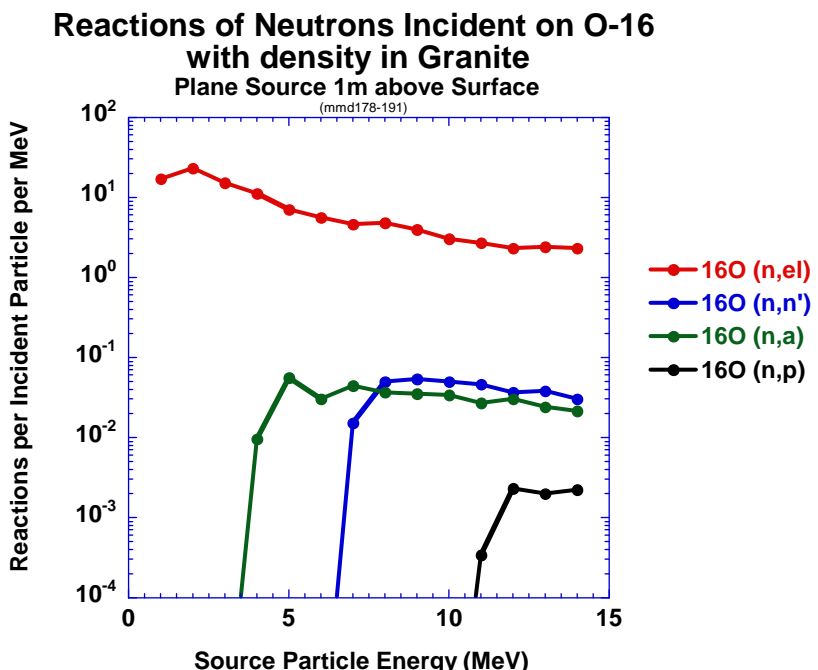


Figure 18: Calculated, total neutron reactions by depth into the ^{16}O component of granite only. Other components are removed from the problem.

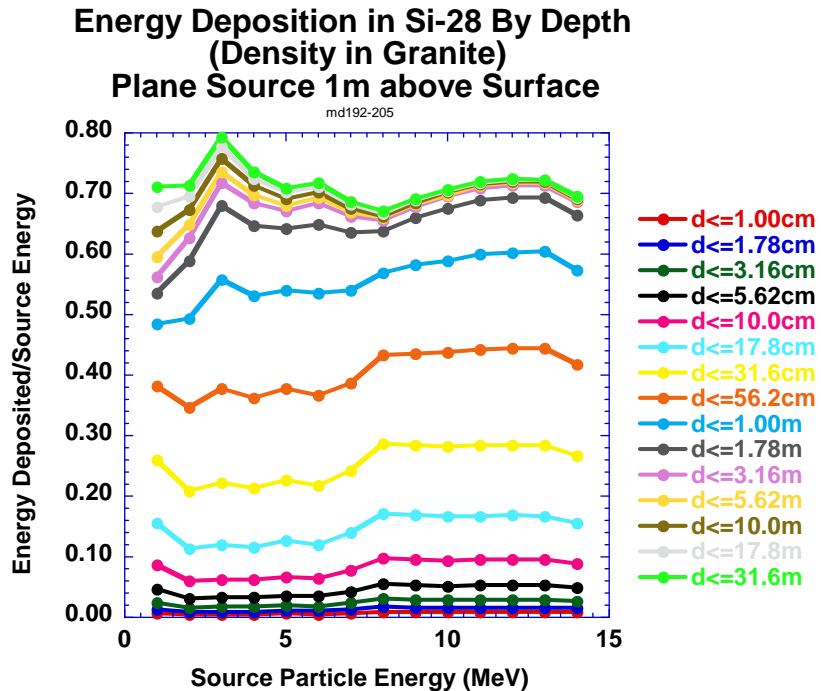


Figure 19: Calculated energy deposition by depth into the ^{28}Si component of granite only. Other components are removed from the problem.

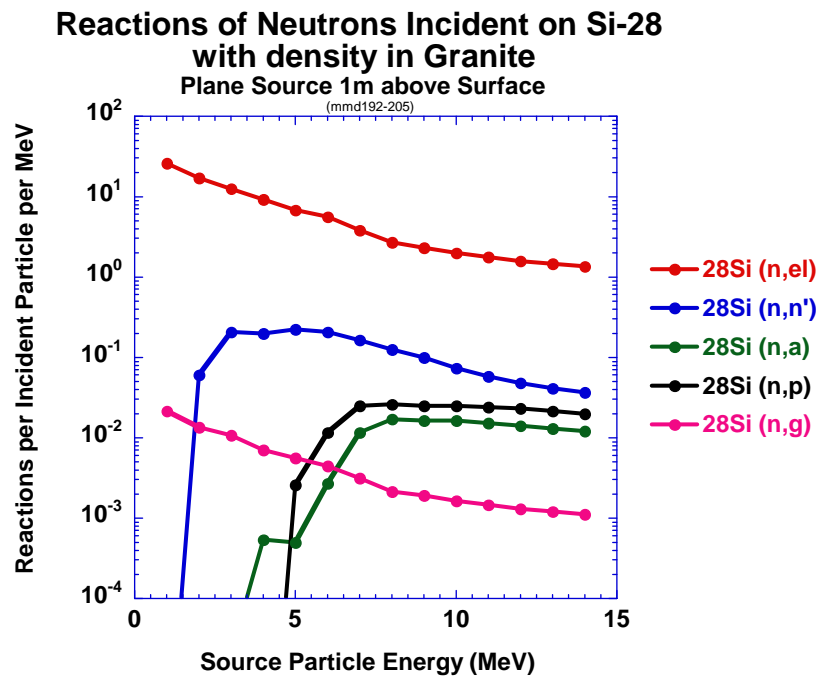


Figure 20: Calculated, total neutron reactions by depth into the ^{28}Si component of granite only. Other components are removed from the problem.

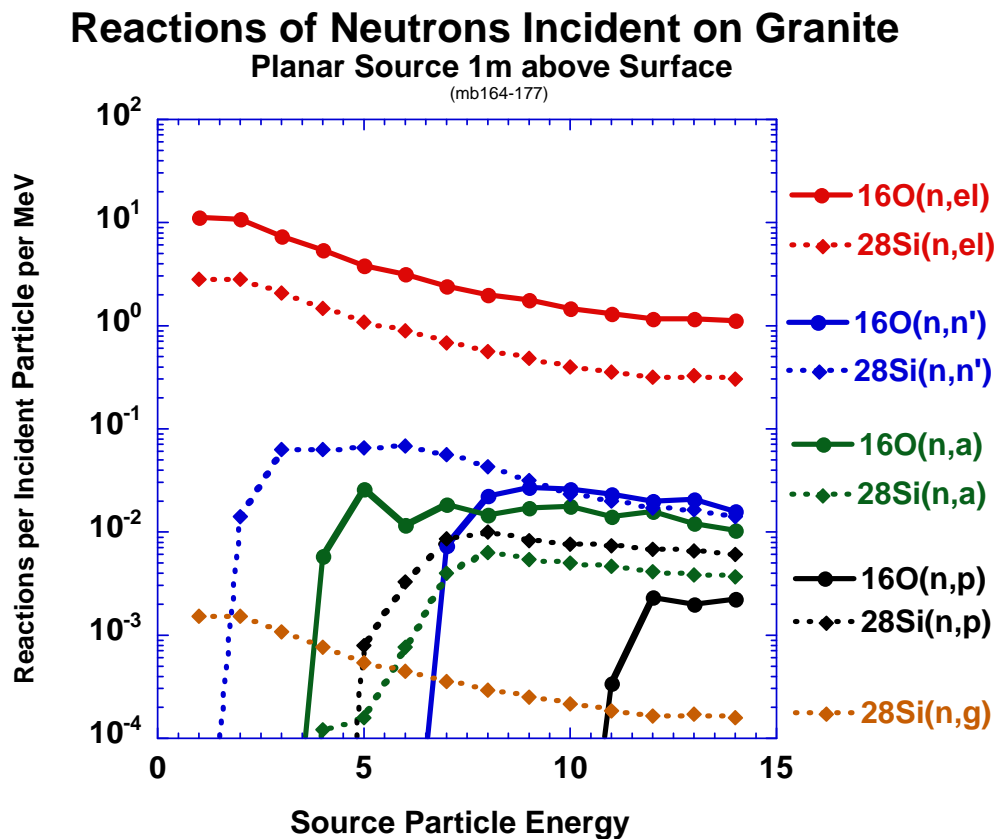


Figure 21: Summary of the dominant reactions for neutrons incident on granite.
 Reactions involving ^{16}O are represented with solid curves, while reactions involving ^{28}Si are represented with dashed curves.

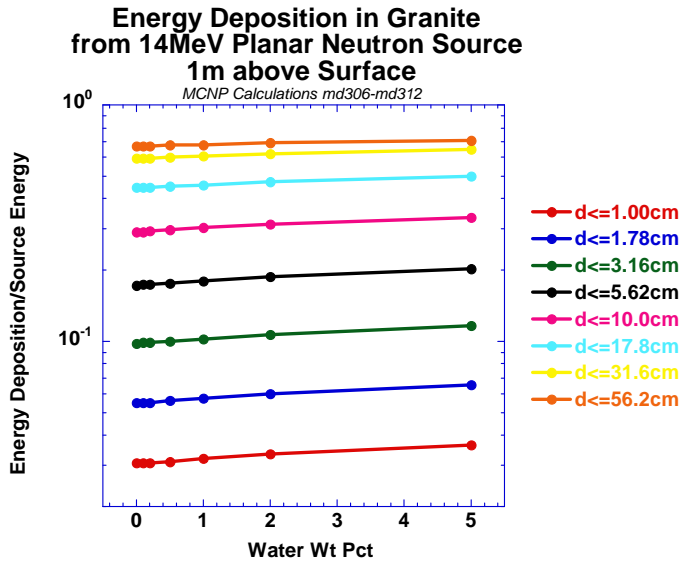


Figure 22: Calculated energy deposition by depth in granite vs. percentage of added water.

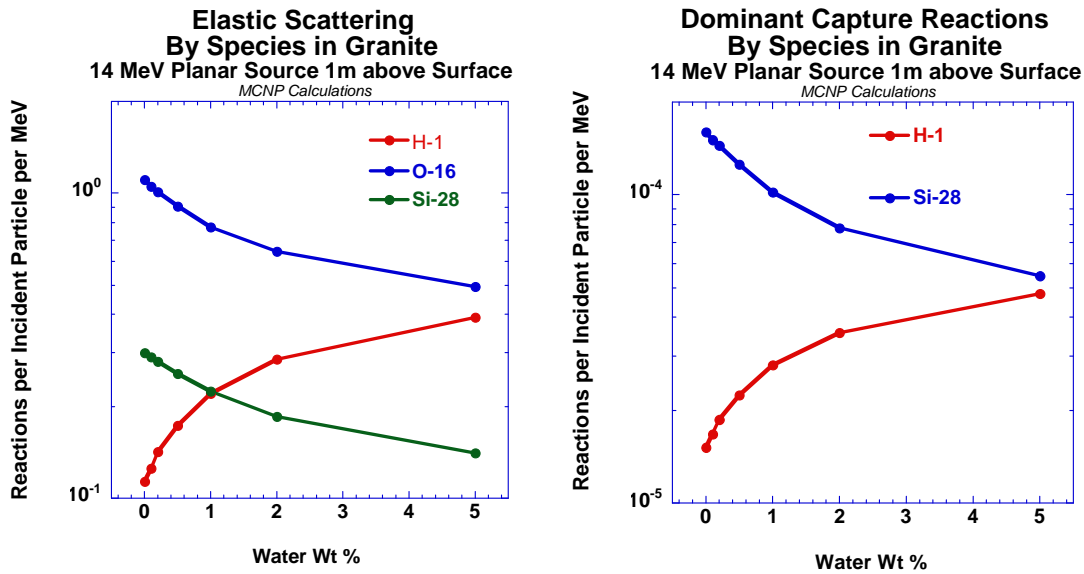


Figure 23: Effects of added water on neutron reactions in granite.

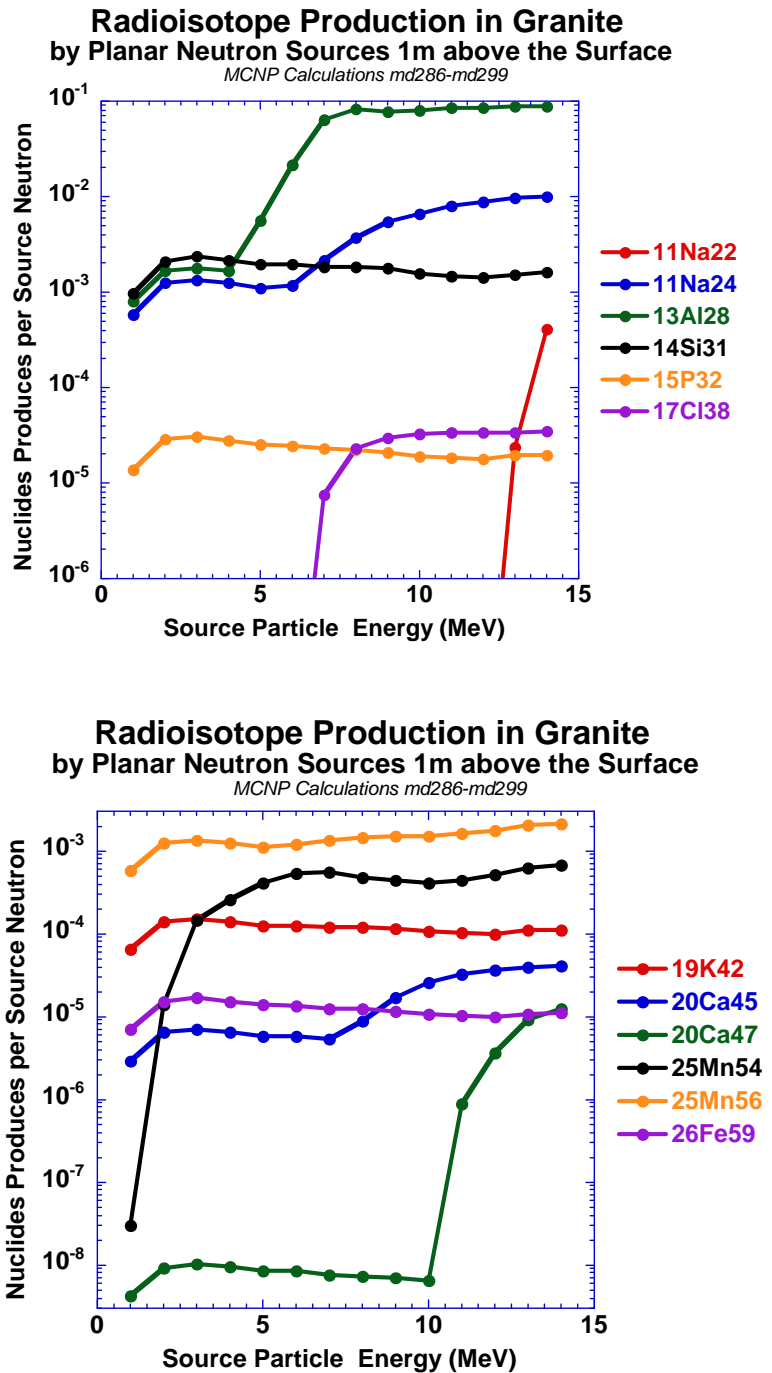


Figure 24: Total production of specific radioisotopes in granite from planar, monoenergetic neutron sources.

Tables

Simplified granite composition.

<u>Species</u>	<u>Wt Fraction</u>	<u>Wt Fraction in Earth's Crust¹¹</u>	<u>Wt Fraction of pure SiO₂</u>
H	0.00093	0.0014	
O	0.49813	0.461	0.533
Na	0.02582	0.0236	
Mg	0.00528	0.0233	
Al	0.07661	0.0823	
Si	0.32751	0.282	0.467
P	0.00083	0.00105	
K	0.02258	0.0209	
Ca	0.01421	0.0415	
Ti	0.00234	0.00565	
Mn	0.00093	0.000095	
Fe	0.02483	0.0563	

Density= 2.63gm/cm³

Table 1: Composition of simplified granite used in this study. The calculations reflect the natural isotopic abundances for each element.

¹¹ Source: CRC Handbook of Chemistry and Physics (Boca Raton: CRC Press, 1998), p. 14-14.

Residual Radionuclides and their decay properties.

<u>Radionuclide</u>	<u>Half-Life</u>	<u>Decay Prod.</u>	<u>Half-Life</u>	<u>Decay Prod.</u>			
6 C	14	5730y	7 N	14			
11 Na	22	2.62y	10 Na	22			
11 Na	24	15h	12 Mg	24			
13 Al	28	2.3m	14 Si	28			
14 Si	31	2.62h	15 P	31			
14 P	32	24d	16 S	32			
17 Cl	38	37.3m	18 Ar	38			
19 K	42	12.36h	20 Ca	42			
20 Ca	45	165d	21 Sc	45			
20 Ca	47	4.535d	21 Sc	47	3.44d	22 Ti	47
25 Mn	54	303d	24 Cr	54			
25 Mn	56	2.576h	26 Fe	56			
26 Fe	59	44.6d	27 Co	59			
27 Co	60	5.26y	28 Ni	60			
28 Ni	65	2.56h	29 Cu	65			
29 Cu	64	12.8h	30 Zn	64 (or 28Ni64)			
30 Zn	65	245d	29 Cu	65			
38 Sr	89	52d	39 Y	89			
39 Sr	91	9.7h	39 Y	91	58d	40 Zr	91

Table 2: Radionuclides included in published lists of contaminant nuclides which may be created by neutron irradiation of ground. Those nuclides shown in red are radioactive. Note that not all of these radionuclides can be produced from the isotopes included in the simplified granite of Table 1, but they may be produced by neutron reactions with trace elements.

Channels with available cross-sections for producing residual radionuclides.

Product	Library	Target	Rxn	Product	Library	Target	Rxn
C-14	ENDFb6	N-15	(n,np)	Ca-47	ACTL	Ca-48	(n,2n)
C-14	ENDL92	C-13	(n,g)	Ca-47	ACTL	Ca-46	(n,g)
C-14	ENDFb6	N-14	(n,p)	Ca-47	ENDFb6	Ti-50	(n,a)
C-14	ENDFb6	N-15	(n,d)	Mn-54	ENDFb6	Mn-55	(n,2n)
C-14	ENDFb6	O-17	(n,a)	Mn-54	ENDFb6	Fe-54	(n,p)
Na-22	ENDFb6	Na-23	(n,2n)	Mn-54	ENDFb6	Fe-56	(n,t)
Na-24	ENDFb6	Na-23	(n,g)	Mn-56	ENDFb6	Fe-57	(n,np)
Na-24	ENDFb6	Mg-24	(n,p)	Mn-56	ENDFb6	Mn-55	(n,g)
Na-24	ENDFb6	Al-27	(n,a)	Mn-56	ENDFb6	Fe-56	(n,p)
Al-28	ENDFb6	Si-29	(n,np)	Mn-56	ACTL	Fe-58	(n,t)
Al-28	ENDFb6	Al-27	(n,g)	Mn-56	ENDFb6	Co-59	(n,a)
Al-28	ENDFb6	Si-28	(n,p)	Fe-59	ENDFb6	Fe-58	(n,g)
Al-28	ENDFb6	P-31	(n,a)	Fe-59	ENDFb6	Co-59	(n,p)
Si-31	ENDFb6	Si-30	(n,g)	Fe-59	ENDFb6	Ni-62	(n,a)
Si-31	ENDFb6	P-31	(n,p)	Co-60	ENDFb6	Ni-61	(n,np)
Si-31	ACTL	S-34	(n,a)	Co-60	ENDFb6	Co-59	(n,g)
P-32	ACTL	S-33	(n,np)	Co-60	ENDFb6	Ni-60	(n,p)
P-32	ENDFb6	P-31	(n,g)	Co-60	ACTL	Ni-61	(n,d)
P-32	ENDFb6	S-32	(n,p)	Co-60	ACTL	Ni-62	(n,t)
P-32	ACTL	S-33	(n,d)	Co-60	ENDFb6	Cu-63	(n,a)
P-32	ACTL	Cl-35	(n,a)	Ni-65	ENDFb6	Ni-64	(n,g)
Cl-38	ACTL	Cl-37	(n,g)	Ni-65	ENDFb6	Cu-65	(n,p)
Cl-38	ACTL	Ar-38	(n,p)	Ni-65	ACTL	Zn-68	(n,a)
Cl-38	ACTL	K-41	(n,a)	Cu-64	ENDFb6	Cu-65	(n,2n)
K-42	ACTL	K-41	(n,g)	Cu-64	ENDFb6	Cu-63	(n,g)
K-42	ACTL	Ca-42	(n,p)	Cu-64	ACTL	Zn-64	(n,p)
K-42	ACTL	Ca-43	(n,d)	Zn-65	ACTL	Zn-66	(n,2n)
K-42	ENDFb6	Sc-45	(n,a)	Zn-65	ACTL	Zn-64	(n,g)
Ca-45	ACTL	Ca-46	(n,2n)	Sr-89	ENDFb6	Sr-88	(n,g)
Ca-45	ACTL	Ti-49	(n,na)	Sr-89	ENDFb6	Zr-92	(n,a)
Ca-45	ACTL	Ca-44	(n,g)	Sr-90	ACTL	Zr-94	(n,na)
Ca-45	ENDFb6	Sc-45	(n,p)	Sr-91	ENDFb6	Zr-94	(n,a)
Ca-45	ENDFb6	Ti-48	(n,a)	Sr-93	ENDFb6	Zr-96	(n,a)

Table 3: Available cross-sections for producing each of the radionuclides listed in Table 2. The reactions included in calculations described in this work are highlighted in yellow. Those which are not highlighted involve target nuclides which are not included in the simplified granite formulation considered here.

Residual Radionuclides with their parent chains and half-lives.

Radionuclides produced by decays from parent chains.

denotes production cross-section availability.

Product	Half-Life	Parent	Half-Life	Parent	Half-Life	Parent	Half-Life	Parent	Half-Life
C-14	5730y	B-14	13.8ms	Be-14	4.35ms				
		N-18	624ms	C-18	95ms				
				C-19	46ms				
Na-22	2.6019y	Al-23	0.47s						
		Mg-22	3.857s	Al-22	70ms	Si-22	6ms		
Na-24	14.959h	Ne-24	3.38m	F-24	0.34s	O-24	61ms		
				F-25	59ms				
Al-28	2.2414m	Mg-28	20.9h	Na-28	30.5ms	Ne-28	17ms		
				Na-29m	44.9ms	Ne-29	0.2s		
Si-31	157.3m	Al-31	644ms	Mg-31	230ms	Na-31	17ms		
				Mg-32	120ms	Na-32	13.2ms		
						Na-32	13.2ms		
						Na-33	8.2ms		
P-32	14.262d	Si-32	150y	Al-32	33ms	Mg-32	120ms	Na-32	13.2ms
						Mg-33	90ms	Na-33	8.2ms
								Na-33	8.2ms
								Na-34	5.5ms
Cl-38	37.24m	S-38	170.3m	P-38	0.64s				
				P-39	0.16s				
K-42	12.36h	Ar42	32.9y	Cl-42	6.8s	S-42	0.56s	P-42	110ms
						S-43	220ms	P-43	33ms
								P-43	33ms
Ca-45	162.61d	K-45	17.3m	Ar-45	21.48s	Cl-45	400ms	S-45	82ms
						Cl-46	223ms		
Ca-47	4.536d	K-47	17.5s	Ar-47	700ms	Cl-47	>200ns		
		K-48	6.8s						
Mn-54	312.3d								
Mn-56	2.5785h	Cr-56	5.94m						
Fe-59	44.503d	Mn-59	4.6s	Cr-59	0.74s	V-59	130ms		
Co-60	5.2714y	Fe-60	1.5e6y	Mn-60	51s	Mn-60m	1.77s		
						Cr-60	0.57s		
Ni-65	2.5172h	Co-65	1.2s	Fe-65	0.4s	Mn65	110ms		
Cu-64	12.7h								
Zn-65	244.26d	Ga-65	15.2m	Ge-65	30.9s	As-65	0.19s	Se-65	<50ms
Sr-89	50.53d	Rb-89	15.15m	Kr-89	3.15m	Br-89	4.348s	Se-89	0.41s
						Br-90	1.91s	Se-91	0.27s
Sr-90	28.78y	Rb-90	158s	Kr-90	3.32m	Br-90	1.91s	Se-91	0.27s
				Rb-90m	258s	Br-91	0.541s	Se-91	0.27s
Sr-91	9.63h	Rb-91	58.4s	Kr-91	8.57s	Br-91	0.541s	Se-91	0.27s
				Kr-92	1.84s	Br-92	0.343s		
						Br-92	0.343s		
				Rb-92	4.492s	Br-93	102ms		
						Br-92	0.343s		
						Br-93	102ms		
						Br-93	102ms		
						Br-94	70ms		
Sr-93	7.423m	Rb-93	5.84s	Kr-93	1.286s	Br-93	102ms		
				Kr-94	0.2s	Br-94	70ms		
				Rb-94	2.702s	Kr-94	0.2s	Br-94	70ms

Table 4: Parent decay chains.

Appendix A: Cross-Sections for Neutron Transport

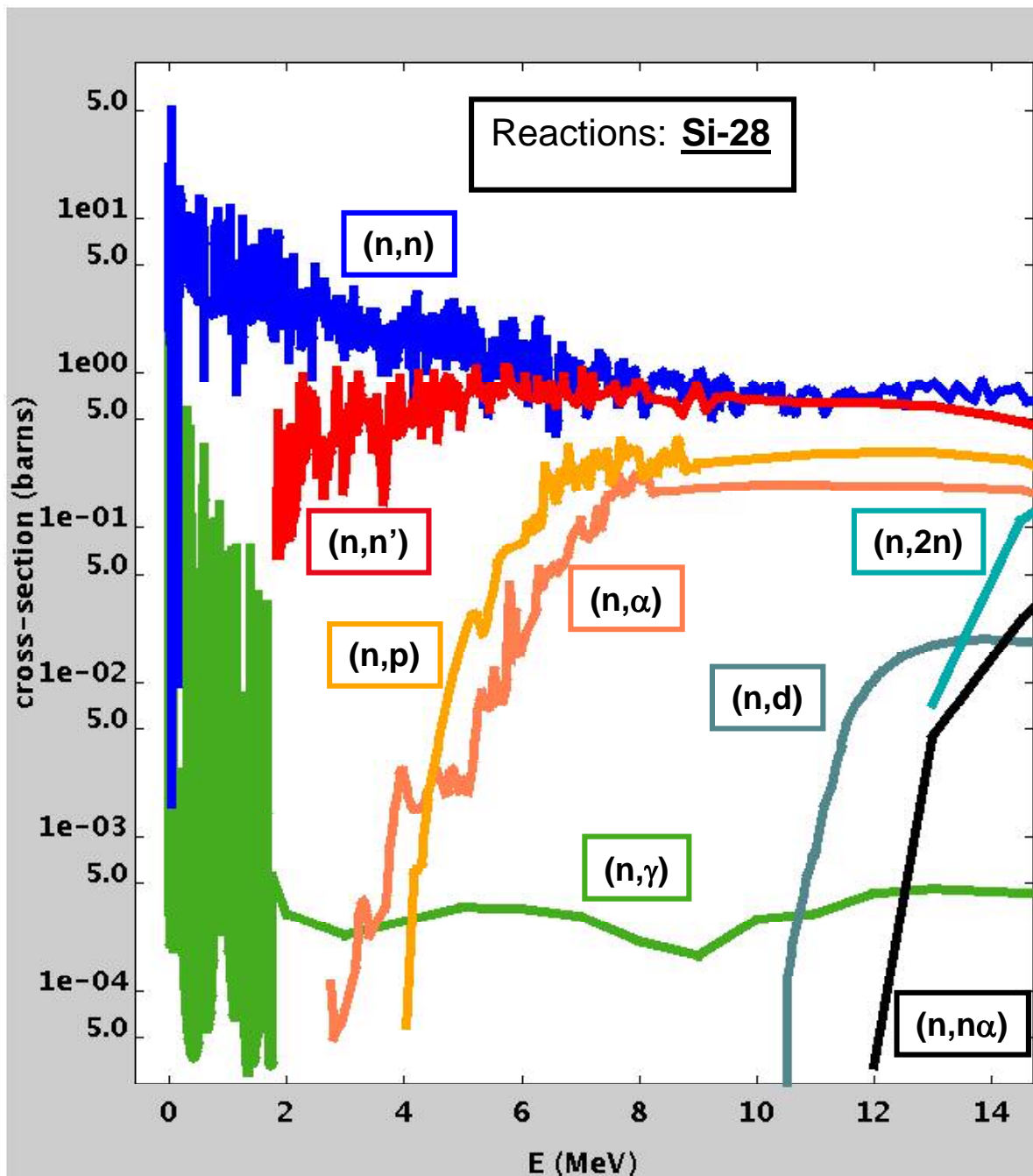


Figure 25: (Appendix A) Neutron cross-sections for target ^{28}Si from ENDF/B-VI.8.

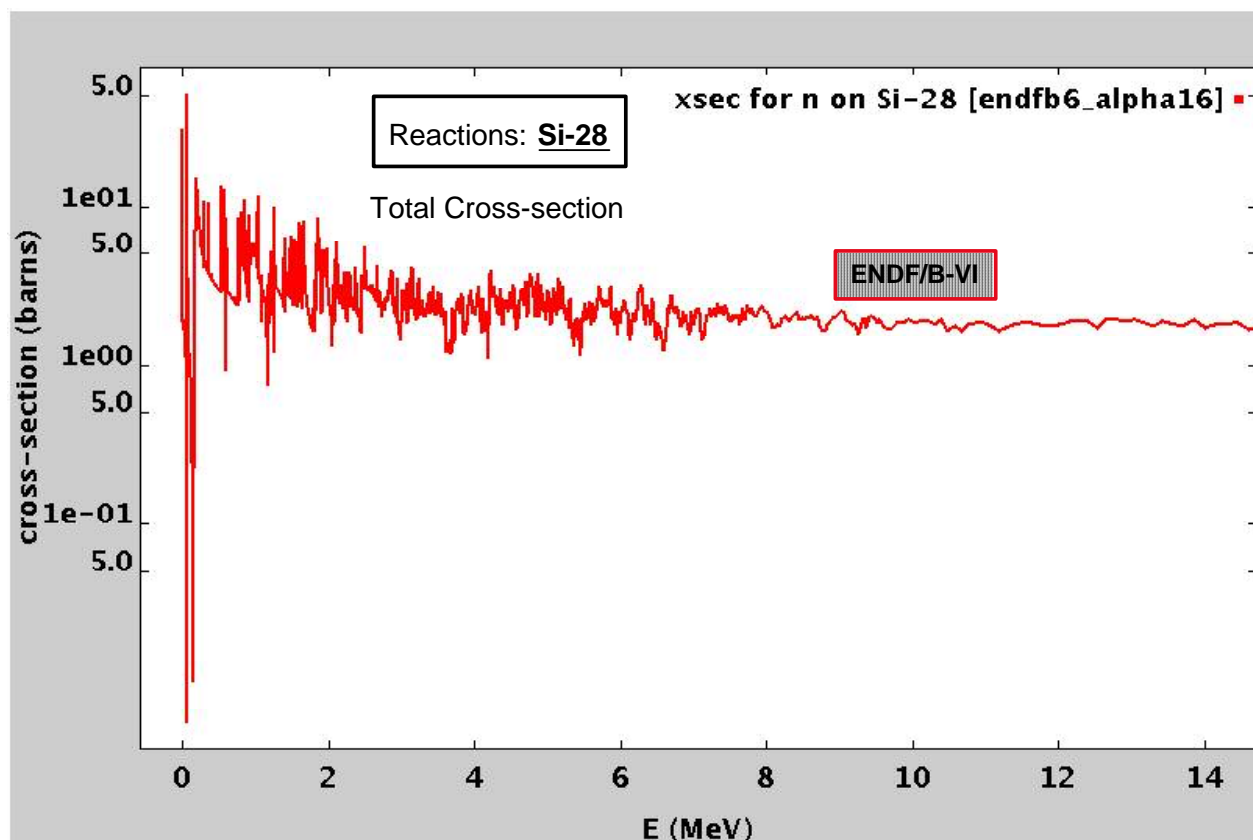


Figure 26: (Appendix A) Total Cross Section for neutrons incident on ^{28}Si , from ENDF/B-VI.8

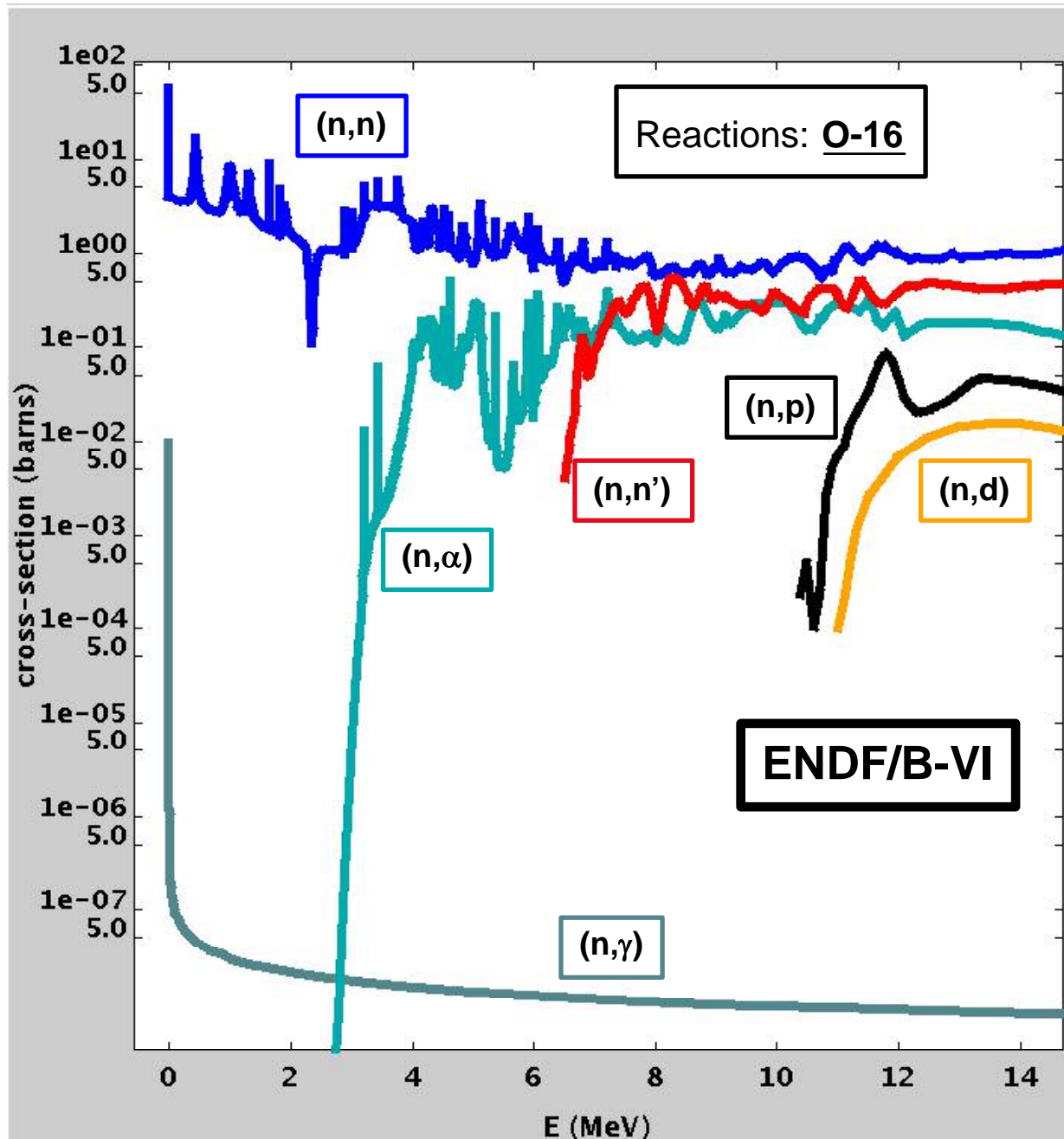


Figure 27: (Appendix A) Neutron cross-sections for target ^{16}O from ENDF/B-VI.8.

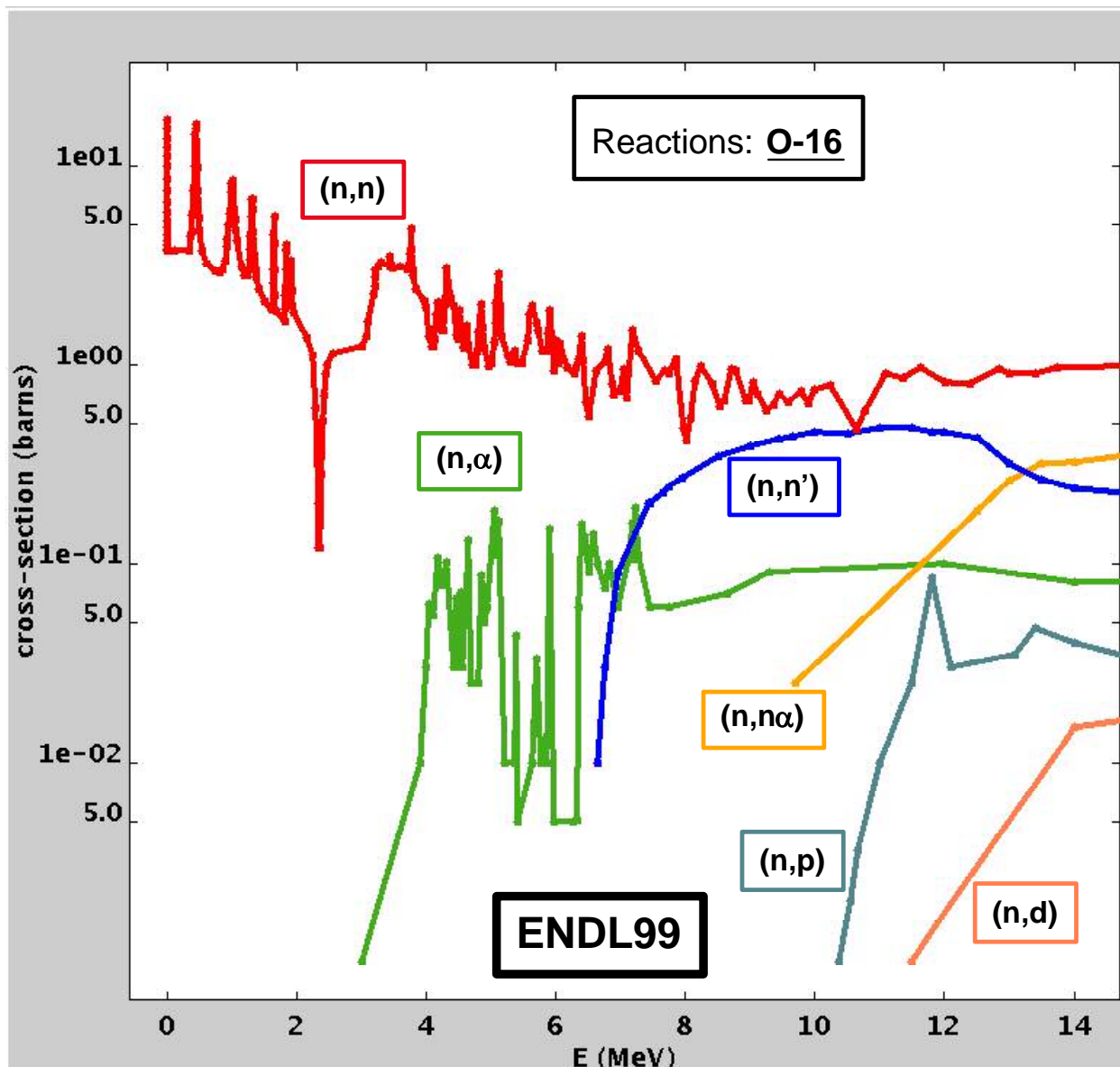


Figure 28: (Appendix A) Neutron cross-sections for target ^{16}O from ENDL99.

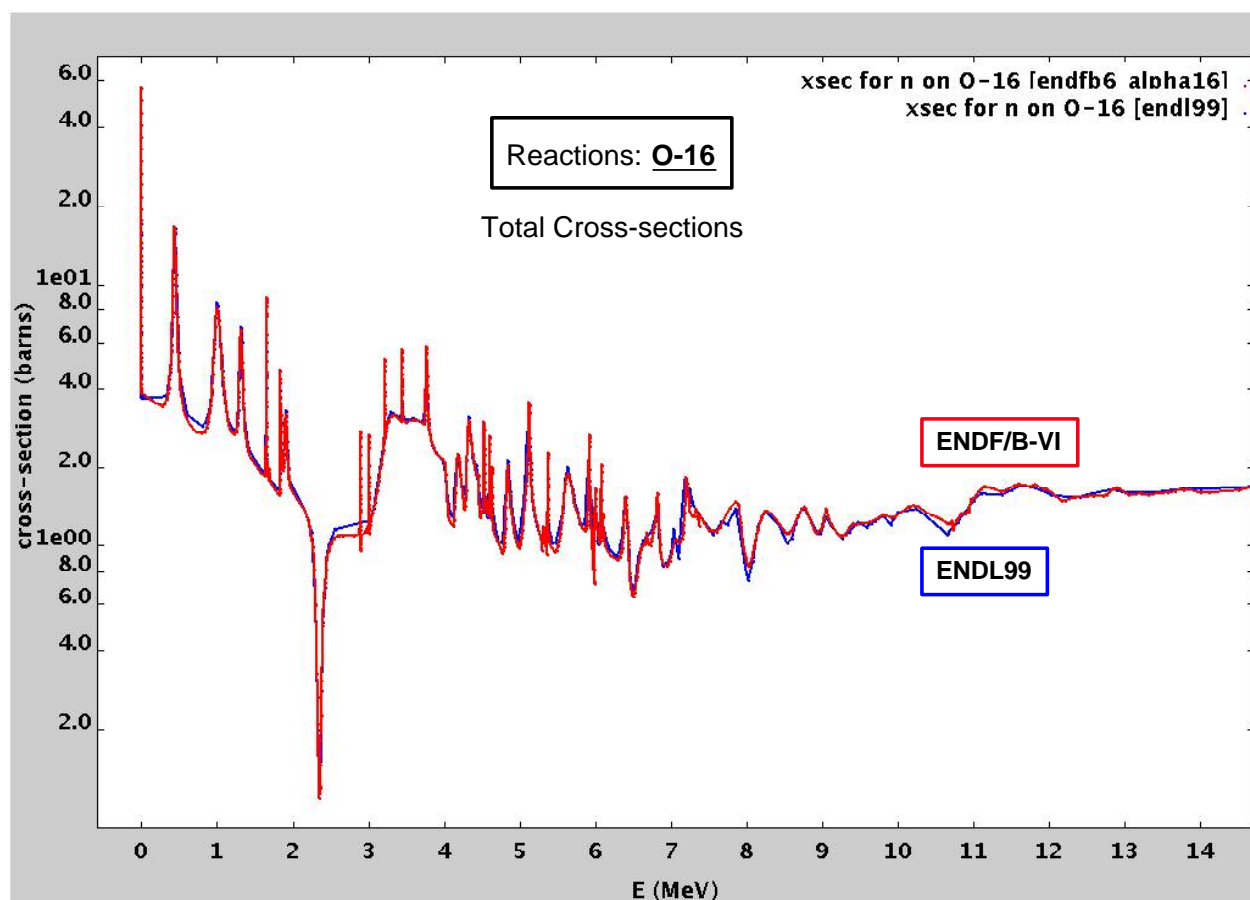


Figure 29: (Appendix A) Total Cross Section for neutrons incident on ${}^{16}\text{O}$, from both ENDF/B-VI.8 and ENDL99.

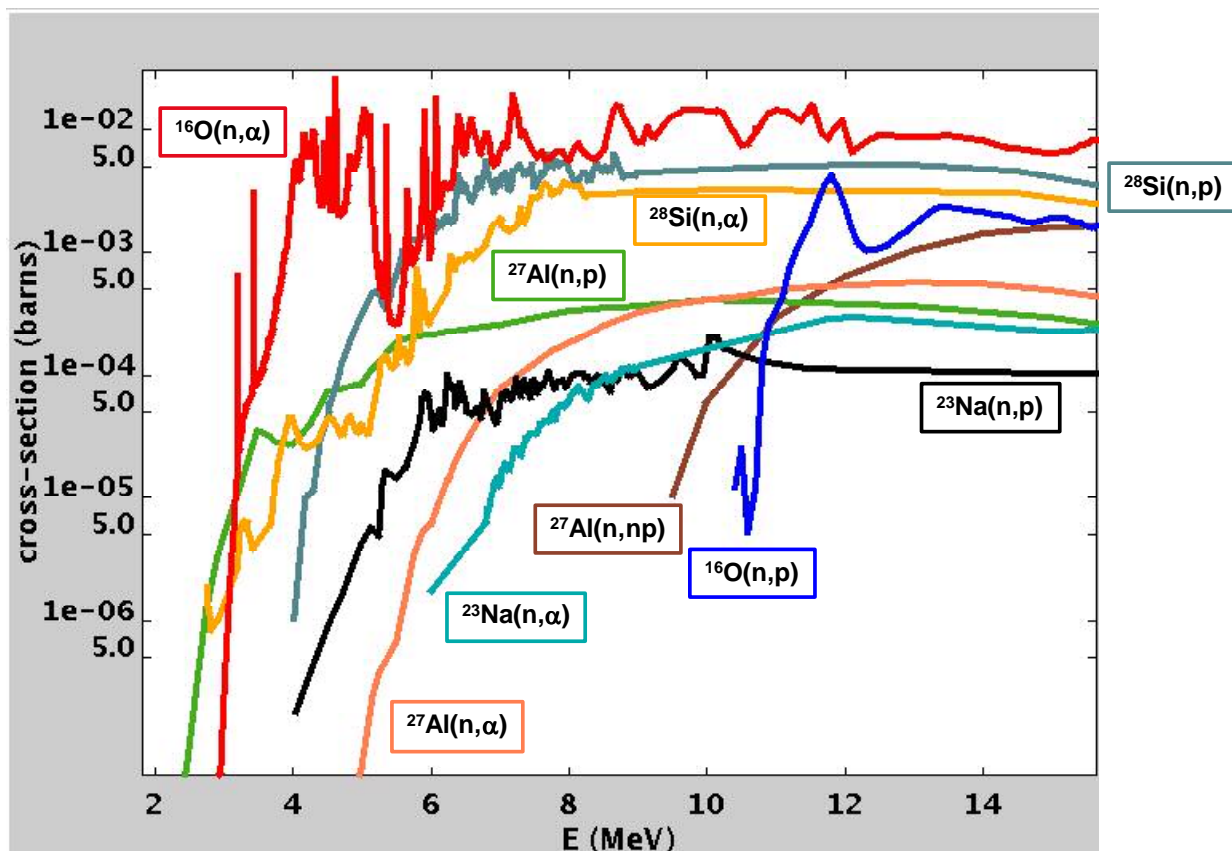


Figure 30: (Appendix A) ENDF/B-VI cross-sections for dominant transmutation reactions in granite, *WEIGHTED BY THE ATOMIC COMPOSITIONS IN GRANITE*. The vertical scale is the cross section multiplied by the number of atoms/barn-cm of the target nuclide.

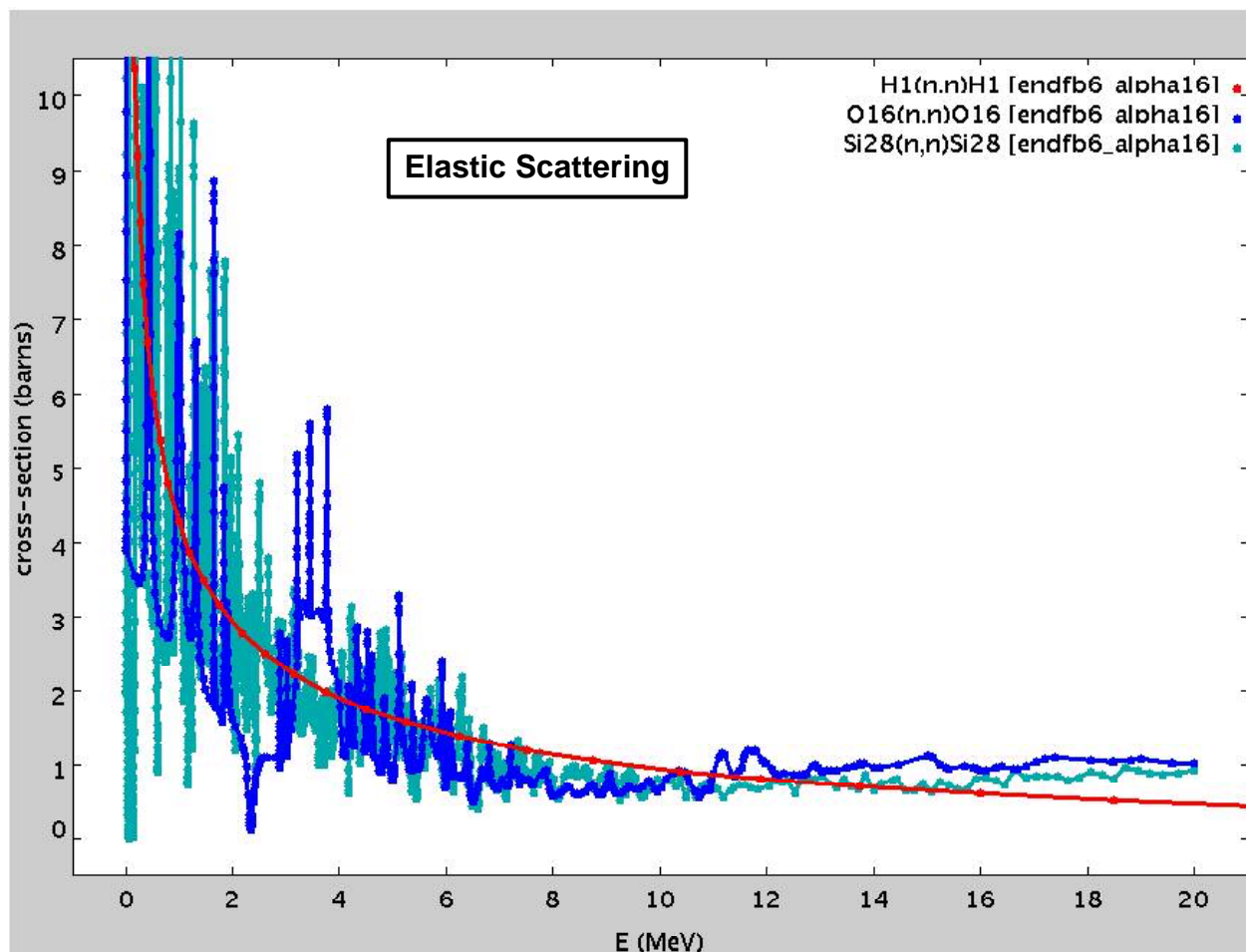


Figure 31: (Appendix A) Neutron elastic cross-sections for 1H , ^{16}O , and ^{28}Si .

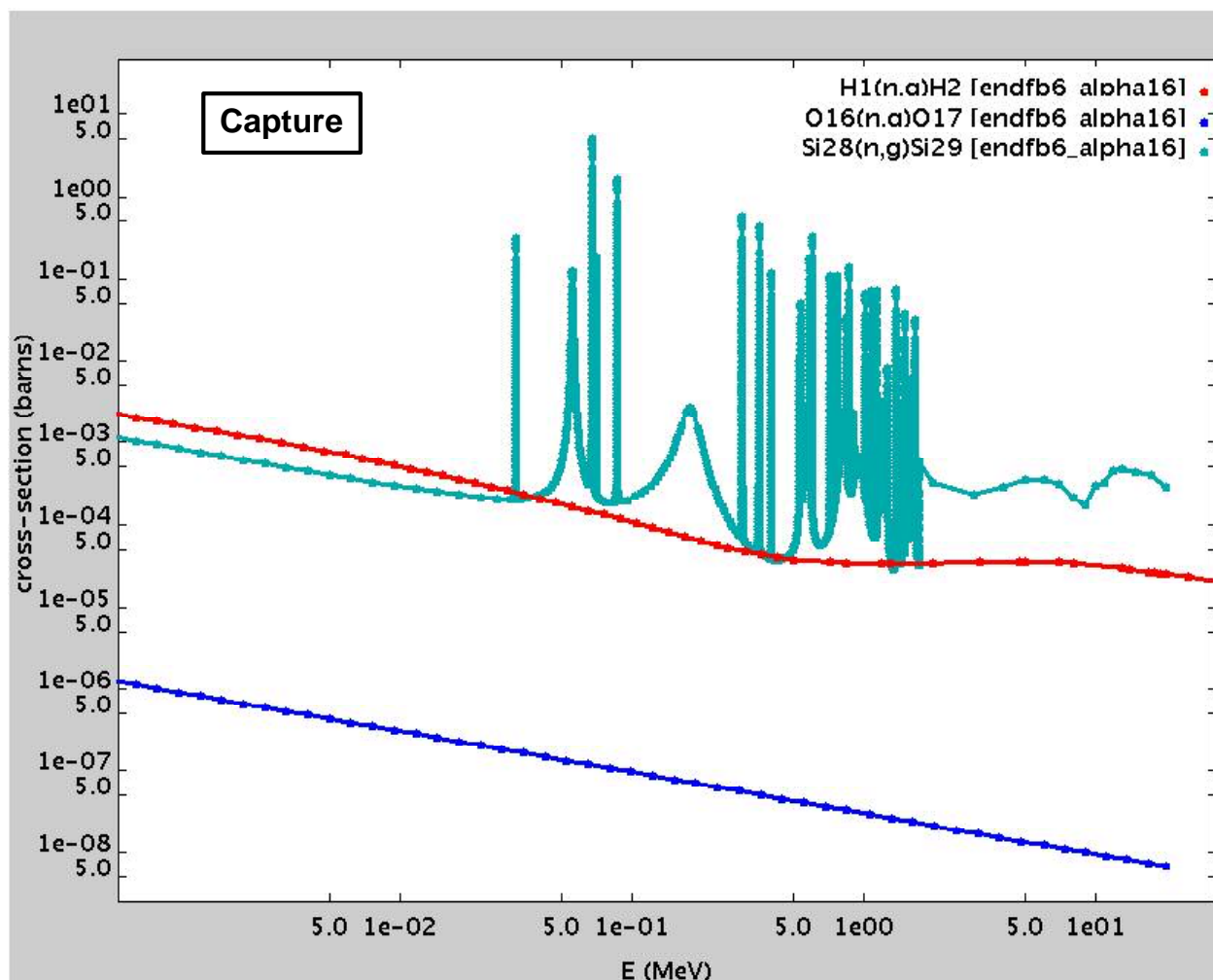
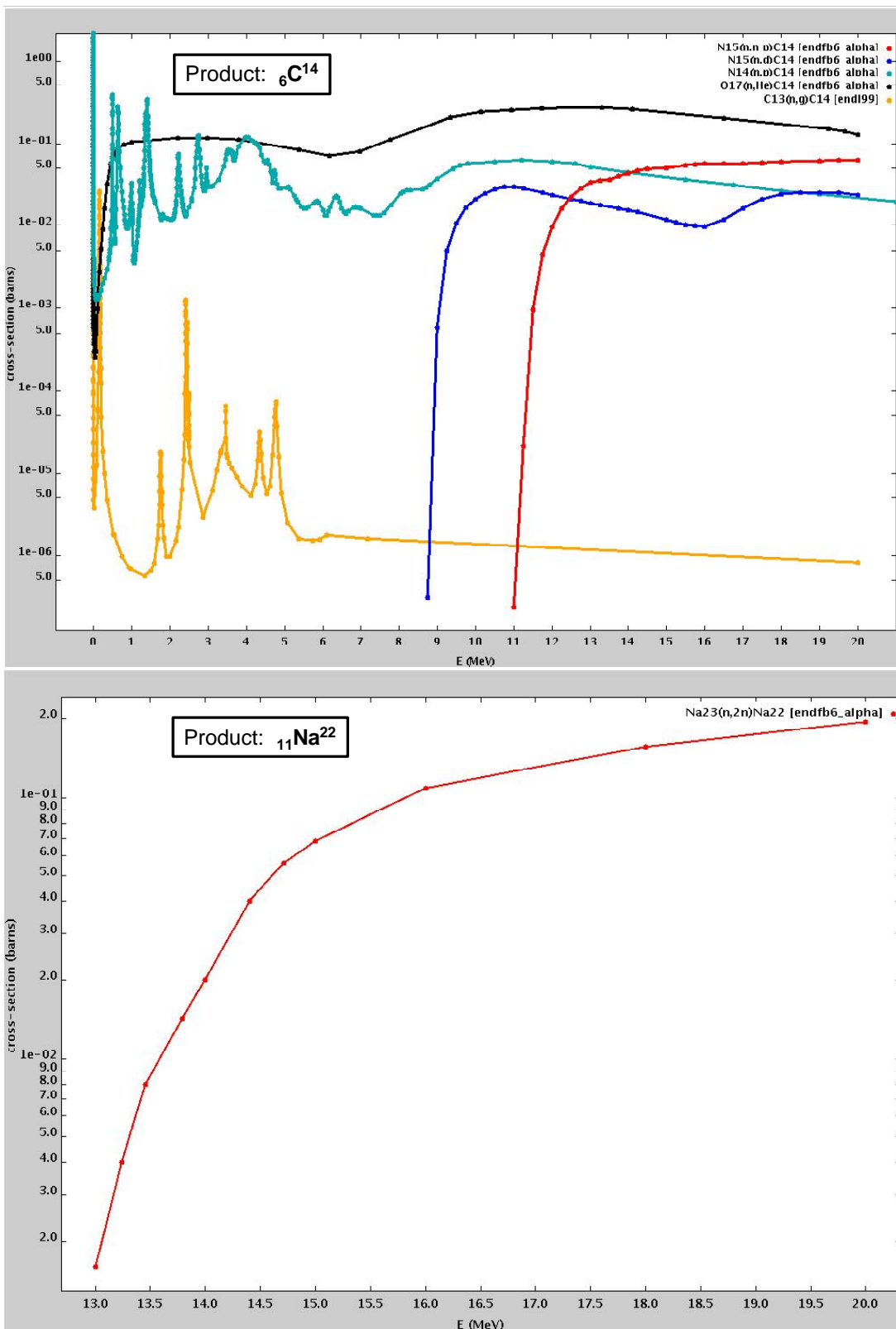
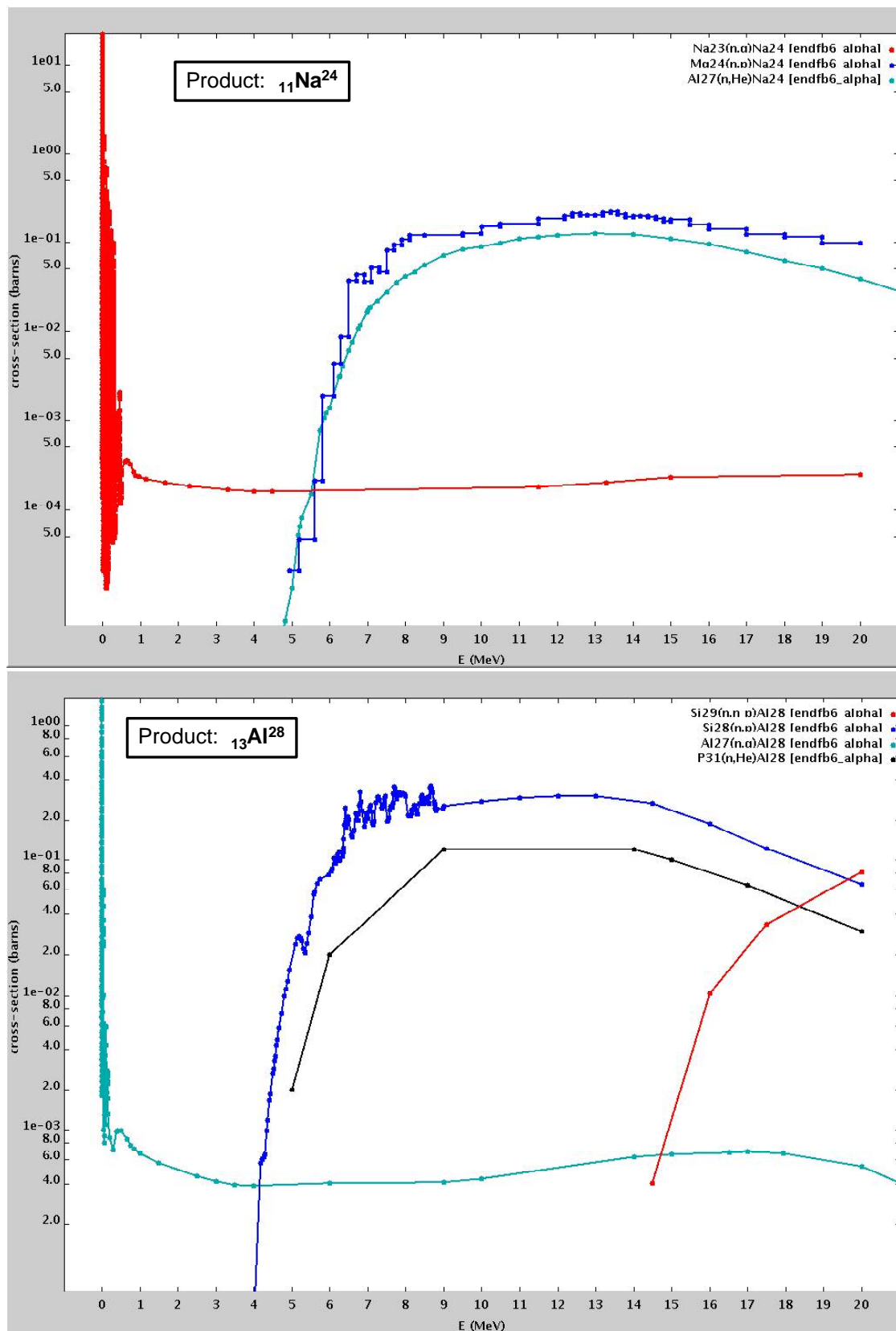
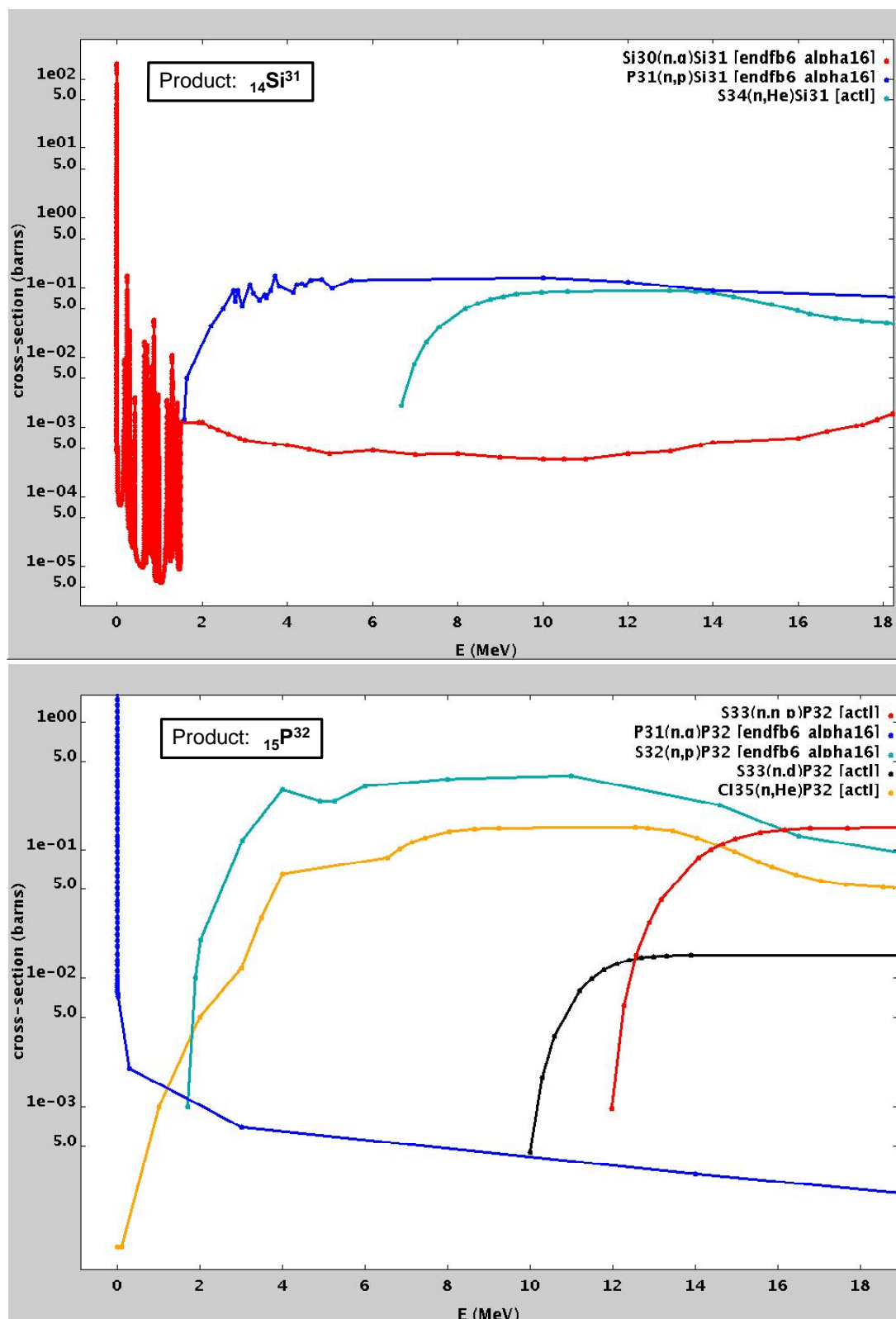


Figure 32: (Appendix A) Capture cross-sections for 1H , ^{16}O , and ^{28}Si .

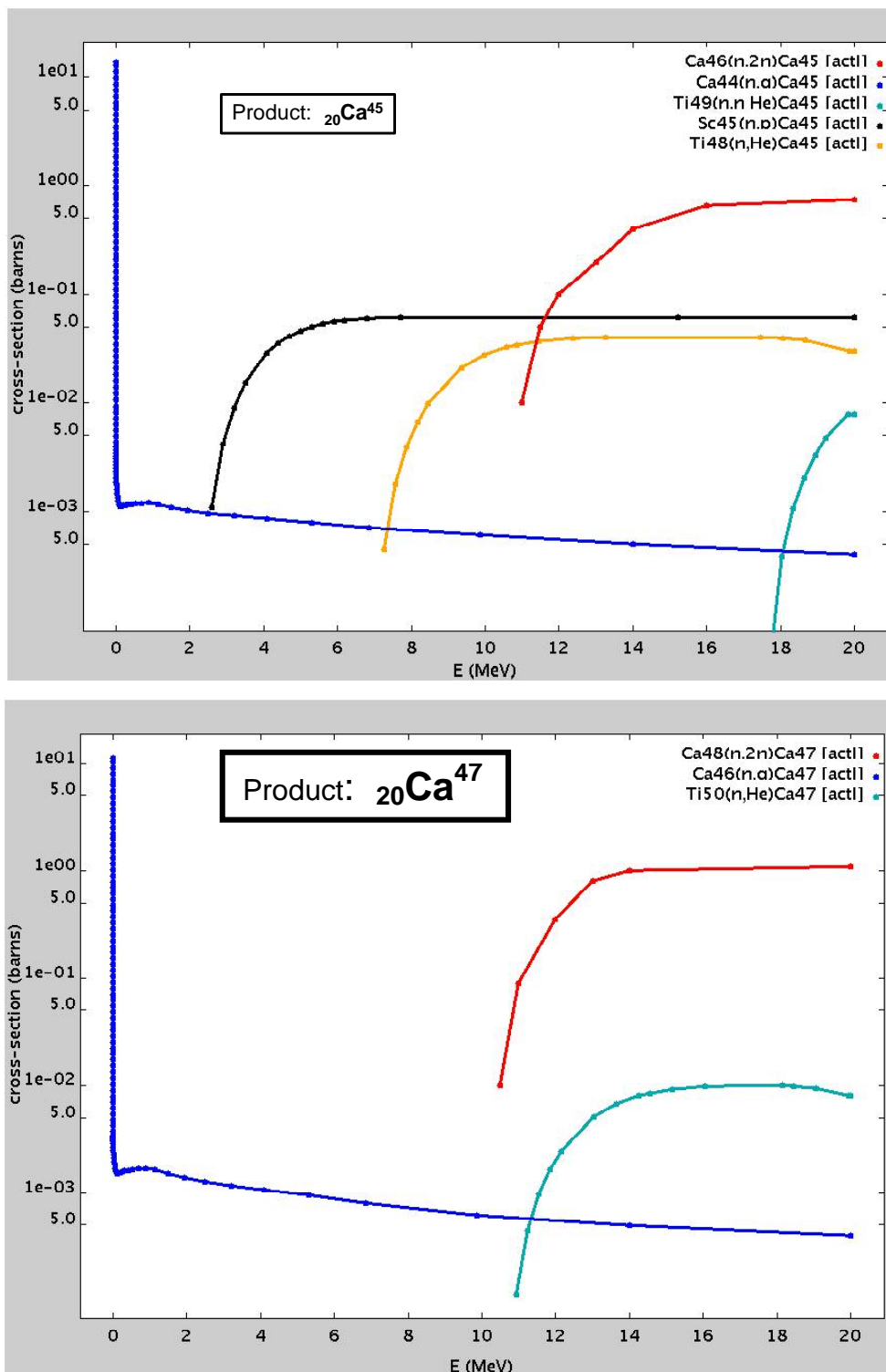
Appendix B: Radionuclide Production Cross-Sections

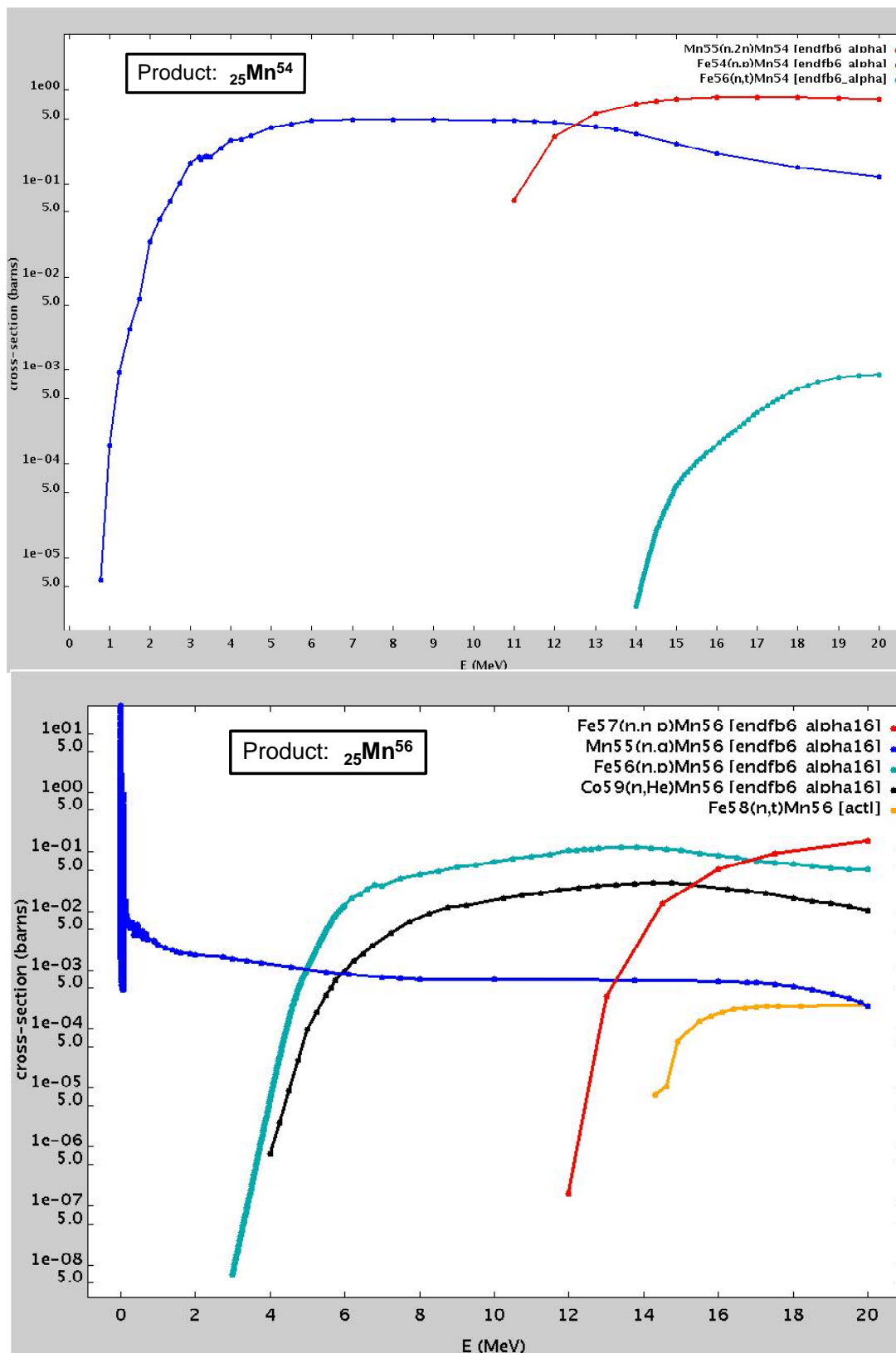


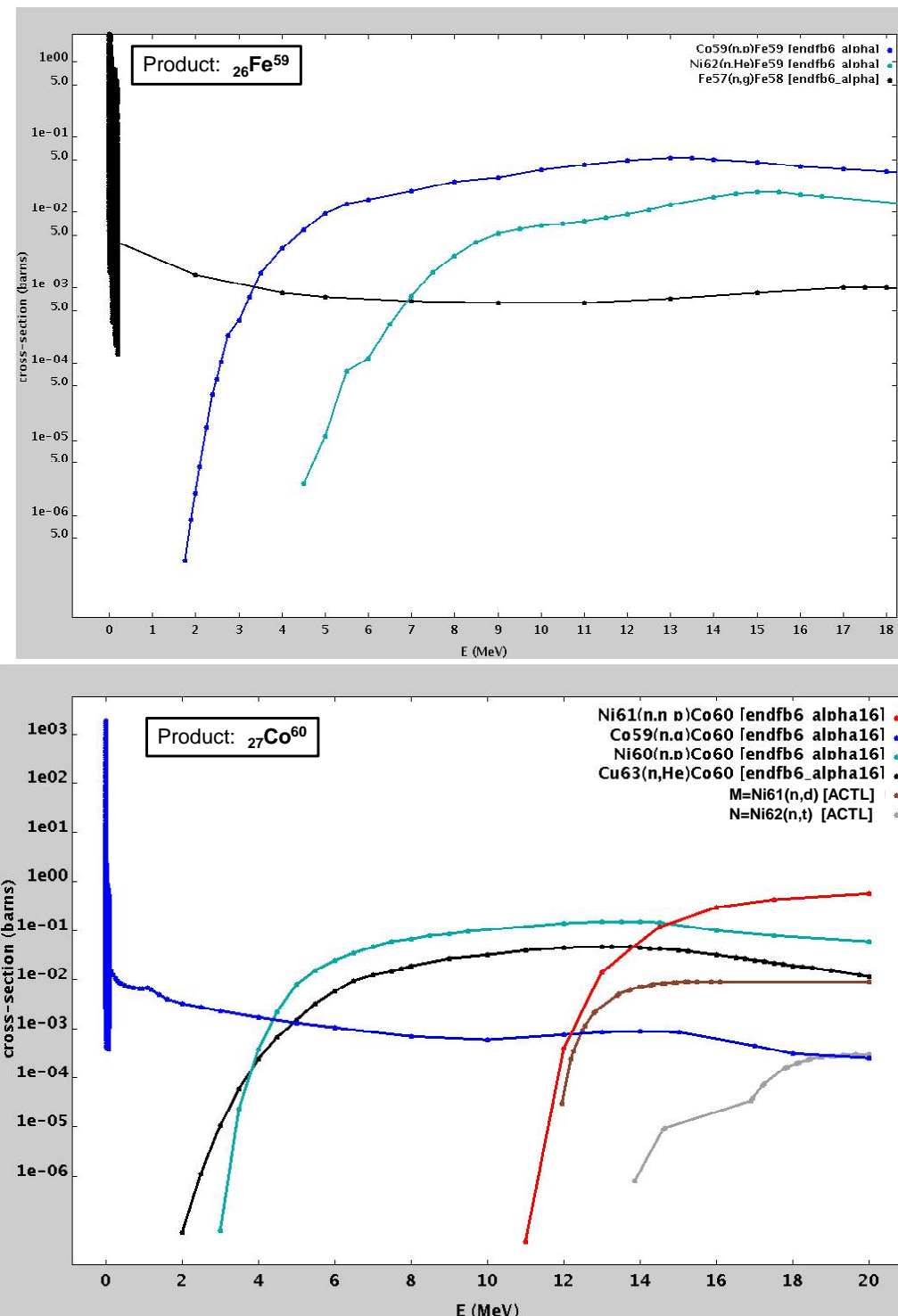


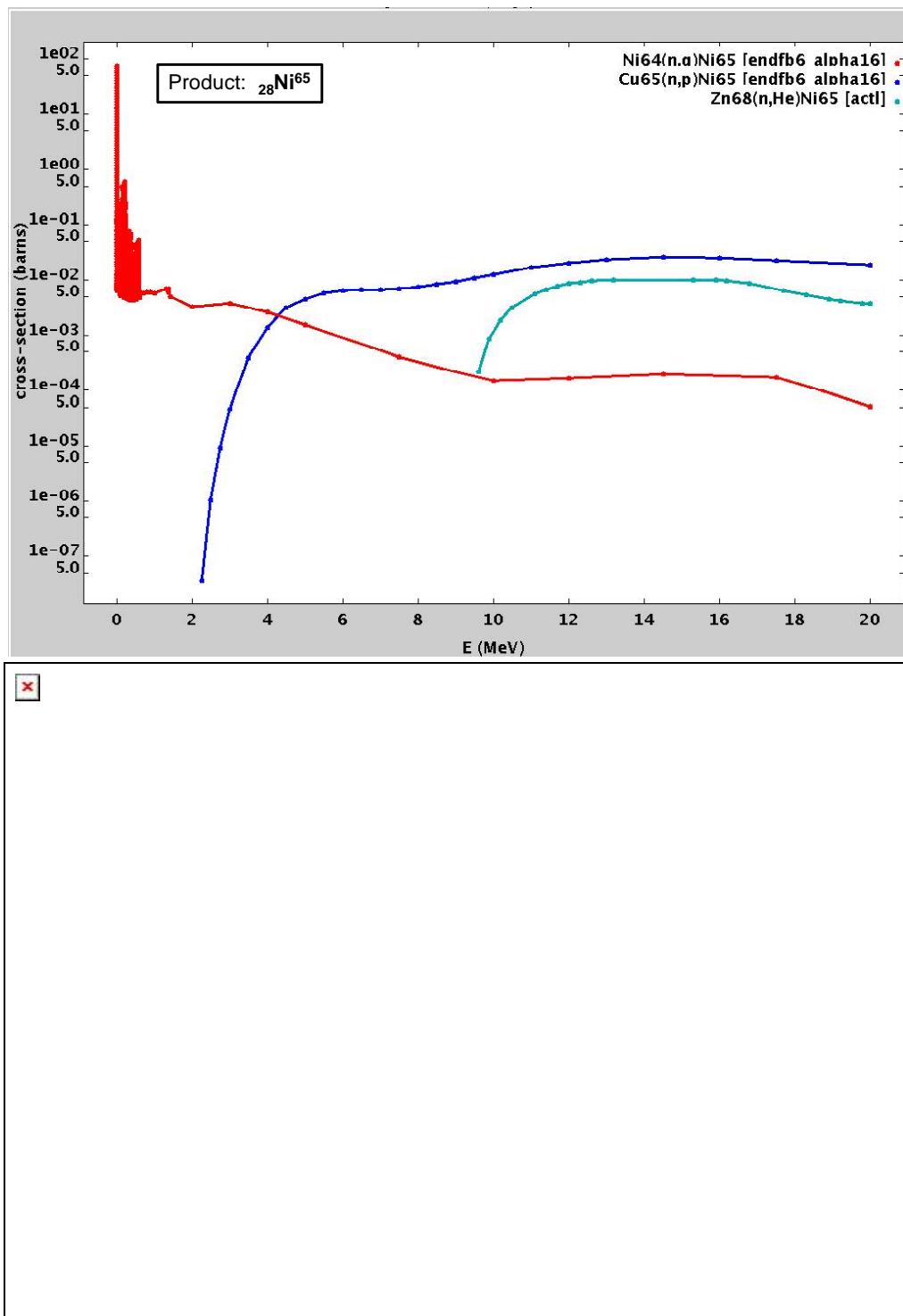


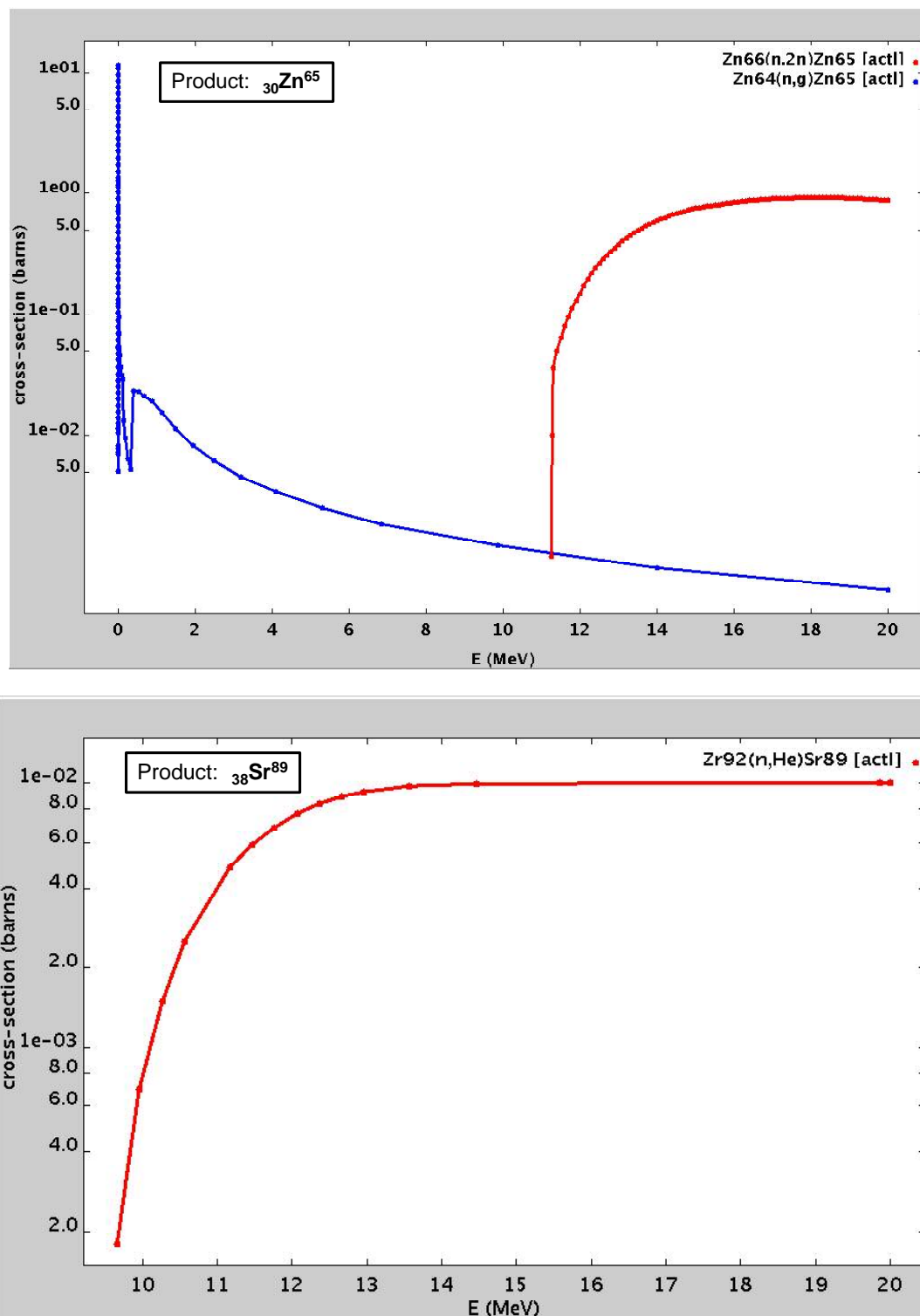


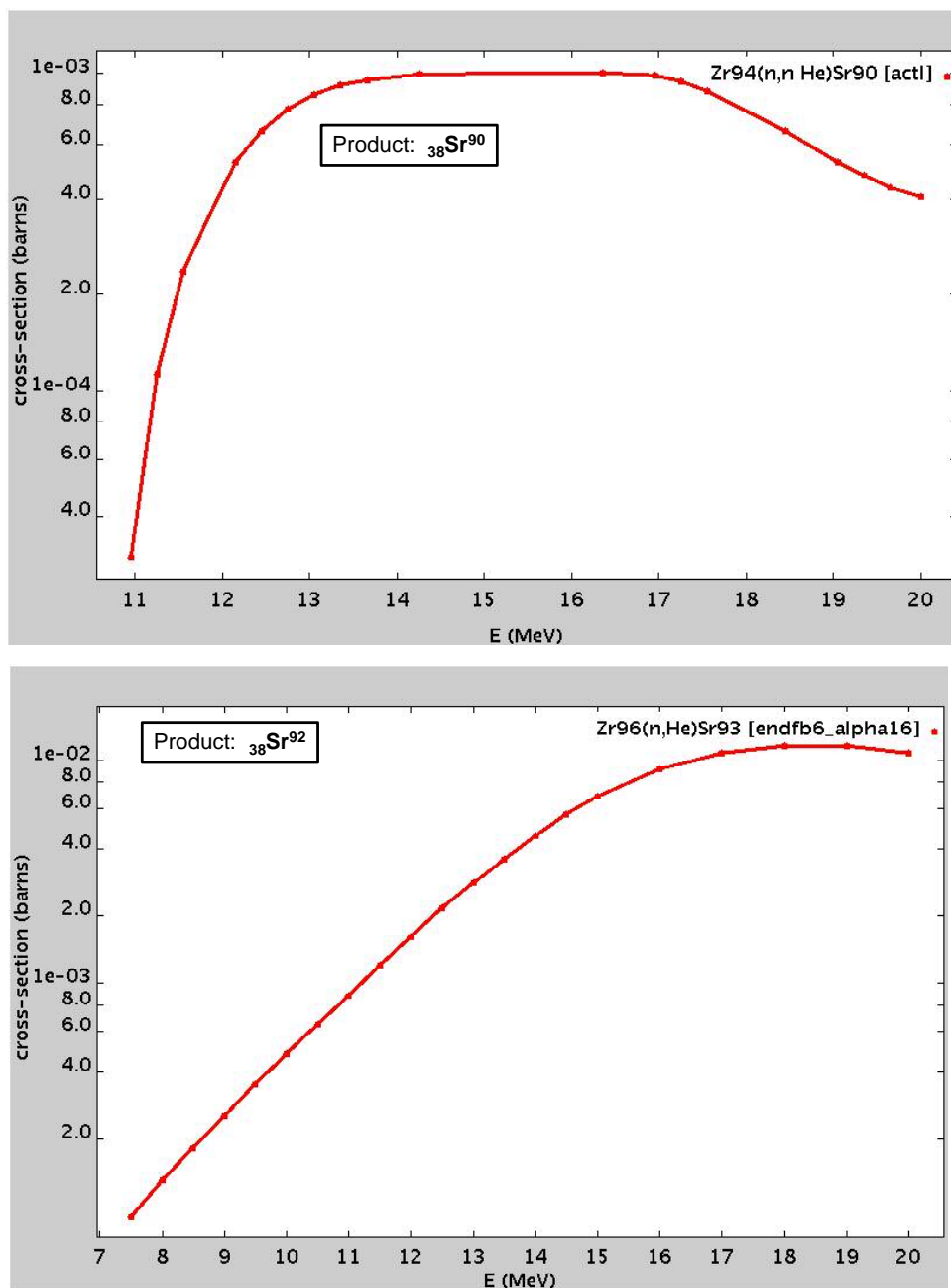












Appendix C: Cross Section Sources for Radionuclide Production

<u>Product</u>	<u>Library</u>	<u>Target</u>	<u>Rxn</u>	<u>O-19</u>	<u>ENDFb6</u>	<u>F-19</u>	<u>(n,p)</u>
H-3	LLNL/ACTL	H-2	(n,g)	F-18	ENDFb5/532dos	F-19	(n,2n)
H-3	ENDFb6	H-2	(n,g)	F-18	LLNL/ACTL	F-19	(n,2n)
H-3	LLNL/ACTL	He-3	(n,p)	F-18	ENDL94	F-19	(n,2n)
H-3	ENDFb6	He-3	(n,p)	F-18	ENDFb6	F-19	(n,2n)
He-6	LLNL/ACTL	Li-6	(n,p)	F-20	LLNL/ACTL	F-19	(n,g)
He-6	ENDFb6	Li-6	(n,p)	F-20	ENDL94	F-19	(n,g)
He-6	ENDFb6	Li-7	(n,d)	F-20	ENDFb6	F-19	(n,g)
He-6	LLNL/ACTL	Be-9	(n,a)	F-20	LLNL/ACTL	Na-23	(n,a)
He-6	ENDFb6	Be-9	(n,a)	F-20	ENDFb6	Na-23	(n,a)
Li-8	ENDFb5/532dos	Li-7	(n,g)	F-20	ENDFb6	Al-27	(n,2a)
Li-8	LLNL/ACTL	Li-7	(n,g)	Ne-19	ENDL94	Ne-20	(n,2n)
Li-8	ENDL94	Li-7	(n,g)	Ne-23	LLNL/ACTL	Na-23	(n,p)
Li-8	ENDFb6	Li-7	(n,g)	Ne-23	ENDFb6	Na-23	(n,p)
Li-8	LLNL/ACTL	Be-9	(n,d)	Ne-23	LLNL/ACTL	Mg-26	(n,a)
Li-8	ENDFb6	Be-9	(n,d)	Ne-23	ENDFb6	Al-27	(n,pa)
Li-8	LLNL/ACTL	B-11	(n,a)	Na-22	LLNL/ACTL	Na-23	(n,2n)
Li-8	ENDFb6	B-11	(n,a)	Na-22	ENDL94	Na-23	(n,2n)
Li-9	LLNL/ACTL	Be-9	(n,p)	Na-22	ENDFb6	Na-23	(n,2n)
Li-9	ENDFb6	Be-9	(n,p)	Na-24	LLNL/ACTL	Na-23	(n,g)
He-4	LLNL/ACTL	Be-9	(n,2n)	Na-24	ENDL94	Na-23	(n,g)
Be-8	ENDFb6	Be-9	(n,2n)	Na-24	ENDFb6	Na-23	(n,g)
Be-8	ENDFb6	B-10	(n,t)	Na-24	ENDFb5/532dos	Mg-24	(n,p)
Be-10	ENDFb6	B-11	(n,np)	Na-24	LLNL/ACTL	Mg-24	(n,p)
Be-10	LLNL/ACTL	Be-9	(n,g)	Na-24	ENDFb6	Mg-24	(n,p)
Be-10	ENDFb6	Be-9	(n,g)	Na-24	ENDFb5/532dos	Al-27	(n,a)
Be-10	ENDFb6	B-10	(n,p)	Na-24	LLNL/ACTL	Al-27	(n,a)
Be-10	LLNL/ACTL	C-13	(n,a)	Na-24	ENDFb6	Al-27	(n,a)
Be-11	LLNL/ACTL	B-11	(n,p)	Na-25	LLNL/ACTL	Mg-25	(n,p)
Be-11	ENDFb6	B-11	(n,p)	Na-26	LLNL/ACTL	Mg-26	(n,p)
B-9	ENDL94	B-10	(n,2n)	Na-26	ENDFb6	Al-27	(n,2p)
B-12	LLNL/ACTL	B-11	(n,g)	Mg-23	LLNL/ACTL	Mg-24	(n,2n)
B-12	ENDL94	B-11	(n,g)	Mg-27	LLNL/ACTL	Mg-26	(n,g)
B-12	ENDFb6	B-11	(n,g)	Mg-27	ENDFb5/532dos	Al-27	(n,p)
B-12	LLNL/ACTL	C-12	(n,p)	Mg-27	LLNL/ACTL	Al-27	(n,p)
B-12	ENDFb6	N-15	(n,a)	Mg-27	ENDFb6	Al-27	(n,p)
B-13	LLNL/ACTL	C-13	(n,p)	Mg-27	LLNL/ACTL	Si-30	(n,a)
C-14	ENDL94	N-15	(n,np)	Mg-27	ENDFb6	Si-30	(n,a)
C-14	ENDFb6	N-15	(n,np)	Al-26	LLNL/ACTL	Al-27	(n,2n)
C-14	LLNL/ACTL	C-13	(n,g)	Al-26	ENDL94	Al-27	(n,2n)
C-14	ENDL94	C-13	(n,g)	Al-26	ENDFb6	Al-27	(n,2n)
C-14	ENDFb5/532dos	N-14	(n,p)	Al-28	LLNL/ACTL	Si-29	(n,np)
C-14	LLNL/ACTL	N-14	(n,p)	Al-28	ENDFb6	Si-29	(n,np)
C-14	ENDFb6	N-14	(n,p)	Al-28	ENDFb5/532dos	Al-27	(n,g)
C-14	ENDFb6	N-15	(n,d)	Al-28	LLNL/ACTL	Al-27	(n,g)
C-14	LLNL/ACTL	O-17	(n,a)	Al-28	ENDL94	Al-27	(n,g)
C-14	ENDFb6	O-17	(n,a)	Al-28	ENDFb6	Al-27	(n,g)
C-15	ENDFb6	N-15	(n,p)	Al-28	LLNL/ACTL	Si-28	(n,p)
N-13	LLNL/ACTL	N-14	(n,2n)	Al-28	ENDFb6	Si-28	(n,p)
N-13	ENDL94	N-14	(n,2n)	Al-28	LLNL/ACTL	P-31	(n,a)
N-13	ENDFb6	N-14	(n,2n)	Al-28	ENDFb6	P-31	(n,a)
N-16	ENDFb6	O-17	(n,np)	Al-29	LLNL/ACTL	Si-30	(n,np)
N-16	ENDL94	N-15	(n,g)	Al-29	ENDFb6	Si-30	(n,np)
N-16	ENDFb6	N-15	(n,g)	Al-29	LLNL/ACTL	Si-29	(n,p)
N-16	ENDFb5/532dos	O-16	(n,p)	Al-29	ENDFb6	Si-29	(n,p)
N-16	LLNL/ACTL	O-16	(n,p)	Al-30	LLNL/ACTL	Si-30	(n,p)
N-16	ENDFb6	O-16	(n,p)	Al-30	ENDFb6	Si-30	(n,p)
N-16	ENDFb6	O-17	(n,d)	Si-27	LLNL/ACTL	Si-28	(n,2n)
N-16	LLNL/ACTL	F-19	(n,a)	Si-27	ENDFb6	Si-28	(n,2n)
N-16	ENDFb6	F-19	(n,a)	Si-31	LLNL/ACTL	Si-30	(n,g)
N-17	ENDFb6	O-17	(n,p)	Si-31	ENDFb6	Si-30	(n,g)
O-15	LLNL/ACTL	O-16	(n,2n)	Si-31	ENDFb5/532dos	P-3I	(n,p)
O-15	ENDL94	O-16	(n,2n)	Si-31	LLNL/ACTL	P-31	(n,p)
O-19	LLNL/ACTL	F-19	(n,p)	Si-31	ENDFb6	P-31	(n,p)

Si-31	LLNL/ACTL	S-34	(n,a)	K-43	LLNL/ACTL	Ca-43	(n,p)
Si-32	LLNL/ACTL	S-36	(n,na)	K-43	LLNL/ACTL	Ca-44	(n,d)
P-30	LLNL/ACTL	P-31	(n,2n)	K-43	ENDFb6	Sc-45	(n,3He)
P-30	ENDL94	P-31	(n,2n)	K-44	LLNL/ACTL	Ca-44	(n,p)
P-30	ENDFb6	P-31	(n,2n)	K-46	LLNL/ACTL	Ca-46	(n,p)
P-30	LLNL/ACTL	S-32	(n,t)	K-48	LLNL/ACTL	Ca-48	(n,p)
P-30	ENDFb6	S-32	(n,t)	Ca-39	LLNL/ACTL	Ca-40	(n,2n)
P-32	LLNL/ACTL	S-33	(n,np)	Ca-41	LLNL/ACTL	Ca-42	(n,2n)
P-32	LLNL/ACTL	P-31	(n,g)	Ca-41	LLNL/ACTL	Ca-40	(n,g)
P-32	ENDL94	P-31	(n,g)	Ca-45	LLNL/ACTL	Ca-46	(n,2n)
P-32	ENDFb6	P-31	(n,g)	Ca-45	LLNL/ACTL	Ti-49	(n,na)
P-32	ENDFb5/532dos	S-.32	(n,p)	Ca-45	LLNL/ACTL	Ca-44	(n,g)
P-32	LLNL/ACTL	S-32	(n,p)	Ca-45	LLNL/ACTL	Sc-45	(n,p)
P-32	ENDFb6	S-32	(n,p)	Ca-45	ENDFb6	Sc-45	(n,p)
P-32	LLNL/ACTL	S-33	(n,d)	Ca-45	ENDFb5/532dos	Ti-48	(n,a)
P-32	LLNL/ACTL	C1-35	(n,a)	Ca-45	LLNL/ACTL	Ti-48	(n,a)
P-33	LLNL/ACTL	C1-37	(n,na)	Ca-45	ENDFb6	Ti-48	(n,a)
P-33	LLNL/ACTL	S-34	(n,np)	Ca-47	LLNL/ACTL	Ca-48	(n,2n)
P-33	LLNL/ACTL	S-33	(n,p)	Ca-47	LLNL/ACTL	Ca-46	(n,g)
P-33	LLNL/ACTL	S-34	(n,d)	Ca-47	ENDFb5/532dos	Ti-50	(n,a)
P-34	LLNL/ACTL	S-34	(n,p)	Ca-47	LLNL/ACTL	Ti-50	(n,a)
P-34	LLNL/ACTL	C1-37	(n,a)	Ca-47	ENDFb6	Ti-50	(n,a)
S-31	LLNL/ACTL	S-32	(n,2n)	Ca-49	LLNL/ACTL	Ca-48	(n,g)
S-31	ENDL94	S-32	(n,2n)	Sc-44	ENDFb5/532dos	Sc-45	(n,2n)
S-31	ENDFb6	S-32	(n,2n)	Sc-44	LLNL/ACTL	Sc-45	(n,2n)
S-35	LLNL/ACTL	S-36	(n,2n)	Sc-44	ENDFb6	Sc-45	(n,2n)
S-35	LLNL/ACTL	S-34	(n,g)	Sc-44	LLNL/ACTL	Ti-46	(n,t)
S-35	LLNL/ACTL	C1-35	(n,p)	Sc-46	LLNL/ACTL	V-50	(n,na)
S-35	LLNL/ACTL	C1-37	(n,t)	Sc-46	ENDFb5/532dos	Ti-47	(n,np)
S-35	LLNL/ACTL	Ar-38	(n,a)	Sc-46	LLNL/ACTL	Ti-47	(n,np)
S-37	LLNL/ACTL	S-36	(n,g)	Sc-46	ENDFb6	Ti-47	(n,np)
S-37	LLNL/ACTL	C1-37	(n,p)	Sc-46	ENDFb5/532dos	Sc-45	(n,g)
S-37	LLNL/ACTL	Ar-40	(n,a)	Sc-46	LLNL/ACTL	Sc-45	(n,g)
C1-34	LLNL/ACTL	C1-35	(n,2n)	Sc-46	ENDFb6	Sc-45	(n,g)
C1-36	LLNL/ACTL	C1-37	(n,2n)	Sc-46	ENDFb5/532dos	Ti-46	(n,p)
C1-36	LLNL/ACTL	C1-35	(n,g)	Sc-46	LLNL/ACTL	Ti-46	(n,p)
C1-36	LLNL/ACTL	Ar-36	(n,p)	Sc-46	ENDFb6	Ti-46	(n,p)
C1-36	LLNL/ACTL	K-39	(n,a)	Sc-46	LLNL/ACTL	Ti-47	(n,d)
C1-38	LLNL/ACTL	C1-37	(n,g)	Sc-47	LLNL/ACTL	V-51	(n,na)
C1-38	LLNL/ACTL	Ar-38	(n,p)	Sc-47	ENDL94	V-51	(n,na)
C1-38	LLNL/ACTL	K-41	(n,a)	Sc-47	ENDFb5/532dos	Ti-48	(n,np)
C1-40	LLNL/ACTL	Ar-40	(n,p)	Sc-47	LLNL/ACTL	Ti-48	(n,np)
Ar-36	LLNL/ACTL	Ar-36	(n,2n)	Sc-47	ENDFb6	Ti-48	(n,np)
Ar-37	LLNL/ACTL	Ar-38	(n,2n)	Sc-47	ENDFb5/532dos	Ti-47	(n,p)
Ar-37	LLNL/ACTL	Ar-36	(n,g)	Sc-47	LLNL/ACTL	Ti-47	(n,p)
Ar-37	LLNL/ACTL	K-39	(n,t)	Sc-47	ENDFb6	Ti-47	(n,p)
Ar-37	LLNL/ACTL	Ca-40	(n,a)	Sc-47	LLNL/ACTL	Ti-48	(n,d)
Ar-39	LLNL/ACTL	Ar-40	(n,2n)	Sc-47	LLNL/ACTL	V-50	(n,a)
Ar-39	LLNL/ACTL	Ca-43	(n,na)	Sc-48	LLNL/ACTL	Ti-49	(n,np)
Ar-39	LLNL/ACTL	Ar-38	(n,g)	Sc-48	ENDFb5/532dos	Ti-48	(n,p)
Ar-39	LLNL/ACTL	K-39	(n,p)	Sc-48	LLNL/ACTL	Ti-48	(n,p)
Ar-39	LLNL/ACTL	K-40	(n,d)	Sc-48	ENDFb6	Ti-48	(n,p)
Ar-39	LLNL/ACTL	K-41	(n,t)	Sc-48	LLNL/ACTL	Ti-49	(n,d)
Ar-39	LLNL/ACTL	Ca-42	(n,a)	Sc-48	LLNL/ACTL	V-51	(n,a)
Ar-41	ENDFb5/532dos	Ar-40	(n,g)	Sc-49	LLNL/ACTL	Ti-50	(n,np)
Ar-41	LLNL/ACTL	Ar-40	(n,g)	Sc-49	LLNL/ACTL	Ti-49	(n,p)
Ar-41	ENDFb6	Ar-40	(n,g)	Sc-50	LLNL/ACTL	Ti-50	(n,p)
Ar-41	ENDFb5/532dos	K-41	(n,p)	Ti-45	LLNL/ACTL	Ti-46	(n,2n)
Ar-41	LLNL/ACTL	K-41	(n,p)	Ti-51	LLNL/ACTL	Ti-50	(n,g)
Ar-41	ENDFb6	K-41	(n,p)	Ti-51	LLNL/ACTL	V-51	(n,p)
Ar-41	LLNL/ACTL	Ca-44	(n,a)	Ti-51	LLNL/ACTL	Cr-54	(n,a)
Ar-43	LLNL/ACTL	Ca-46	(n,a)	Ti-51	ENDFb6	Cr-54	(n,a)
K-38	LLNL/ACTL	K-39	(n,2n)	V-48	LLNL/ACTL	Cr-50	(n,t)
K-38	LLNL/ACTL	Ca-40	(n,t)	V-49	LLNL/ACTL	V-50	(n,2n)
K-40	LLNL/ACTL	K-41	(n,2n)	V-49	LLNL/ACTL	Cr-50	(n,np)
K-40	LLNL/ACTL	K-39	(n,g)	V-49	ENDFb6	Cr-50	(n,np)
K-40	LLNL/ACTL	Ca-40	(n,p)	V-49	LLNL/ACTL	Cr-50	(n,d)
K-42	LLNL/ACTL	K-41	(n,g)	V-49	ENDFb6	Cr-50	(n,d)
K-42	LLNL/ACTL	Ca-42	(n,p)	V-50	LLNL/ACTL	V-51	(n,2n)
K-42	LLNL/ACTL	Ca-43	(n,d)	V-50	ENDL94	V-51	(n,2n)
K-42	LLNL/ACTL	Sc-45	(n,a)	V-50	LLNL/ACTL	Cr-50	(n,p)
K-42	ENDFb6	Sc-45	(n,a)	V-50	ENDFb6	Cr-50	(n,p)

V-50	LLNL/ACTL	Cr-52	(n,t)	Fe-55	LLNL/ACTL	Fe-57	(n,3n)
V-52	LLNL/ACTL	Cr-53	(n,np)	Fe-55	LLNL/ACTL	Fe-54	(n,g)
V-52	ENDFb6	Cr-53	(n,np)	Fe-55	ENDFb6	Fe-54	(n,g)
V-52	LLNL/ACTL	V-51	(n,g)	Fe-55	ENDFb5/532dos	Ni-58	(n,a)
V-52	ENDL94	V-51	(n,g)	Fe-55	LLNL/ACTL	Ni-58	(n,a)
V-52	LLNL/ACTL	Cr-52	(n,p)	Fe-55	ENDFb6	Ni-58	(n,a)
V-52	ENDFb6	Cr-52	(n,p)	Fe-59	LLNL/ACTL	Fe-58	(n,g)
V-52	LLNL/ACTL	Cr-53	(n,d)	Fe-59	ENDFb6	Fe-58	(n,g)
V-52	LLNL/ACTL	Cr-54	(n,t)	Fe-59	LLNL/ACTL	Co-59	(n,p)
V-52	LLNL/ACTL	Mn-55	(n,a)	Fe-59	ENDFb6	Co-59	(n,p)
V-52	ENDFb6	Mn-55	(n,a)	Fe-59	ENDFb5/532dos	Ni-62	(n,a)
V-52	ENDFb6	Co-59	(n,2a)	Fe-59	LLNL/ACTL	Ni-62	(n,a)
V-53	LLNL/ACTL	Cr-54	(n,np)	Fe-59	ENDFb6	Ni-62	(n,a)
V-53	LLNL/ACTL	Cr-53	(n,p)	Fe-60	LLNL/ACTL	Ni-64	(n,na)
V-53	ENDFb6	Cr-53	(n,p)	Fe-60	ENDFb6	Ni-64	(n,na)
V-53	LLNL/ACTL	Cr-54	(n,d)	Fe-60	ENDFb6	Ni-61	(n,2p)
V-53	ENDFb6	Cr-54	(n,d)	Fe-61	LLNL/ACTL	Ni-64	(n,a)
V-53	ENDFb6	Mn-55	(n,3He)	Fe-61	ENDFb6	Ni-64	(n,a)
V-54	LLNL/ACTL	Cr-54	(n,p)	Co-56	LLNL/ACTL	Ni-58	(n,t)
V-54	ENDFb6	Cr-54	(n,p)	Co-57	LLNL/ACTL	Ni-58	(n,np)
Cr-49	ENDFb5/532dos	Cr-50	(n,2n)	Co-57	ENDL94	Ni-58	(n,np)
Cr-49	LLNL/ACTL	Cr-50	(n,2n)	Co-57	ENDFb6	Ni-58	(n,np)
Cr-49	ENDFb6	Cr-50	(n,2n)	Co-57	ENDFb5/532dos	Ni-58	(n,d)
Cr-51	ENDFb5/532dos	Cr-52	(n,2n)	Co-57	LLNL/ACTL	Ni-58	(n,d)
Cr-51	LLNL/ACTL	Cr-52	(n,2n)	Co-57	ENDFb6	Ni-58	(n,d)
Cr-51	ENDFb6	Cr-52	(n,2n)	Co-58	LLNL/ACTL	Co-59	(n,2n)
Cr-51	ENDFb5/532dos	Cr-50	(n,g)	Co-58	ENDL94	Co-59	(n,2n)
Cr-51	LLNL/ACTL	Cr-50	(n,g)	Co-58	ENDFb6	Co-59	(n,2n)
Cr-51	ENDFb6	Cr-50	(n,g)	Co-58	ENDFb5/532dos	Ni-58	(n,p)
Cr-51	LLNL/ACTL	Fe-54	(n,a)	Co-58	LLNL/ACTL	Ni-58	(n,p)
Cr-51	ENDFb6	Fe-54	(n,a)	Co-58	ENDFb6	Ni-58	(n,p)
Fe-55	ENDFb5/532dos	Fe-54	(n,g)	Co-58	ENDFb6	Ni-58	(n,p)
Cr-55	LLNL/ACTL	Cr-54	(n,g)	Co-58	LLNL/ACTL	Ni-60	(n,t)
Cr-55	ENDFb6	Cr-54	(n,g)	Co-60	LLNL/ACTL	Ni-61	(n,np)
Cr-55	LLNL/ACTL	Mn-55	(n,p)	Co-60	ENDFb6	Ni-61	(n,np)
Cr-55	ENDFb6	Mn-55	(n,p)	Co-60	LLNL/ACTL	Co-59	(n,g)
Cr-55	LLNL/ACTL	Fe-58	(n,a)	Co-60	ENDL94	Co-59	(n,g)
Cr-55	ENDFb6	Fe-58	(n,a)	Co-60	ENDFb6	Co-59	(n,g)
Cr-55	ENDFb6	Co-59	(n,pa)	Co-60	ENDFb5/532dos	Ni-60	(n,p)
Mn-52	LLNL/ACTL	Fe-54	(n,t)	Co-60	LLNL/ACTL	Ni-60	(n,p)
Mn-52	LLNL/ACTL	Fe-54	(n,np)	Co-60	ENDFb6	Ni-60	(n,p)
Mn-53	ENDFb6	Fe-54	(n,np)	Co-60	LLNL/ACTL	Ni-61	(n,d)
Mn-53	LLNL/ACTL	Fe-54	(n,d)	Co-60	LLNL/ACTL	Ni-62	(n,t)
Mn-53	ENDFb6	Fe-54	(n,d)	Co-60	ENDFb5/532dos	Cu-63	(n,a)
Mn-54	LLNL/ACTL	Mn-55	(n,2n)	Co-60	LLNL/ACTL	Cu-63	(n,a)
Mn-54	ENDL94	Mn-55	(n,2n)	Co-60	ENDFb6	Cu-63	(n,a)
Mn-54	ENDFb6	Mn-55	(n,2n)	Co-61	LLNL/ACTL	Cu-65	(n,na)
Mn-54	LLNL/ACTL	Fe-54	(n,p)	Co-61	ENDFb6	Cu-65	(n,na)
Mn-54	ENDFb6	Fe-54	(n,p)	Co-61	LLNL/ACTL	Ni-62	(n,np)
Mn-54	LLNL/ACTL	Fe-56	(n,t)	Co-61	ENDFb6	Ni-62	(n,np)
Mn-54	ENDFb6	Fe-56	(n,t)	Co-61	LLNL/ACTL	Ni-61	(n,p)
Mn-56	LLNL/ACTL	Fe-57	(n,np)	Co-61	ENDFb6	Ni-61	(n,p)
Mn-56	ENDFb6	Fe-57	(n,np)	Co-61	LLNL/ACTL	Ni-62	(n,d)
Mn-56	LLNL/ACTL	Mn-55	(n,g)	Co-61	ENDFb6	Ni-62	(n,d)
Mn-56	ENDL94	Mn-55	(n,g)	Co-61	ENDFb6	Cu-63	(n,3He)
Mn-56	ENDFb6	Mn-55	(n,g)	Co-62	LLNL/ACTL	Ni-62	(n,p)
Mn-56	LLNL/ACTL	Fe-56	(n,p)	Co-62	ENDFb6	Ni-62	(n,p)
Mn-56	ENDFb6	Fe-56	(n,p)	Co-62	LLNL/ACTL	Ni-64	(n,t)
Mn-56	LLNL/ACTL	Fe-58	(n,t)	Co-62	LLNL/ACTL	Cu-65	(n,a)
Mn-56	LLNL/ACTL	Co-59	(n,a)	Co-62	ENDFb6	Cu-65	(n,a)
Mn-56	ENDFb6	Co-59	(n,a)	Co-63	LLNL/ACTL	Ni-64	(n,np)
Mn-57	LLNL/ACTL	Fe-58	(n,np)	Co-63	ENDFb6	Ni-64	(n,np)
Mn-57	ENDFb6	Fe-58	(n,np)	Co-63	LLNL/ACTL	Ni-64	(n,d)
Mn-57	LLNL/ACTL	Fe-57	(n,p)	Co-63	ENDFb6	Ni-64	(n,d)
Mn-57	ENDFb6	Fe-57	(n,p)	Co-63	ENDFb6	Cu-65	(n,3He)
Mn-57	ENDFb6	Co-59	(n,3He)	Co-64	LLNL/ACTL	Ni-64	(n,p)
Mn-58	LLNL/ACTL	Fe-58	(n,p)	Co-64	ENDFb6	Ni-64	(n,p)
Mn-58	ENDFb6	Fe-58	(n,p)	Ni-57	ENDFb5/532dos	Ni-58	(n,2n)
Mn-58	ENDFb6	Co-59	(n,2p)	Ni-57	LLNL/ACTL	Ni-58	(n,2n)
Fe-53	LLNL/ACTL	Fe-54	(n,2n)	Ni-57	ENDL94	Ni-58	(n,2n)
Fe-53	ENDFb6	Fe-54	(n,2n)	Ni-57	ENDFb6	Ni-58	(n,2n)
Fe-55	LLNL/ACTL	Fe-56	(n,2n)	Ni-59	ENDFb5/532dos	Ni-60	(n,2n)
Fe-55	ENDFb6	Fe-56	(n,2n)	Ni-59	LLNL/ACTL	Ni-60	(n,2n)

Ni-59	ENDFb6	Ni-60	(n, 2n)	As-73	ENDL94	As-75	(n, 3n)
Ni-55	ENDFb5/532dos	Ni-58	(n, g)	As-74	LLNL/ACTL	As-75	(n, 2n)
Ni-59	LLNL/ACTL	Ni-58	(n, g)	As-74	ENDL94	As-75	(n, 2n)
Ni-59	ENDFb6	Ni-58	(n, g)	As-76	LLNL/ACTL	As-75	(n, g)
Ni-63	LLNL/ACTL	Ni-64	(n, 2n)	As-76	ENDL94	As-75	(n, g)
Ni-63	ENDFb6	Ni-64	(n, 2n)	As-76	ENDFb6	As-75	(n, g)
Ni-63	LLNL/ACTL	Zn-67	(n, na)	As-76	LLNL/ACTL	Br-79	(n, a)
Ni-63	ENDFb5/532dos	Ni-62	(n, g)	As-77	LLNL/ACTL	Br-81	(n, na)
Ni-63	LLNL/ACTL	Ni-62	(n, g)	Se-73	LLNL/ACTL	Se-74	(n, 2n)
Ni-63	ENDFb6	Ni-62	(n, g)	Se-75	LLNL/ACTL	Se-76	(n, 2n)
Ni-62	ENDFb5/532dos	Cu-63	(n, p)	Se-75	ENDFb6	Se-74	(n, g)
Ni-63	LLNL/ACTL	Cu-63	(n, p)	Se-75	ENDFb6	Kr-78	(n, a)
Ni-63	ENDFb6	Cu-63	(n, p)	Se-79	LLNL/ACTL	Se-80	(n, 2n)
Ni-63	ENDFb6	Cu-65	(n, t)	Se-79	ENDFb6	Se-78	(n, g)
Ni-63	LLNL/ACTL	Zn-66	(n, a)	Se-79	LLNL/ACTL	Br-79	(n, p)
Ni-65	LLNL/ACTL	Ni-64	(n, g)	Se-79	ENDFb6	Kr-82	(n, a)
Ni-65	ENDFb6	Ni-64	(n, g)	Se-81	LLNL/ACTL	Se-82	(n, 2n)
Ni-65	LLNL/ACTL	Cu-65	(n, p)	Se-81	ENDFb6	Se-80	(n, g)
Ni-65	ENDFb6	Cu-65	(n, p)	Se-81	ENDFb6	Kr-83	(n, 3He)
Ni-65	LLNL/ACTL	Zn-68	(n, a)	Se-81	ENDFb6	Kr-84	(n, a)
Ni-66	LLNL/ACTL	Zn-70	(n, na)	Se-82	ENDFb6	Kr-84	(n, 3He)
Ni-67	LLNL/ACTL	Zn-70	(n, a)	Se-83	ENDFb6	Se-82	(n, g)
Cu-62	LLNL/ACTL	Cu-63	(n, 2n)	Br-76	ENDFb6	Kr-78	(n, t)
Cu-62	ENDFb6	Cu-63	(n, 2n)	Br-77	ENDFb6	Kr-78	(n, d)
Cu-64	ENDFb5/532dos	Cu-65	(n, 2n)	Br-78	LLNL/ACTL	Br-79	(n, 2n)
Cu-64	LLNL/ACTL	Cu-65	(n, 2n)	Br-78	ENDFb6	Kr-78	(n, p)
Cu-64	ENDFb6	Cu-65	(n, 2n)	Br-78	ENDFb6	Kr-80	(n, t)
Cu-64	ENDFb5/532dos	Cu-63	(n, g)	Br-80	LLNL/ACTL	Br-81	(n, 2n)
Cu-64	LLNL/ACTL	Cu-63	(n, g)	Br-80	ENDFb6	Br-79	(n, g)
Cu-64	ENDFb6	Cu-63	(n, g)	Br-80	ENDFb6	Kr-80	(n, p)
Cu-64	LLNL/ACTL	Zn-64	(n, p)	Br-80	ENDFb6	Kr-82	(n, t)
Cu-66	LLNL/ACTL	Zn-67	(n, np)	Br-82	LLNL/ACTL	Br-81	(n, g)
Cu-66	LLNL/ACTL	Cu-65	(n, g)	Br-82	ENDFb6	Br-81	(n, g)
Cu-66	ENDFb6	Cu-65	(n, g)	Br-82	ENDFb6	Kr-82	(n, p)
Cu-66	LLNL/ACTL	Zn-66	(n, p)	Br-82	ENDFb6	Kr-83	(n, d)
Cu-67	LLNL/ACTL	Zn-68	(n, np)	Br-82	ENDFb6	Kr-84	(n, t)
Cu-67	LLNL/ACTL	Zn-67	(n, p)	Br-82	ENDFb6	Rb-85	(n, a)
Cu-68	LLNL/ACTL	Zn-68	(n, p)	Br-83	ENDFb6	Rb-87	(n, na)
Cu-70	LLNL/ACTL	Zn-70	(n, p)	Br-83	ENDFb6	Kr-83	(n, p)
Zn-63	LLNL/ACTL	Zn-64	(n, 2n)	Br-83	ENDFb6	Kr-84	(n, d)
Zn-65	LLNL/ACTL	Zn-66	(n, 2n)	Br-83	ENDFb6	Rb-85	(n, 3He)
Zn-65	LLNL/ACTL	Zn-64	(n, g)	Br-84	ENDFb6	Kr-84	(n, p)
Zn-79	LLNL/ACTL	Zn-70	(n, 2n)	Br-84	ENDFb6	Kr-86	(n, t)
Zn-69	LLNL/ACTL	Ge-73	(n, na)	Br-84	ENDFb6	Rb-87	(n, a)
Zn-69	LLNL/ACTL	Zn-68	(n, g)	Br-85	ENDFb6	Kr-86	(n, d)
Zn-69	LLNL/ACTL	Ge-72	(n, a)	Br-85	ENDFb6	Rb-87	(n, 3He)
Zn-71	LLNL/ACTL	Zn-70	(n, g)	Br-86	ENDFb6	Kr-86	(n, p)
Zn-71	LLNL/ACTL	Ge-74	(n, a)	Kr-77	ENDFb6	Kr-78	(n, 2n)
Zn-72	LLNL/ACTL	Ge-76	(n, na)	Kr-79	ENDFb6	Kr-80	(n, 2n)
Zn-73	LLNL/ACTL	Ge-76	(n, a)	Kr-79	ENDFb6	Kr-78	(n, g)
Ga-68	LLNL/ACTL	Ga-69	(n, 2n)	Kr-81	ENDFb6	Kr-82	(n, 2n)
Ga-70	LLNL/ACTL	Ga-71	(n, 2n)	Kr-81	ENDFb6	Kr-83	(n, 3n)
Ga-70	LLNL/ACTL	Ge-70	(n, p)	Kr-81	ENDFb6	Kr-80	(n, g)
Ga-72	LLNL/ACTL	Ge-73	(n, np)	Kr-85	ENDFb6	Kr-86	(n, 2n)
Ga-72	LLNL/ACTL	Ga-71	(n, g)	Kr-85	ENDFb6	Kr-84	(n, g)
Ga-72	LLNL/ACTL	Ge-72	(n, p)	Kr-85	ENDFb6	Rb-85	(n, p)
Ga-72	LLNL/ACTL	As-75	(n, a)	Kr-85	ENDFb6	Rb-87	(n, t)
Ga-73	LLNL/ACTL	Ge-74	(n, np)	Kr-87	ENDFb6	Kr-86	(n, g)
Ga-73	LLNL/ACTL	Ge-73	(n, p)	Kr-87	ENDFb6	Rb-87	(n, p)
Ga-74	LLNL/ACTL	Ge-74	(n, p)	Rb-84	LLNL/ACTL	Rb-85	(n, 2n)
Ga-75	LLNL/ACTL	Ge-76	(n, np)	Rb-84	ENDFb6	Rb-85	(n, 2n)
Ga-76	LLNL/ACTL	Ge-76	(n, p)	Rb-86	LLNL/ACTL	Rb-87	(n, 2n)
Ge-69	LLNL/ACTL	Ge-70	(n, 2n)	Rb-86	ENDFb6	Rb-87	(n, 2n)
Ge-71	LLNL/ACTL	Ge-72	(n, 2n)	Rb-86	ENDFb6	Rb-85	(n, g)
Ge-71	LLNL/ACTL	Ge-73	(n, 3n)	Rb-88	ENDFb6	Rb-87	(n, g)
Ge-71	LLNL/ACTL	Ge-70	(n, g)	Sr-83	LLNL/ACTL	Sr-84	(n, 2n)
Ge-75	LLNL/ACTL	Ge-76	(n, 2n)	Sr-85	ENDFb6	Sr-84	(n, g)
Ge-75	LLNL/ACTL	Ge-74	(n, g)	Sr-89	ENDFb6	Sr-88	(n, g)
Ge-75	ENDFb6	Ge-74	(n, g)	Sr-89	LLNL/ACTL	Zr-92	(n, a)
Ge-75	LLNL/ACTL	As-75	(n, p)	Sr-89	ENDFb6	Zr-92	(n, a)
Ge-77	LLNL/ACTL	Ge-76	(n, g)	Sr-90	LLNL/ACTL	Zr-94	(n, na)
Ge-77	ENDFb6	Ge-76	(n, g)	Sr-91	LLNL/ACTL	Zr-94	(n, a)

Sr-91	ENDFb6	Zr-94	(n,a)	Mo-101	ENDFb5/532dos	Md-I00	(n,g)
Sr-93	ENDFb6	Zr-96	(n,a)	Mo-101	LLNL/ACTL	Mo-100	(n,g)
Y-90	LLNL/ACTL	Zr-91	(n,np)	Mo-101	ENDFb6	Mo-100	(n,g)
Y-90	LLNL/ACTL	Zr-90	(n,p)	Ru-97	ENDFb6	Pd-102	(n,2na)
Y-90	ENDFb6	Zr-90	(n,p)	Ru-97	ENDFb6	Ru-96	(n,g)
Y-90	LLNL/ACTL	Zr-91	(n,d)	Ru-103	ENDFb6	Pd-108	(n,2na)
Y-90	LLNL/ACTL	Nb-93	(n,a)	Ru-103	ENDFb6	Ru-102	(n,g)
Y-90	ENDFb6	Nb-93	(n,a)	Ru-103	ENDFb6	Pd-106	(n,a)
Y-91	LLNL/ACTL	Zr-92	(n,np)	Ru-105	ENDFb6	Pd-110	(n,2na)
Y-91	ENDFb6	Y-90	(n,g)	Ru-105	ENDFb6	Ru-104	(n,g)
Y-91	LLNL/ACTL	Zr-91	(n,p)	Ru-105	ENDFb6	Pd-108	(n,a)
Y-91	ENDFb6	Zr-91	(n,p)	Ru-106	ENDFb6	Pd-110	(n,na)
Y-91	LLNL/ACTL	Zr-92	(n,d)	Ru-107	ENDFb6	Pd-110	(n,a)
Y-92	LLNL/ACTL	Zr-92	(n,p)	Rh-100	ENDFb6	Pd-102	(n,nd)
Y-92	ENDFb6	Zr-92	(n,p)	Rh-100	ENDFb6	Pd-102	(n,2np)
Y-94	LLNL/ACTL	Zr-94	(n,p)	Rh-101	ENDFb6	Pd-102	(n,np)
Y-94	ENDFb6	Zr-94	(n,p)	Rh-101	ENDFb6	Pd-102	(n,d)
Zr-E9	ENDFb5/532dos	Zr-90	(n,2n)	Rh-102	LLNL/ACTL	Rh-103	(n,2n)
Zr-89	LLNL/ACTL	Zr-90	(n,2n)	Rh-102	ENDFb6	Rh-103	(n,2n)
Zr-89	ENDFb6	Zr-90	(n,2n)	Rh-102	ENDFb6	Pd-104	(n,nd)
Zr-89	LLNL/ACTL	Zr-91	(n,3n)	Rh-102	ENDFb6	Pd-104	(n,2np)
Zr-89	LLNL/ACTL	Mo-92	(n,a)	Rh-102	ENDFb6	Pd-102	(n,p)
Zr-93	LLNL/ACTL	Zr-94	(n,2n)	Rh-104	ENDFb6	Pd-105	(n,np)
Zr-93	ENDFb6	Zr-94	(n,2n)	Rh-104	ENDFb6	Pd-106	(n,nd)
Zr-93	ENDFb5/532dos	Zr-92	(n,g)	Rh-104	ENDFb6	Pd-106	(n,2np)
Zr-93	LLNL/ACTL	Zr-92	(n,g)	Rh-104	ENDFb6	Rh-103	(n,g)
Zr-93	ENDFb6	Zr-92	(n,g)	Rh-104	ENDFb6	Pd-104	(n,p)
Zr-93	LLNL/ACTL	Nb-93	(n,p)	Rh-104	ENDFb6	Pd-105	(n,d)
Zr-93	ENDFb6	Nb-93	(n,p)	Rh-104	LLNL/ACTL	Ag-107	(n,a)
Zr-93	LLNL/ACTL	Mo-96	(n,a)	Rh-104	ENDFb6	Ag-107	(n,a)
Zr-95	LLNL/ACTL	Zr-96	(n,2n)	Rh-105	ENDFb6	Ag-109	(n,na)
Zr-95	ENDFb6	Zr-96	(n,2n)	Rh-105	ENDFb6	Pd-106	(n,np)
Zr-95	ENDFb5/532dos	Zr-94	(n,g)	Rh-105	ENDFb6	Pd-105	(n,p)
Zr-95	LLNL/ACTL	Zr-94	(n,g)	Rh-105	ENDFb6	Pd-106	(n,d)
Zr-95	ENDFb6	Zr-94	(n,g)	Rh-105	ENDFb6	Ag-107	(n,3He)
Zr-95	LLNL/ACTL	Mo-98	(n,a)	Rh-106	ENDFb6	Pd-108	(n,nd)
Zr-97	ENDFb6	Zr-96	(n,g)	Rh-106	ENDFb6	Pd-108	(n,2np)
Zr-97	LLNL/ACTL	Mo-100	(n,a)	Rh-106	ENDFb6	Pd-106	(n,p)
Nb-90	LLNL/ACTL	Mo-92	(n,t)	Rh-106	LLNL/ACTL	Ag-109	(n,a)
Nb-91	LLNL/ACTL	Nb-93	(n,3n)	Rh-106	ENDFb6	Ag-109	(n,a)
Nb-91	ENDL94	Nb-93	(n,3n)	Rh-107	ENDFb6	Pd-108	(n,np)
Nb-91	ENDFb6	Nb-93	(n,3n)	Rh-107	ENDFb6	Pd-108	(n,d)
Nb-91	LLNL/ACTL	Mo-92	(n,np)	Rh-107	ENDFb6	Ag-109	(n,3He)
Nb-91	LLNL/ACTL	Mo-92	(n,d)	Rh-108	ENDFb6	Pd-110	(n,nd)
Nb-92	LLNL/ACTL	Nb-93	(n,2n)	Rh-108	ENDFb6	Pd-110	(n,2np)
Nb-92	ENDL94	Nb-93	(n,2n)	Rh-108	ENDFb6	Pd-108	(n,p)
Nb-92	ENDFb6	Nb-93	(n,2n)	Rh-109	ENDFb6	Pd-110	(n,np)
Nb-92	LLNL/ACTL	Mo-92	(n,p)	Rh-109	ENDFb6	Pd-110	(n,d)
Nb-92	LLNL/ACTL	Mo-94	(n,t)	Rh-110	ENDFb6	Pd-110	(n,p)
Nb-94	LLNL/ACTL	Mo-95	(n,np)	Pd-100	ENDFb6	Pd-102	(n,3n)
Nb-94	LLNL/ACTL	Nb-93	(n,g)	Pd-101	ENDFb6	Pd-102	(n,2n)
Nb-94	ENDL94	Nb-93	(n,g)	Pd-103	ENDFb6	Pd-104	(n,2n)
Nb-94	ENDFb6	Nb-93	(n,g)	Pd-103	ENDFb6	Pd-105	(n,3n)
Nb-94	LLNL/ACTL	Mo-94	(n,p)	Pd-103	ENDFb6	Pd-102	(n,g)
Nb-94	LLNL/ACTL	Mo-95	(n,d)	Pd-103	ENDFb6	Cd-106	(n,a)
Nb-95	LLNL/ACTL	Mo-96	(n,np)	Pd-107	ENDFb6	Pd-108	(n,2n)
Nb-95	LLNL/ACTL	Mo-95	(n,p)	Pd-107	ENDFb6	Cd-111	(n,na)
Nb-95	LLNL/ACTL	Mo-96	(n,d)	Pd-107	ENDFb6	Pd-106	(n,g)
Nb-96	LLNL/ACTL	Mo-96	(n,p)	Pd-107	LLNL/ACTL	Ag-107	(n,p)
Nb-97	LLNL/ACTL	Mo-97	(n,p)	Pd-107	ENDFb6	Ag-107	(n,p)
Nb-98	LLNL/ACTL	Mo-98	(n,p)	Pd-107	ENDFb6	Ag-109	(n,t)
Nb-98	LLNL/ACTL	Mo-100	(n,p)	Pd-107	ENDFb6	Cd-110	(n,a)
Mo-91	LLNL/ACTL	Mo-92	(n,2n)	Pd-109	ENDFb6	Pd-110	(n,2n)
Mo-93	LLNL/ACTL	Mo-94	(n,2n)	Pd-109	ENDFb6	Cd-113	(n,na)
Mo-93	LLNL/ACTL	Mo-95	(n,3n)	Pd-109	ENDFb6	Pd-108	(n,g)
Mo-93	ENDFb5/532dos	Mo-92	(n,g)	Pd-109	LLNL/ACTL	Ag-109	(n,p)
Mo-93	LLNL/ACTL	Mo-92	(n,g)	Pd-109	ENDFb6	Ag-109	(n,p)
Mo-93	ENDFb6	Mo-92	(n,g)	Pd-109	ENDFb6	Cd-111	(n,3He)
Mo-99	LLNL/ACTL	Mo-100	(n,2n)	Pd-109	LLNL/ACTL	Cd-112	(n,a)
Mo-99	ENDFb5/532dos	Mo-99	(n,g)	Pd-109	ENDFb6	Cd-112	(n,a)
Mo-99	LLNL/ACTL	Mo-98	(n,g)	Pd-111	LLNL/ACTL	Pd-110	(n,g)
Mo-99	ENDFb6	Mo-98	(n,g)	Pd-111	ENDFb6	Pd-110	(n,g)

Pd-111	ENDFb6	Cd-113	(n, 3He)	Cd-113	ENDFb6	Cd-112	(n, g)
Pd-111	ENDFb6	Cd-114	(n, a)	Cd-113	LLNL/ACTL	In-113	(n, p)
Pd-112	ENDFb6	Cd-116	(n, na)	Cd-115	LLNL/ACTL	Cd-116	(n, 2n)
Pd-112	ENDFb6	Cd-114	(n, 3He)	Cd-115	ENDFb6	Cd-114	(n, g)
Pd-113	ENDFb6	Cd-116	(n, a)	Cd-115	ENDFb6	In-115	(n, p)
Pd-114	ENDFb6	Cd-116	(n, 3He)	Cd-115	LLNL/ACTL	Sn-118	(n, a)
Ag-103	ENDFb6	Cd-106	(n, nt)	Cd-115	LLNL/ACTL	Cd-116	(n, g)
Ag-104	ENDFb6	Cd-106	(n, nd)	Cd-117	ENDFb6	Sn-112	(n, np)
Ag-104	ENDFb6	Cd-106	(n, t)	In-111	LLNL/ACTL	Sn-112	(n, d)
Ag-105	LLNL/ACTL	Ag-107	(n, 3n)	In-111	LLNL/ACTL	In-113	(n, 2n)
Ag-105	ENDL94	Ag-107	(n, 3n)	In-112	LLNL/ACTL	Sn-112	(n, p)
Ag-105	ENDFb6	Ag-107	(n, 3n)	In-112	LLNL/ACTL	In-115	(n, np)
Ag-105	ENDFb6	Cd-106	(n, np)	In-114	LLNL/ACTL	Sn-115	(n, np)
Ag-105	ENDFb6	Cd-106	(n, nt)	In-114	LLNL/ACTL	In-113	(n, g)
Ag-105	ENDFb6	Cd-106	(n, d)	In-114	LLNL/ACTL	In-113	(n, g)
Ag-106	LLNL/ACTL	Ag-107	(n, 2n)	In-114	ENDFb6	In-113	(n, g)
Ag-106	ENDL94	Ag-107	(n, 2n)	In-114	LLNL/ACTL	Sn-114	(n, p)
Ag-106	ENDFb6	Ag-107	(n, 2n)	In-115	LLNL/ACTL	Sn-116	(n, np)
Ag-106	ENDFb6	Cd-108	(n, nd)	In-115	ENDFb5/532dos	In-Ii5	(n, n'), 1
Ag-106	ENDFb6	Cd-106	(n, p)	In-115	LLNL/ACTL	Sn-115	(n, p)
Ag-106	ENDFb6	Cd-108	(n, t)	In-116	LLNL/ACTL	In-115	(n, g)
Ag-108	LLNL/ACTL	Ag-109	(n, 2n)	In-116	ENDFb6	In-115	(n, g)
Ag-108	ENDL94	Ag-109	(n, 2n)	In-116	LLNL/ACTL	Sn-116	(n, p)
Ag-108	ENDFb6	Ag-109	(n, 2n)	In-117	LLNL/ACTL	Sn-117	(n, p)
Ag-108	ENDFb6	Cd-110	(n, nd)	In-118	LLNL/ACTL	Sn-118	(n, p)
Ag-108	ENDFb6	Cd-111	(n, nt)	In-119	LLNL/ACTL	Sn-119	(n, p)
Ag-108	LLNL/ACTL	Ag-107	(n, g)	In-120	LLNL/ACTL	Sn-120	(n, p)
Ag-108	ENDL94	Ag-107	(n, g)	In-122	LLNL/ACTL	Sn-122	(n, p)
Ag-108	ENDFb6	Ag-107	(n, g)	In-124	LLNL/ACTL	Sn-124	(n, p)
Ag-108	ENDFb6	Cd-108	(n, p)	Sn-111	LLNL/ACTL	Sn-112	(n, 2n)
Ag-108	ENDFb6	Cd-110	(n, t)	Sn-113	LLNL/ACTL	Sn-114	(n, 2n)
Ag-110	ENDFb6	Cd-111	(n, np)	Sn-113	LLNL/ACTL	Sn-112	(n, g)
Ag-110	ENDFb6	Cd-112	(n, nd)	Sn-113	ENDFb6	Sn-112	(n, g)
Ag-110	ENDFb6	Cd-113	(n, nt)	Sn-121	LLNL/ACTL	Sn-122	(n, 2n)
Ag-110	LLNL/ACTL	Ag-109	(n, g)	Sn-121	ENDFb5/532dos	Sn-120	(n, g)
Ag-110	ENDL94	Ag-109	(n, g)	Sn-121	LLNL/ACTL	Sn-120	(n, g)
Ag-110	ENDFb6	Ag-109	(n, g)	Sn-121	ENDFb6	Sn-120	(n, g)
Ag-110	ENDFb6	Cd-110	(n, p)	Sn-121	LLNL/ACTL	Sb-121	(n, p)
Ag-110	ENDFb6	Cd-111	(n, d)	Sn-123	LLNL/ACTL	Sn-124	(n, 2n)
Ag-110	ENDFb6	Cd-112	(n, t)	Sn-123	ENDFb5/532dos	Sn-I22	(n, g)
Ag-110	LLNL/ACTL	In-113	(n, a)	Sn-123	LLNL/ACTL	Sn-122	(n, g)
Ag-111	ENDFb6	Cd-112	(n, np)	Sn-123	ENDFb6	Sn-122	(n, g)
Ag-111	ENDFb6	Cd-113	(n, nd)	Sn-123	LLNL/ACTL	Sb-123	(n, p)
Ag-111	ENDFb6	Cd-114	(n, nt)	Sn-125	ENDFb5/532dos	Sn-I24	(n, g)
Ag-111	LLNL/ACTL	Cd-111	(n, p)	Sn-125	LLNL/ACTL	Sn-124	(n, g)
Ag-111	ENDFb6	Cd-111	(n, p)	Sn-125	ENDFb6	Sn-124	(n, g)
Ag-111	ENDFb6	Cd-112	(n, d)	Sb-120	LLNL/ACTL	Sb-121	(n, 2n)
Ag-111	ENDFb6	Cd-113	(n, t)	Sb-122	LLNL/ACTL	Sb-123	(n, 2n)
Ag-112	ENDFb6	Cd-113	(n, np)	Sb-122	LLNL/ACTL	Sb-121	(n, g)
Ag-112	ENDFb6	Cd-114	(n, nd)	Sb-122	ENDFb6	Sb-121	(n, g)
Ag-112	ENDFb6	Cd-112	(n, p)	Sb-124	LLNL/ACTL	Sb-123	(n, g)
Ag-112	ENDFb6	Cd-113	(n, d)	Sb-124	ENDFb6	Sb-123	(n, g)
Ag-112	ENDFb6	Cd-114	(n, t)	Sb-124	ENDFb6	I-127	(n, a)
Ag-109	LLNL/ACTL	In-115	(n, a)	Te-121	ENDFb6	Te-120	(n, g)
Ag-113	ENDFb6	Cd-114	(n, np)	Te-121	ENDFb6	Xe-124	(n, a)
Ag-113	ENDFb6	Cd-116	(n, nt)	Te-123	ENDFb6	Te-122	(n, g)
Ag-113	ENDFb6	Cd-113	(n, p)	Te-123	ENDFb6	Xe-126	(n, a)
Ag-113	ENDFb6	Cd-114	(n, d)	Te-127	ENDFb6	Te-126	(n, g)
Ag-114	ENDFb6	Cd-116	(n, nd)	Te-127	ENDFb6	I-127	(n, p)
Ag-114	ENDFb6	Cd-114	(n, p)	Te-127	ENDFb6	Xe-130	(n, a)
Ag-114	ENDFb6	Cd-116	(n, t)	Te-128	ENDFb6	Xe-131	(n, a)
Ag-115	ENDFb6	Cd-116	(n, np)	Te-129	ENDFb6	Te-128	(n, g)
Ag-115	ENDFb6	Cd-116	(n, d)	Te-129	ENDFb6	Xe-132	(n, a)
Ag-116	ENDFb6	Cd-116	(n, p)	Te-131	ENDFb6	Te-130	(n, g)
Cd-105	LLNL/ACTL	Cd-106	(n, 2n)	Te-131	ENDFb6	Xe-134	(n, a)
Cd-105	ENDFb6	Cd-106	(n, 2n)	Te-133	ENDFb6	Xe-136	(n, a)
Cd-107	ENDFb6	Cd-108	(n, 2n)	I-122	ENDFb6	Xe-124	(n, t)
Cd-107	ENDFb6	Cd-106	(n, g)	I-123	ENDFb6	Xe-124	(n, d)
Cd-109	ENDFb6	Cd-110	(n, 2n)	I-124	ENDFb6	Xe-124	(n, p)
Cd-109	ENDFb6	Cd-111	(n, 3n)	I-124	ENDFb6	Xe-126	(n, t)
Cd-109	ENDFb6	Cd-108	(n, g)	I-125	ENDL94	I-127	(n, 3n)
Cd-113	ENDFb6	Cd-114	(n, 2n)	I-125	ENDFb6	I-127	(n, 3n)

I-125	ENDFb6	Xe-126	(n,d)	Pr-140	LLNL/ACTL	Pr-141	(n,2n)
I-126	ENDFb5/532dos	I-127	(n,2n)	Pr-140	ENDFb6	Pr-141	(n,2n)
I-126	LLNL/ACTL	I-127	(n,2n)	Pr-142	ENDFb6	Nd-143	(n,np)
I-126	ENDL94	I-127	(n,2n)	Pr-142	ENDFb6	Pr-141	(n,g)
I-126	ENDFb6	I-127	(n,2n)	Pr-142	ENDFb6	Nd-143	(n,d)
I-126	ENDFb6	Xe-126	(n,p)	Pr-143	ENDFb6	Pm-147	(n,na)
I-126	ENDFb6	Xe-128	(n,t)	Pr-143	ENDFb6	Nd-143	(n,p)
I-128	ENDFb5/532dos	I-127	(n,g)	Pr-143	ENDFb6	Nd-145	(n,t)
I-128	ENDL94	I-127	(n,g)	Pr-144	ENDFb6	Nd-145	(n,np)
I-128	ENDFb6	I-127	(n,g)	Pr-144	ENDFb6	Nd-145	(n,d)
I-128	ENDFb6	Xe-128	(n,p)	Pr-144	ENDFb6	Nd-146	(n,t)
I-128	ENDFb6	Xe-129	(n,d)	Pr-144	ENDFb6	Pm-147	(n,a)
I-128	ENDFb6	Xe-130	(n,t)	Pr-145	ENDFb6	Nd-146	(n,np)
I-129	ENDFb6	Xe-129	(n,p)	Pr-145	ENDFb6	Nd-145	(n,p)
I-129	ENDFb6	Xe-130	(n,d)	Pr-145	ENDFb6	Nd-146	(n,d)
I-129	ENDFb6	Xe-131	(n,t)	Pr-145	ENDFb6	Pm-147	(n,3He)
I-130	ENDFb6	Xe-130	(n,p)	Pr-146	ENDFb6	Nd-146	(n,p)
I-130	ENDFb6	Xe-131	(n,d)	Pr-146	ENDFb6	Nd-148	(n,t)
I-130	ENDFb6	Xe-132	(n,t)	Pr-147	ENDFb6	Nd-148	(n,np)
I-130	ENDFb6	Cs-133	(n,a)	Pr-147	ENDFb6	Nd-148	(n,d)
I-131	ENDFb6	Xe-131	(n,p)	Pr-148	ENDFb6	Nd-148	(n,p)
I-131	ENDFb6	Xe-132	(n,d)	Pr-148	ENDFb6	Nd-150	(n,t)
I-132	ENDFb6	Xe-132	(n,p)	Pr-149	ENDFb6	Nd-150	(n,np)
I-132	ENDFb6	Xe-134	(n,t)	Pr-149	ENDFb6	Nd-150	(n,d)
I-133	ENDFb6	Xe-134	(n,d)	Pr-150	ENDFb6	Nd-150	(n,p)
I-134	ENDFb6	Xe-134	(n,p)	Nd-141	LLNL/ACTL	Nd-142	(n,2n)
I-134	ENDFb6	Xe-136	(n,t)	Nd-141	ENDFb6	Nd-143	(n,3n)
I-135	ENDFb6	Xe-136	(n,d)	Nd-144	ENDFb6	Nd-145	(n,2n)
I-136	ENDFb6	Xe-136	(n,p)	Nd-144	ENDFb6	Nd-146	(n,3n)
Xe-122	ENDFb6	Xe-124	(n,3n)	Nd-144	ENDFb6	Nd-143	(n,g)
Xe-123	ENDFb6	Xe-124	(n,2n)	Nd-147	LLNL/ACTL	Nd-148	(n,2n)
Xe-125	ENDFb6	Xe-126	(n,2n)	Nd-147	ENDFb6	Nd-148	(n,2n)
Xe-125	ENDFb6	Xe-124	(n,g)	Nd-147	ENDFb6	Sm-151	(n,na)
Xe-127	ENDFb6	Xe-128	(n,2n)	Nd-147	ENDFb6	Nd-146	(n,g)
Xe-127	ENDFb6	Xe-129	(n,3n)	Nd-147	ENDFb6	Pm-147	(n,p)
Xe-127	ENDFb6	Xe-126	(n,g)	Nd-149	LLNL/ACTL	Nd-150	(n,2n)
Xe-133	ENDL94	Xe-134	(n,2n)	Nd-149	ENDFb6	Nd-150	(n,2n)
Xe-133	ENDFb6	Xe-134	(n,2n)	Nd-149	ENDFb6	Nd-148	(n,g)
Xe-133	ENDFb6	Xe-132	(n,g)	Nd-149	ENDFb6	Sm-151	(n,3He)
Xe-133	ENDFb6	Cs-133	(n,p)	Nd-151	ENDFb6	Nd-150	(n,g)
Xe-135	ENDFb6	Xe-136	(n,2n)	Pm-145	ENDFb6	Pm-147	(n,3n)
Xe-135	ENDL94	Xe-134	(n,g)	Pm-146	ENDFb6	Pm-147	(n,2n)
Xe-135	ENDFb6	Xe-134	(n,g)	Pm-148	ENDFb6	Eu-152	(n,na)
Xe-135	ENDFb6	Ba-138	(n,a)	Pm-148	ENDFb6	Pm-147	(n,g)
Xe-137	ENDFb6	Xe-136	(n,g)	Pm-149	ENDFb6	Pm-148	(n,g)
Cs-132	LLNL/ACTL	Cs-133	(n,2n)	Pm-149	ENDFb6	Pm-148	(n,g)
Cs-132	ENDFb6	Cs-133	(n,2n)	Pm-149	ENDFb6	Sm-151	(n,t)
Cs-134	ENDFb6	Cs-133	(n,g)	Pm-149	ENDFb6	Eu-152	(n,a)
Cs-138	ENDFb6	Ba-138	(n,p)	Pm-150	ENDFb6	Eu-154	(n,na)
Ba-133	ENDFb6	Ba-134	(n,2n)	Pm-150	ENDFb6	Sm-151	(n,np)
Ba-139	ENDFb6	Ba-138	(n,g)	Pm-150	ENDFb6	Pm-149	(n,g)
La-137	ENDFb6	Pr-141	(n,na)	Pm-150	ENDFb6	Sm-151	(n,d)
La-140	ENDFb5/532dos	La-139	(n,g)	Pm-150	ENDFb6	Eu-152	(n,3He)
La-140	ENDFb6	La-139	(n,g)	Pm-151	ENDFb6	Eu-155	(n,na)
Ce-139	LLNL/ACTL	Ce-140	(n,2n)	Pm-151	ENDFb6	Sm-151	(n,p)
Ce-139	ENDFb6	Nd-143	(n,na)	Pm-151	ENDFb6	Eu-154	(n,a)
Ce-139	ENDFb6	Pr-141	(n,t)	Pm-152	ENDFb6	Eu-154	(n,3He)
Ce-141	LLNL/ACTL	Ce-142	(n,2n)	Pm-152	ENDFb6	Eu-155	(n,a)
Ce-141	ENDFb6	Nd-145	(n,na)	Pm-153	ENDFb6	Eu-155	(n,3He)
Ce-141	ENDFb6	Ce-140	(n,g)	Sm-151	ENDFb6	Eu-152	(n,np)
Ce-141	ENDFb6	Pr-141	(n,p)	Sm-151	ENDFb6	Eu-152	(n,d)
Ce-141	ENDFb6	Nd-143	(n,3He)	Sm-153	ENDFb6	Eu-154	(n,np)
Ce-143	ENDFb6	Ce-142	(n,g)	Sm-153	ENDFb6	Eu-154	(n,d)
Ce-143	ENDFb6	Nd-145	(n,3He)	Sm-153	ENDFb6	Eu-155	(n,t)
Ce-143	ENDFb6	Nd-146	(n,a)	Sm-155	ENDFb6	Eu-155	(n,p)
Ce-144	ENDFb6	Nd-148	(n,na)	Eu-150	ENDFb6	Eu-152	(n,3n)
Ce-144	ENDFb6	Nd-146	(n,3He)	Eu-152	ENDFb6	Eu-154	(n,3n)
Ce-145	ENDFb6	Nd-148	(n,a)	Eu-154	ENDFb6	Eu-155	(n,2n)
Ce-146	ENDFb6	Nd-150	(n,na)	Eu-154	ENDL94	Eu-156	(n,3n)
Ce-146	ENDFb6	Nd-148	(n,3He)	Eu-155	ENDL94	Eu-156	(n,2n)
Ce-147	ENDFb6	Nd-150	(n,a)	Eu-155	ENDFb6	Eu-154	(n,g)
Pr-139	ENDFb6	Pr-141	(n,3n)	Eu-156	ENDFb6	Eu-155	(n,g)

Eu-157	ENDL94	Eu-156	(n,g)	Ta-184	ENDFb6	W-184	(n,p)
Eu-157	ENDFb6	Eu-156	(n,g)	Ta-185	ENDFb6	W-186	(n,np)
Eu-158	ENDFb6	Eu-157	(n,g)	Ta-186	LLNL/ACTL	W-186	(n,p)
Tb-161	ENDFb6	Tb-160	(n,g)	Ta-186	ENDFb6	W-186	(n,p)
Dy-166	LLNL/ACTL	Ho-166	(n,p)	W-178	LLNL/ACTL	W-180	(n,3n)
Ho-162	LLNL/ACTL	Ho-164	(n,3n)	W-179	LLNL/ACTL	W-180	(n,2n)
Ho-163	LLNL/ACTL	Ho-164	(n,2n)	W-181	LLNL/ACTL	W-182	(n,2n)
Ho-164	LLNL/ACTL	Ho-166	(n,3n)	W-181	ENDFb6	W-182	(n,2n)
Ho-167	LLNL/ACTL	Ho-166	(n,g)	W-181	LLNL/ACTL	W-183	(n,3n)
Tm-168	LLNL/ACTL	Tm-169	(n,2n)	W-181	ENDFb6	W-183	(n,3n)
Tm-170	LLNL/ACTL	Tm-169	(n,g)	W-181	LLNL/ACTL	W-180	(n,g)
Tm-172	ENDFb6	Lu-175	(n,a)	W-185	LLNL/ACTL	W-186	(n,2n)
Tm-173	ENDFb6	Lu-176	(n,a)	W-185	ENDFb6	W-186	(n,2n)
Yb-175	ENDFb6	Lu-175	(n,p)	W-185	LLNL/ACTL	W-184	(n,g)
Lu-173	LLNL/ACTL	Lu-175	(n,3n)	W-185	ENDFb6	W-184	(n,g)
Lu-173	ENDFb6	Lu-175	(n,3n)	W-185	LLNL/ACTL	Re-185	(n,p)
Lu-174	LLNL/ACTL	Lu-175	(n,2n)	W-187	LLNL/ACTL	W-186	(n,g)
Lu-174	ENDFb6	Lu-175	(n,2n)	W-187	ENDFb6	W-186	(n,g)
Lu-174	LLNL/ACTL	Lu-176	(n,3n)	W-187	LLNL/ACTL	Re-187	(n,p)
Lu-174	ENDFb6	Lu-176	(n,3n)	Re-183	LLNL/ACTL	Re-185	(n,3n)
Lu-174	LLNL/ACTL	Hf-174	(n,p)	Re-183	ENDL94	Re-185	(n,3n)
Lu-176	LLNL/ACTL	Lu-175	(n,g)	Re-183	ENDFb6	Re-185	(n,3n)
Lu-176	ENDFb6	Lu-175	(n,g)	Re-184	LLNL/ACTL	Re-185	(n,2n)
Lu-176	LLNL/ACTL	Hf-176	(n,p)	Re-184	ENDL94	Re-185	(n,2n)
Lu-177	LLNL/ACTL	Ta-181	(n,na)	Re-184	ENDFb6	Re-185	(n,2n)
Lu-177	LLNL/ACTL	Lu-176	(n,g)	Re-186	LLNL/ACTL	Re-187	(n,2n)
Lu-177	ENDFb6	Lu-176	(n,g)	Re-186	ENDL94	Re-187	(n,2n)
Lu-177	LLNL/ACTL	Hf-177	(n,p)	Re-186	ENDFb6	Re-187	(n,2n)
Lu-177	LLNL/ACTL	Ta-180	(n,a)	Re-186	LLNL/ACTL	Re-185	(n,g)
Lu-178	LLNL/ACTL	Hf-178	(n,p)	Re-186	ENDL94	Re-185	(n,g)
Lu-179	LLNL/ACTL	Hf-179	(n,p)	Re-186	ENDFb6	Re-185	(n,g)
Lu-180	LLNL/ACTL	Hf-180	(n,p)	Re-188	LLNL/ACTL	Re-187	(n,g)
Hf-172	LLNL/ACTL	Hf-174	(n,3n)	Re-188	ENDL94	Re-187	(n,g)
Hf-173	LLNL/ACTL	Hf-174	(n,2n)	Re-188	ENDFb6	Re-187	(n,g)
Hf-173	ENDFb6	Hf-174	(n,2n)	Ir-190	LLNL/ACTL	Ir-191	(n,2n)
Hf-174	LLNL/ACTL	Hf-176	(n,3n)	Ir-190	ENDFb6	Ir-191	(n,2n)
Hf-175	LLNL/ACTL	Hf-176	(n,2n)	Ir-190	LLNL/ACTL	Pt-190	(n,p)
Hf-175	ENDFb6	Hf-176	(n,2n)	Ir-192	LLNL/ACTL	Ir-193	(n,2n)
Hf-175	LLNL/ACTL	Hf-177	(n,3n)	Ir-192	ENDFb6	Ir-193	(n,2n)
Hf-181	LLNL/ACTL	Hf-180	(n,g)	Ir-192	LLNL/ACTL	Pt-192	(n,p)
Hf-181	LLNL/ACTL	Ta-181	(n,p)	Ir-194	LLNL/ACTL	Pt-194	(n,p)
Hf-181	ENDFb6	Ta-181	(n,p)	Ir-194	LLNL/ACTL	Au-197	(n,a)
Hf-181	LLNL/ACTL	W-184	(n,a)	Ir-194	ENDFb6	Au-197	(n,a)
Hf-181	ENDFb6	W-184	(n,a)	Ir-195	LLNL/ACTL	Pt-195	(n,p)
Hf-182	LLNL/ACTL	W-186	(n,na)	Ir-196	LLNL/ACTL	Pt-196	(n,p)
Hf-183	LLNL/ACTL	W-186	(n,a)	Ir-198	LLNL/ACTL	Pt-198	(n,p)
Hf-183	ENDFb6	W-186	(n,a)	Pt-188	LLNL/ACTL	Pt-190	(n,3n)
Ta-178	LLNL/ACTL	Ta-180	(n,3n)	Pt-189	LLNL/ACTL	Pt-190	(n,2n)
Ta-179	LLNL/ACTL	Ta-180	(n,2n)	Pt-190	LLNL/ACTL	Pt-192	(n,3n)
Ta-179	LLNL/ACTL	Ta-181	(n,3n)	Pt-191	LLNL/ACTL	Pt-192	(n,2n)
Ta-179	ENDL94	Ta-181	(n,3n)	Pt-193	LLNL/ACTL	Pt-194	(n,2n)
Ta-179	ENDFb6	Ta-181	(n,3n)	Pt-193	LLNL/ACTL	Pt-195	(n,3n)
Ta-179	LLNL/ACTL	W-180	(n,np)	Pt-197	LLNL/ACTL	Pt-198	(n,2n)
Ta-179	LLNL/ACTL	W-180	(n,d)	Pt-197	LLNL/ACTL	Au-197	(n,p)
Ta-180	LLNL/ACTL	Ta-181	(n,2n)	Pt-197	ENDFb6	Au-197	(n,p)
Ta-180	ENDL94	Ta-181	(n,2n)	Pt-199	LLNL/ACTL	Hg-202	(n,a)
Ta-180	ENDFb6	Ta-181	(n,2n)	Pt-201	LLNL/ACTL	Hg-204	(n,a)
Ta-180	LLNL/ACTL	W-180	(n,p)	Au-195	LLNL/ACTL	Au-197	(n,3n)
Ta-182	LLNL/ACTL	W-183	(n,np)	Au-195	ENDFb6	Au-197	(n,3n)
Ta-182	ENDFb6	W-183	(n,np)	Au-196	LLNL/ACTL	Au-197	(n,2n)
Ta-182	LLNL/ACTL	Ta-181	(n,g)	Au-196	ENDFb6	Au-197	(n,2n)
Ta-182	ENDL94	Ta-181	(n,g)	Au-198	LLNL/ACTL	Au-197	(n,g)
Ta-182	ENDFb6	Ta-181	(n,g)	Au-198	ENDFb6	Au-197	(n,g)
Ta-182	LLNL/ACTL	W-182	(n,p)	Au-201	LLNL/ACTL	Hg-202	(n,np)
Ta-182	ENDFb6	W-182	(n,p)	Au-202	LLNL/ACTL	Hg-202	(n,p)
Ta-182	LLNL/ACTL	W-183	(n,d)	Au-203	LLNL/ACTL	Hg-204	(n,np)
Ta-183	LLNL/ACTL	W-184	(n,np)	Au-204	LLNL/ACTL	Hg-204	(n,p)
Ta-183	ENDFb6	W-184	(n,np)	Hg-203	LLNL/ACTL	Hg-204	(n,2n)
Ta-183	LLNL/ACTL	W-183	(n,p)	Hg-203	LLNL/ACTL	Pb-207	(n,na)
Ta-183	ENDFb6	W-183	(n,p)	Hg-203	ENDFb6	Pb-208	(n,2na)
Ta-183	LLNL/ACTL	W-184	(n,d)	Hg-203	LLNL/ACTL	Hg-202	(n,g)
Ta-184	LLNL/ACTL	W-184	(n,p)	Hg-203	LLNL/ACTL	Tl-203	(n,p)

Hg-203	LLNL/ACTL	Pb-206	(n, a)	Th-231	LLNL/ACTL	Th-232	(n, 2n)
Hg-203	ENDFb6	Pb-206	(n, a)	Th-231	ENDL94	Th-232	(n, 2n)
Hg-205	LLNL/ACTL	Hg-204	(n, g)	Th-231	ENDFb6	Th-232	(n, 2n)
Hg-205	LLNL/ACTL	Tl-205	(n, p)	Th-233	LLNL/ACTL	Th-232	(n, g)
Tl-201	LLNL/ACTL	Tl-203	(n, 3n)	Th-233	ENDL94	Th-232	(n, g)
Tl-202	LLNL/ACTL	Tl-203	(n, 2n)	Th-233	ENDFb6	Th-232	(n, g)
Tl-202	LLNL/ACTL	Pb-204	(n, t)	Pa-229	ENDFb6	Pa-231	(n, 3n)
Tl-204	LLNL/ACTL	Tl-205	(n, 2n)	Pa-230	ENDFb6	Pa-231	(n, 2n)
Tl-204	LLNL/ACTL	Tl-203	(n, g)	Pa-232	ENDFB5/532dos	Pa-231	(n, g)
Tl-204	LLNL/ACTL	Pb-204	(n, p)	Pa-232	ENDFb6	Pa-231	(n, g)
Tl-204	LLNL/ACTL	Pb-206	(n, t)	U-232	LLNL/ACTL	U-234	(n, 3n)
Tl-204	ENDFb6	Pb-206	(n, t)	U-232	ENDL94	U-234	(n, 3n)
Tl-206	ENDFb6	Pb-208	(n, nd)	U-232	ENDFb6	U-234	(n, 3n)
Tl-206	ENDFb6	Pb-208	(n, 2np)	U-232	LLNL/ACTL	U-235	(n, 4n)
Tl-206	LLNL/ACTL	Tl-205	(n, g)	U-232	ENDL94	U-235	(n, 4n)
Tl-206	LLNL/ACTL	Pb-206	(n, p)	U-232	ENDFb6	U-235	(n, 4n)
Tl-206	ENDFb6	Pb-206	(n, p)	U-233	LLNL/ACTL	U-234	(n, 2n)
Tl-206	LLNL/ACTL	Bi-209	(n, a)	U-233	ENDL94	U-234	(n, 2n)
Tl-207	ENDFb6	Pb-208	(n, np)	U-233	ENDFb6	U-234	(n, 2n)
Tl-207	LLNL/ACTL	Pb-207	(n, p)	U-233	LLNL/ACTL	U-235	(n, 3n)
Tl-207	ENDFb6	Pb-207	(n, p)	U-233	ENDL94	U-235	(n, 3n)
Pb-204	LLNL/ACTL	Pb-206	(n, 3n)	U-233	ENDFb6	U-235	(n, 3n)
Pb-204	ENDFb6	Pb-206	(n, 3n)	U-234	LLNL/ACTL	U-235	(n, 2n)
Pb-205	LLNL/ACTL	Pb-206	(n, 2n)	U-234	ENDL94	U-235	(n, 2n)
Pb-205	ENDFb6	Pb-206	(n, 2n)	U-234	ENDFb6	U-235	(n, 2n)
Pb-205	LLNL/ACTL	Pb-207	(n, 3n)	U-235	LLNL/ACTL	U-238	(n, 4n)
Pb-205	ENDFb6	Pb-207	(n, 3n)	U-235	ENDL94	U-238	(n, 4n)
Pb-205	LLNL/ACTL	Pb-204	(n, g)	U-235	ENDFB6	U-238	(n, 4n)
Pb-209	LLNL/ACTL	Pb-208	(n, g)	U-235	LLNL/ACTL	U-234	(n, g)
Pb-209	LLNL/ACTL	Bi-209	(n, p)	U-235	ENDL94	U-234	(n, g)
Bi-209	LLNL/ACTL	Bi-209	(n, 3n)	U-235	ENDFb6	U-234	(n, g)
Bi-207	ENDL94	Bi-209	(n, 3n)	U-236	LLNL/ACTL	U-238	(n, 3n)
Bi-207	LLNL/ACTL	Bi-209	(n, 2n)	U-236	ENDL94	U-238	(n, 3n)
Bi-208	ENDL94	Bi-209	(n, 2n)	U-236	ENDFb6	U-238	(n, 3n)
Bi-210	LLNL/ACTL	Bi-209	(n, g)	U-236	LLNL/ACTL	U-235	(n, g)
Bi-210	ENDL94	Bi-209	(n, g)	U-236	ENDL94	U-235	(n, g)
Th-229	LLNL/ACTL	Th-232	(n, 4n)	U-236	ENDFB6	U-235	(n, g)
Th-229	ENDL94	Th-232	(n, 4n)	U-237	LLNL/ACTL	U-238	(n, 2n)
Th-230	LLNL/ACTL	Th-232	(n, 3n)	U-237	ENDL94	U-238	(n, 2n)
Th-230	ENDL94	Th-232	(n, 3n)	U-237	ENDFb6	U-238	(n, 2n)
Th-230	ENDFb6	Th-232	(n, 3n)				